INVESTIGATING THE BIOLOGICAL ROLE OF SIALIDASE NEU4 AND GM3 SYNTHASE ENZYMES IN A MOUSE MODEL OF TAY-SACHS DISEASE

A Thesis Submitted to
the Graduate School of Engineering and Sciences of
İzmir Institute of Technology
in Partial Fulfillment of the Requirements for the Degree of

MASTER OF SCIENCE

In Molecular Biology and Genetics

By
Talha BARNAR

July 2017
IZMIR

We approved the thesis of **Talha BARNAR**

Examining Committee Member

_____

Prof. Dr. Volkan SEYRANTEPE
Department of Molecular Biology and Genetics,
İzmir Institute of Technology

_____

Prof. Dr. Gülperi ÖKTEM

Department of Histology and Embryology,
Ege University Medical School

_____

Assoc. Prof. Bünyamin AKGÜL
Department of Molecular Biology and Genetics,
İzmir Institute of Technology

28 July 2017

_____

Prof. Dr. Volkan SEYRANTEPE
Supervisor, Department of Molecular Biology and Genetics,
İzmir Institute of Technology

_____

Prof. Dr. Volkan SEYRANTEPE
Head of the Department of Molecular
Biology and genetics

_____

Prof. Dr. Aysun SOFUOĞLU
Dean of the Graduate School of
Engineering and Sciences

ACKNOWLEDGEMENTS

I would like to say thank to my family deeply, my mother always inspires me to being a successful. She always shows me being honest. She gives me a good lesson about facing to difficulties. She teaches me not escape, and focusing of a study.

I am greatly thankful to Intensified cooperation (IntenC) of German-Turkish bilateral agreement and TUBITAK (113T025)

I would like to express my thanks to my supervisor Prof. Volkan Seyrantepe for helping my study and teaching. He gave me a wonderful opportunity to do this project. I am also greatly thankful about his support for this study due to understanding, guidance and encouragement.

I am greatly thankful my thesis committee professors; Assoc. Prof. Bünyamin Akgül, and Prof. Dr. Gülperi Öktem for their advice and contribution. Their suggestion is improved this research and enlighten my point of view.

I would like to express special thanks to Zehra K. Timur teaching, encouragement, motivation, and understanding. Her efforts cannot be remained unregarded because of truthful and suggestive attitude.

I would like to say thank also Osman Yipkin Çalhan and Seçil akyıldız for their support, encouragement, understanding motivation

I also place on record, my sense of gratitude to my other lab members for their helping, understanding, and supports.

ABSTRACT

INVESTIGATING THE BIOLOGICAL ROLE OF SIALIDASE NEU4 AND GM3 SYNTHASE ENZYMES IN A MOUSE MODEL OF TAY-SACHS DISEASE

β-Hexaminidase A which has role in GM2 degradation in glycosphingolipid pathway is known to be main enzyme for Tay-Sachs disease. Although recessive mutant phenotype of this enzyme causes disease in human, Hexa gene knockout mice show less accumulation of GM2 ganglioside than human. To avoid excess GM2 accumulation, mice uses neuraminidases convert GM2 into GA2. In addition, among neuraminidases, it has been found that *Neu4*$^{-/-}$*Hexa*$^{-/-}$ mice can be good model for Tay-Sachs diseases (Seyrantepe et al., 2010). On the other hand, to prevent GM2 accumulation, blocking GM3 synthase is the finest method because GM3 synthase plays a big part in ganglioside synthesis pathway by producing GM3 that is later converted into GM2 or GD3 ganglioside. In addition, GM3 synthase deficient mice can live longer than 1 year. In this study, *Hexa*$^{-/-}$*GM3S*$^{-/-}$*Neu4*$^{-/-}$ mice with single and double variants were produced and brain regions were analyzed with thin-layer chromatography, immunohistochemistry, and real-time PCR methods. This investigation was conducted to clarify real function of *GM3S* on Tay-Sachs mice model and to search for possible effects of *Neu4* in ganglioside pathway. Although GM2 accumulation are present in *Hexa*$^{-/-}$ and *Neu4*$^{-/-}$*Hexa*$^{-/-}$mice, analysis of *Hexa*$^{-/-}$*GM3S*$^{-/-}$*Neu4*$^{-/-}$and *Hexa*$^{-/-}$*GM3S*$^{-/-}$ mice revealed that there is no GM2 accumulation without GM3 synthase enzyme. These results are consistent with known ganglioside synthesis pathway. *Hexa*$^{-/-}$*GM3S*$^{-/-}$*Neu4*$^{-/-}$ and double deficient *Neu4*$^{-/-}$mice variants disclosed change of *Neu3* and *Neu2* concentration to the wild type mice. In regard of these results, change in other neuraminidase expression is to compensate Neu4 function.

Key Words: GM3 synthase, GM2 ganglioside, Neuraminidase, Sialidase, Hexaminidase, Mice.

ÖZET

SİALİDAZ *NEU4* VE GM3 SENTAZ ENZİMLERİNİN TAY-SACHS FARE MODELLERİNDE BİYOLOJİK ROLÜNÜN ARAŞTIRILMASI

GM2 yıkımında rol alan β-hekzosaminidaz A'nın tay sachs hastalığında esas enzim olduğu bilinmektedir. Bu enzimin ressesif mutant fenotipi insanda hastalığa sebebiyet vermesine rağmen, hekzosaminidaz A nakavt fare insana göre daha az GM2 gangliosit birikimi göstermektedir. Farelerde, GM2 birikiminin fazla artışından kaçınmak için fareler GM2'yi, GA2'ye neuraminidazlarla çevirirler. Buna ek olarak, sialidazlar arasından, *Neu4*$^{-/-}$*Hexa*$^{-/-}$ farelerinin Tay-Sachs hastalığı için iyi bir model organizma olabileceğini bulunmuştur (Seyrantepe et al., 2010). Öte yandan, GM2 brikimini önlemek için, GM3 sentaz'ı bloklamak en iyi yöntemdir çünkü GM3 sentaz gangliosit sentez yol izinde büyük bir rol oynar ve sonradan GM2 ya da GD3'e dönüşencek olan GM3'ü sentezler. Bu çalışmada, *Hexa*$^{-/-}$*GM3S*$^{-/-}$*Neu4*$^{-/-}$ fare ve onun tekli ve ikili varyantları üretildi ve beyin bölgeleri ince tabaka kromatografisi, immünohistokimya, ve gerçek zamanlı PCR metodlarıyla analiz edildi. Bu araştırma *GM3S*'in gangliosit metabolizmasındaki gerçek rolünün açıklanması ve *Neu4*'un gangliosit yol izindeki muhtemel etkilerini aramak için yürütüldü. GM2 birikimi *Hexa*$^{-/-}$ ve *Neu4*$^{-/-}$*Hexa*$^{-/-}$ farelerinde olmasına ragmen, *Hexa*$^{-/-}$ *GM3S*$^{-/-}$*Neu4*$^{-/-}$ve *Hexa*$^{-/-}$*GM3S*$^{-/-}$ faresinin analizi göstermiştirki GM3 sentaz enzimininin yokluğunda GM2 birikimi yoktur. Bu sonuçlar bilinen gangliosit sentez yol iziyle tutarlıdır. *Hexa*$^{-/-}$*GM3S*$^{-/-}$*Neu4*$^{-/-}$ ve *Neu4*$^{-/-}$olmayan ikili varyantları *Neu3* ve *Neu2*'nin konsantrasyonunda değişimi açığa vurmuştur. Bu sonuçlar bakımından, diğer neuraminidaszlardaki değişim Neu4'un yokluğunu kompanse etmek içindir.

Anahtar Kelimeler : GM3 sentaz, GM2 gangliosit, Nöraminidaz, Sialidaz, Hekzosaminidaz, Fare.

TABLE OF CONTENTS

LIST OF FIGURES

Figure **Page**

LIST OF TABLES

CHAPTER 1

INTRODUCTION

1.1. Glycolipid

Glycolipids are defined as any compounds which have one or more monosaccharides bounded to a hydrophobic moiety by glyosidic linkage, but in IUPAC/IUBMB, it means acyl glycerols, ceramides and prenols (Brandenburg et al., 2015), (Malhotra, 2012). They are generally embedded in membrane and have role in receiving or delivering signals but some spread in cytosol (Brandenburg et al., 2015), (Malhotra, 2012). Glycolipids are synthesized from Golgi and transferred its final destination by small vesicles (Malhotra, 2012). Glycolipids are divided into two groups: Glycoglycerolipids (especially for plants) and Glycosphingolipids.

1.2. Sphingolipid

Amino alcohol derivatives which are called Sphingolipids play important role in signal transduction and (Borodzicz et.al., 2015). Sphingolipids which are synthesized from endoplasmic reticulum play a part as structural lipid (Iqbal et al., 2017). Ceramide which is crucial for various sphingolipid synthesis, when glycosylated, called glycosphingolipid, or it can take polar head group and is called sphingomyelin (Iqbal et al., 2017).

1.2.1. Glycosphingolipids

Glycosphingolipids which are composed of glycan conjugate and ceramide containing lipids are found abundantly in the outer leaflet of plasma membrane, especially brain and have functions as specific receptors such as certain pituitary hormones, growth factors, viruses and cell–cell interactions (Bhavanandan & Gowda, 2014). Glycosphingolipids (GSLs), which are amphipathic molecules in terms of carbohydrate hydrophilicity and lipid hydrophobicity, are generally needed glucosylceramide precursor for synthesis (Furukawa et al., 2014). GSLs divide into 4 group according to carbohydrate moiety; glio-, globo-, lacto/neolacto-, and asialo-series (Furukawa et al., 2014). Most of the ganglioside are obtained from lactosylceramide by adding galactose (Furukawa et al., 2014).

Table 1. 1: Schematic overview for structure of major glycolipids found in mammals (Source: Bhavanandan & Gowda, 2014).

Type	Structure
lacto	Galβ1-3G1cNAcβ1-3Galβ1-4Glcβ1-1-ceramide
lactoneo	Galβ1-4G1cNAcβ1-3Galβ1-4Glcβ1-1-ceramide
Globo	GaINAcβ1-3Galα1-4Galβ1 -4G1cβ1-1-ceramide
Globoneo	GaINAcβ1-3Galα1-3Ga1β1-4G1cβ1-1-ceramide
Isoglobo	GaINAcβ1-3Galα1-3Ga1β1-4G1cβ1-1-ceramide
Ganglio	Galβ1-3G1cNAcβ1-4Galβ1 -4G1cβ1-1-ceramide
Muco	Galβ1 -3Galβ1 -3Galβ1-4G1cβ1-1-ceramide
Galαcto	Galα1 -4Galβ1- 1 -ceramide
Sulfatides	3-*0*-Sulfo-Galβ1 -ceramide

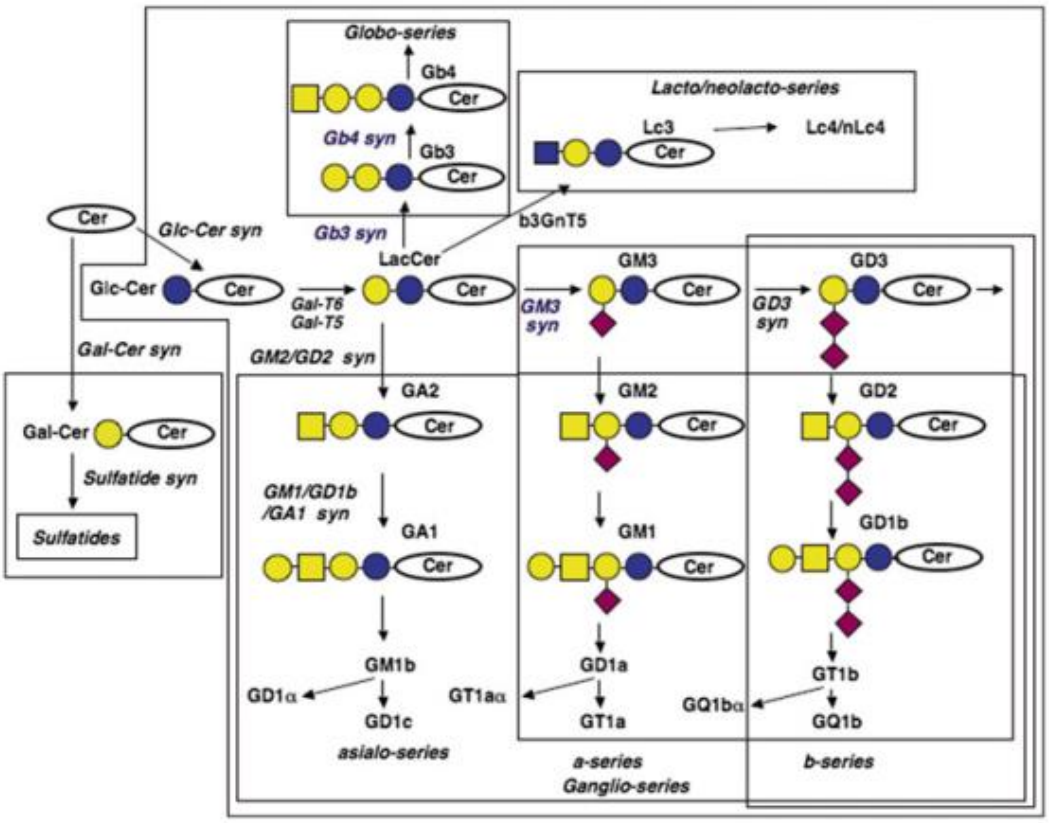

Figure 1.1: Schematic representation of glycosphingolipid synthesis Source: (Furukawa et al., 2014).

Glycosphingolipids are divided into 2 groups: neutral and acidic glycosphingolipids. Gangliosides are member of acidic GSLs due to containing sialic acid residue, but neutral GSLs are precursor for synthesis of gangliosides and have role in cytoprotection, myelinogenesis, cell adhesion, and recognition (Kojima et al., 2015).

1.2.1.1. Gangliosides

Gangliosides which are first isolated by Ernst Klenk in 1942 from human brain of Niemann-Pick patient and later Tay-Sachs patient (Yu, 1984). And ganglioside name come from mainly existence in ganglion cells (Degroote et al., 2017), (Svennerholm 1956), (Yu, 1984). Klenk and other scientist also found sialic acid in carbohydrate moiety (Yu, 1984). In 50's and 60's, Klenk and his coworker detect ,detailed structure of ganglioside (Yu, 1984). Kuhn and Wiegandt have discovered 4 gangliosides structure these are GI, GII' GIII and GIV and later it’s called GM1, GD1a, GD1b and GT1c (Yu,

1984). Nomenclature of Gangliosides, especially for brain are proposed by Lars Svennerholm (Svennerholm, 1956), (Kolter & Thomas, 2012)].

In general, gangliosides which are defined as GSL that has one or more sialic acid residue in carbohydrate moiety are found in outer leaflet of the plasma membrane and interact with cholesterol, transmembrane proteins and forming in lipid rafts (Degroote et al., 2017). Non-nervous tissues have ten-fold lower ganglioside according to brain ganglioside which composes one-twelfth plasma membrane glycerophospholipids in outer leaflet (Aureli et al., 2014). Gangliosides oligosaccharide chain is variable due to sugar structure and sequence (Sonnino et al., 2006). Neuronal gangliosides have large saccharide head group and acidic group, and it shows strong amphiphilicity (Aureli et al., 2014). In addition to neuronal ganglioside, stearic acid is the most common fatty acid and gives neuronal membrane plasticity (Aureli et al., 2014).

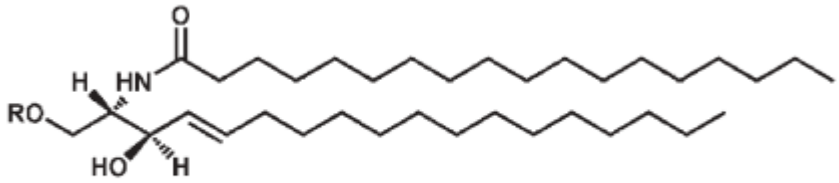

Figure 1.2**:** Structure of ganglioside with polysialyl chains Source: (Sonnino et al., 2006). By ketosidic and ester linkage, sialic acids are linked together.

Sialic acids are named due to neuraminic acid derivatives and healthy human have only 5. 5-N-acetyl-, and the 5-N-acetyl-9-O-acetyl-glycol among 3 main sialic acid derivatives (Sonnino et al., 2006). Human most common sialic acid is N-acetylneuraminic acid, but N-glycolylneuraminic also common in other species (Kolter & Thomas, 2012).

Table 1. 2**:** Main Gangliosides in mammalian with their structure (Source: Kolter & Thomas, 2012).

Type	**Structure**
Cer	Ceramide, N-Acylsphingosine
GA1	Galβ1,3GalNAcβ1,4Galβ1,4Glcβ1Cer(Gg4Cer)
GA2	GalNAcβ1,4Galβ1,4Glcβ1Cer (Gg3Cer)
GalCer	Galβ1Cer
GalNAc-GD1a	GalNAcβ1,4Galβ1,3GalNAcβ1,4(Neu5Acα2,3)Galβ1,4Glcβ1Cer (IV3Neu5AcII3Neu5AcGg5Cer)
GbOse3Cer	Galα1,4Galβ1,4Glcβ1Cer (Gb3Cer)
GbOse4Cer	GalNAcβ1,3Galα1,4Galβ1,4Glcβ1Cer(Gb4Cer)
GD1a	Neu5Acα2,3Galβ1,3GalNAcβ1,4(Neu5Acα2,3)Galβ1,4Glcβ1Cer (IV3Neu5AcII3Neu5AcGg4Cer)
GD1b	Galβ1,3GalNAcβ1,4(Neu5Acα2,8Neu5Acα2,3)Galβ1,4Glcβ1Cer (II3(Neu5Ac)2Gg4Cer)
GD1b-lactone	II3[Neu5Ac-(2−8,1−9)-Neu5Ac]Gg4Cer
GD1c	Neu5Acα2,8Neu5Acα2,3Galβ1,3GalNAcβ1,4Galβ1,4Glcβ1Cer (IV3(Neu5Ac)2Gg4Cer)
GD1α	Neu5Acα2,3Galβ1,3(Neu5Acα2,6)GalNAcβ1,4Galβ1,4Glcβ1Cer (IV3Neu5AcIII6Neu5AcGg4Cer)
GD2	GalNAcβ1,4(Neu5Acα2,8Neu5Acα2,3)Galβ1,4Glcβ1Cer (II3(Neu5Ac)2Gg3Cer)
GD3	Neu5Acα2,8Neu5Acα2,3Galβ1,4Glcβ1Cer (II3(Neu5Ac)2LacCer)
GlcCer	Glcβ1Cer
GM1a	Galβ1,3GalNAcβ1,4(Neu5Acα2,3)Galβ1,4Glcβ1Cer (II3Neu5AcGg4Cer)
GM1b	Neu5Acα2,3Galβ1,3GalNAcβ1,4Galβ1,4Glcβ1Cer (IV3Neu5AcGg4Cer)

(CONT ON NEXT PAGE)

Table 1.2: (cont).

GM2	GalNAcβ1,4(Neu5Acα2,3)Galβ1,4Glcβ1Cer (II3Neu5AcGg3Cer)
GM3	Neu5Acα2,3Galβ1,4Glcβ1Cer(II3Neu5AcLacCer)
GM4	Neu5Acα2-3Galβ1Cer(I3Neu5AcαGalCer)
GP1c	Neu5Acα2,8Neu5Acα2,3Galβ1,3GalNAcβ1,4 (Neu5Acα2,8Neu5Acα2,8Neu5Acα2,3)Galβ1,4Glcβ1Cer (IV3(Neu5Ac)2II3(Neu5Ac)3Gg4Cer)
GP1cα	Neu5Acα2,3Galβ1,3(Neu5Acα2,6)GalNAcβ1,4 (Neu5Acα2,8Neu5Acα2,8Neu5Acα2,3)Galβ1,4Glcβ1Cer (IV3Neu5AcIII6Neu5Ac,II3(Neu5Ac)3Gg4Cer)
GQ1b	Neu5Acα2,8Neu5Acα2,3Galβ1,3GalNAcβ1,4 (Neu5Acα2,8Neu5Acα2,3)Galβ1,4Glcβ1Cer (IV3(Neu5Ac)2II3(Neu5Ac)2Gg4Cer)
GQ1bα	Neu5Acα2,3Galβ1,3(Neu5Acα2,6)GalNAcβ1,4 (Neu5Acα2,8Neu5Acα2,3)Galβ1,4Glcβ1Cer (IV3(Neu5Ac)2III6(Neu5Ac)2Gg4Cer)
GQ1c	Neu5Acα2,3Galβ1,3GalNAcβ1,4 (Neu5Acα2,8Neu5Acα2,8Neu5Acα2,3)Galβ1,4Glcβ1Cer (IV3Neu5AcII3(Neu5Ac)3Gg4Cer)
GT1a	Neu5Acα2,8Neu5Acα2,3Galβ1,3GalNAcβ1,4 (Neu5Acα2,3)Galβ1,4Glcβ1Cer (V3(Neu5Ac)2II3Neu5AcGg4Cer)
GT1b	Neu5Acα2,3Galβ1,3GalNAcβ1,4 (Neu5Acα2,8Neu5Acα2,3)Galβ1,4Glcβ1Cer (IV3Neu5AcII3(Neu5Ac)2Gg4Cer)
GT1c	Galβ1,3GalNAcβ1,4 (Neu5Acα2,8Neu5Acα2,8Neu5Acα2,3)Galβ1,4Glcβ1Cer (II3(Neu5Ac)3Gg4Cer)

(CONT ON NEXT PAGE)

Table 1.2: (cont).

GT1α	Neu5Acα2,3Galβ1,3(Neu5Acα2,6)GalNAcβ1,4 (Neu5Acα2,3)Galβ1,4Glcβ1Cer (IV3Neu5AcIII6(Neu5Ac)2Gg4Cer)
GT2	GalNAcβ1,4 (Neu5Acα2,8Neu5Acα2,8Neu5Acα2,3)Galβ1,4Glcβ1Cer (II3(NeuAc)-Gg3Cer)
GT3	Neu5Acα2,8Neu5Acα2,8Neu5Acα2,3Galβ1,4Glcβ1Cer (II3(NeuAc)3LacCer)
LacCer	Galβ1,4Glcβ1Cer
Sulfatide	Sulfate3Galβ1Cer (I3-sulfate,GalCer)

1.2.1.1.1. Metabolism

Brain ganglioside and expression levels are conserved among mammals and GM1, GD1a, GD1b and GT1b consist of majority of total ganglioside within healthy brain (Schnaar, 2010). Expression level of gangliosides is controlled by developmentally and also change with differentiation state and type of cell (Yu et al., 2004). Gangliosides are synthesized in intracellular membrane and deliver the plasma membrane via exocytotic flow of membrane (Kolter et al., 2002). When lifetime of ganglioside is ended, membrane site goes endocytosis and degraded by lysosomal enzymes with the help of activator proteins (Kolter et al., 2002). Condensation of serine and palmityl-CoA causes 3-ketodihydrosphingosine and this ketone later converted into ceramide in the cytosolic face of endoplasmic reticulum in mammals (Funato & Riezman, 2001). Ceramide transferred with both CERT transfer protein and vesicular transport to the Golgi apparatus to start GSL synthesis (Levy & Futerman, 2010). Glucosyltransferase synthesize glucosyl ceramide within cytosolic site of Golgi, and then with addition of a galactose, lactosylceramide are synthesized in luminal site of Golgi (Allende & Proia, 2002).

Glycosylceramides are converted into lactosylceramides with lactosylceramidase family which are called β1,4-galactosyltransferase (β4GalT) and it has 7 members (Tokuda et al., 2013). Function of β4GalT is to transfer galactose from UDP-galactose to glycosylceramide (Chatterjee & Pandey, 2008). Addition one sialic acid to lactosylceramide results in GM3 by GM3 synthase enzyme, or it can be converted GA2 via UDP-GalNAc in other words beta-1,4-N-acetylgalactosaminyltransferase (Giraudo et al., 1999). GM3 ganglioside can be converted into GM2 by GalNAc which adds N-acetyl-galactoseamine (Giraudo et al., 1999), or GD3 by GD3 synthase ST8SIA1 (Bobowski et al., 2013) which binds a one more sialic acid. GD3 can be further synthesized into GD2 by GalNAc enzyme (Giraudo et al., 1999), or GT3 by adding one more sialic acid with ST-III or GT3 synthase enzyme (Nakayama et al., 1996). GT3 can also be synthesized into GT2 by GalNAc (Giraudo et al., 1999). GalNAc enzyme adds one N-acetyl-galactoseamine to its substrate (Giraudo et al., 1999). GA2, GM2, GD2, and GT2 can further changed into GA1, GM1a, GD1a and GT1c by adding one more N-acetyl-galactoseamine. Most of the ganglioside is depend on GM3 synthesis. However, GM4 do not need GM3 and it can be synthesized from ceramide (Kolter et al., 2002). B3GALT4 is homologue of rat GM1/GD1 synthase which binds N-acetylgalactosamine residue to GM2/GD2 ganglioside and involves in GM1/GD1b/GA1 synthesis (Shiina et al., 2000),(Amado et al., 1998),(Miyazaki et al., 1997).

For degradation of gangliosides, β-galactosidase or BGAL has role in hydrolysis of GM1 and GA1 into GM2 and GA2 respectively (Hahn et al., 1997),(Matsuda et al., 1997),(Pinsky et al., 1974),(Hauser et al., 2004). To degrade GM2 ganglioside into GM3, it is necessary to have both β-Hexaminidase, α and β (Cordeiro et al., 2000). β-Hexaminidase (HEX) have 2 variants: A and B (Cordeiro et al., 2000). Hexa deficiency causes Tay-Sachs disease via GM2 accumulation in human. Hexb deficiency causes GM2 and GA2 accumulation in both mice (Arthur et al., 2012) and human. Hexb also causes globotetraosylceramide accumulation in human non-nervous tissues (Okuda, 2017). Neuraminidase which cleaves α-ketosidic linkage between sialic acid and an adjacent sugar residue is exosialidase (Shtyrya et al., 2009). Neuraminidases also participate ganglioside degradation in ganglioside metabolism (Yang et al., 2015).

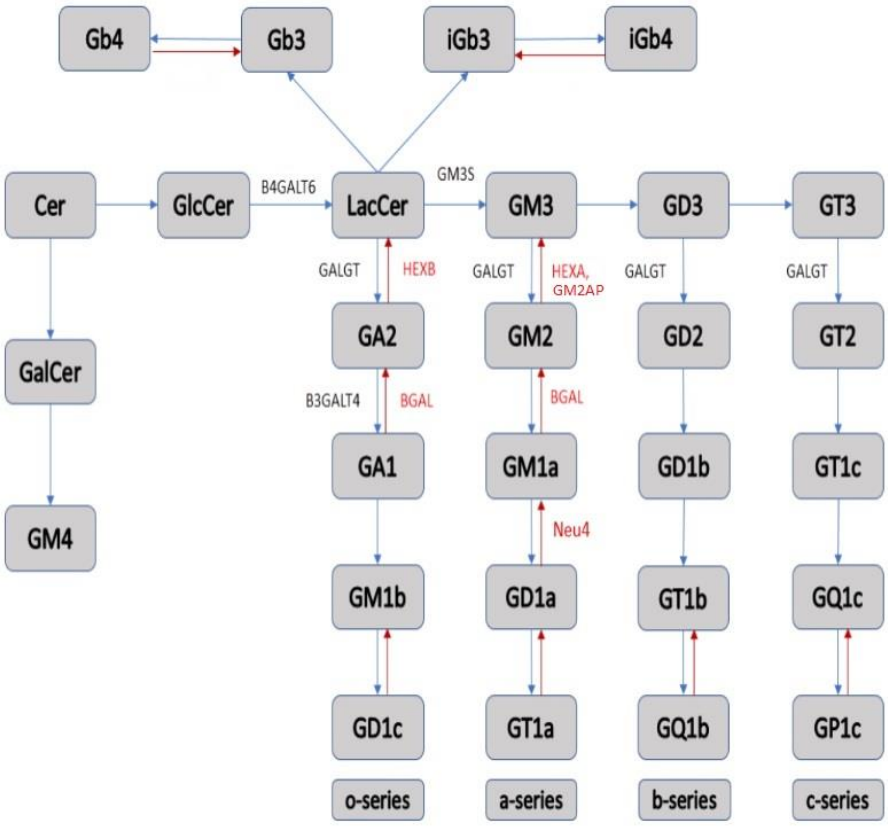

Figure 1.3:General view of ganglioside synthesis and degradation in mammals. Lactosylceramide (LacCer) is key precursor of ganglioside biosynthesis. Ceramide (Cer) can be converted into Galactosylceramide (GalCer). GM4 ganglioside can be converted from lactosylceramide (Kolter et al., 2002),(Gesellschaft et al., 1962) via galactosylceramide (GalCer) intermediate with GalT-III and ST-VI enzyme respectively (Krengel & Bousquet, 2014). β4GalT6 can synthesize glycosylceramide (GlcCer) into LacCer (Tokuda et al., 2013). GALGT defines GalNAc. BGAL or beta-galactosidase are thought to convert both GA1 and GM1a into GA2 and GM2 respectively. HEXA defines β-Hexaminidase A and HEXB defines β-Hexaminidase B which are variant of β-Hexaminidase. Gb4 is globotetraosylceramide and Gb4 is isoform of Gb4. GM1a defines GM1 but GM1b represents cis GM1. Most of the ganglioside is in ganlio series but there are also globo and isoglobo series gangliosides in mammals such as Gb3 and iGb3.

1.2.1.1.2. Function

Gangliosides are effective tissue and body fluids on nervous system, and other (Yu et al., 2011). Since it is found in plasma membrane, gangliosides take part in adhesion, signal-transduction and cell-cell interaction (Yu et al., 2011). Gangliosides

sometimes exist in nuclear envelope and are involve in Na^+ / Ca^{2+} exchange (Wu et al., 1995)(Ledeen & Wu, 2006). And they play in cytoprotective role in cell (Ledeen & Wu, 2006). In addition, gangliosides contribute formation of glycosynapses (Chaves & Sipione, 2010). Glycosynapses are necessary for cell-cell recognition adhesion and signaling (Chaves & Sipione, 2010). For example, laminin1-induced GM1 promotes neurite outgrowth (Ichikawa et al., 2009).

GM1, GD1a, GD1b, and GT1b are the most frequently synthesized gangliosides in central nervous system (Yu et al., 2012)(Kreutz et al., 2013). In Sandhoff disease patients, presence of GM2 and GA2 accumulation in CNS are known (Lecommandeur et al., 2017).

Ganglioside GM4 are identified as a minor ganglioside in the human brain (Li et al., 2002). Although GM4 myelin related function are reported in human (Ledeen et al., it can also be found in extra neural tissues (Li et. al., 1978) such as mouse erythrocytes (Seyfried et al., 1992), rat kidney (Tadano & Ishizuka, 1980) and chicken liver (Shiraishi & Uda, 1986)(Li et al., 2002).

GM3 is the main ganglioside in monocyte and lymphocyte (Kiguchi et al., 1990)(Prokazova, et al., 2009). GM3 and to lesser extent GM1 have role in cell proliferation via controlling EGF growth factor (Bremer et al., 1986). GM3 inhibits invasiveness of tumors by promoting the interaction of integrin with anti-metastatic membrane proteins and enhancing the cell adhesion in human with CD9 expression (Ono et al., 2001)(Kawakami et al., 2002)(Prokazova et al., 2009).

All membrane sialyl transferase indicates type 2 transmembrane glycoprotein compartment in trans-Golgi compartment(Harduin-Lepers et al, 2005). Although sialyl transferase sialylate a few of lipid substrate, GM3 synthase and GD3 synthase which belongs to ST3Gal subfamily of sialyl transferase are highly specific to its substrate (Prokazova et al., 2009).

Table 1.3 GM3 ganglioside contents in some human tissues. -, represents no data *, displays lipid-bound sialic acid (SA) concentration (nmol/g in wet tissue). **, lipid bound Sialic acid amount. (Source: Prokazova et al., 2009).

Tissue	Gangliosides	GM3, % of the total ganglioside content	Method of GM3 determination
Liver	214-220*	90-91.6	TLC, colorimetry
Kidneys	30-60*	74	The same
Spleen	200-300*	–	_"_
Placenta	100-200*	–	_"_
Muscles			TLC and immunostaining
skeletal muscles	50-80*	70	
heart	–	50	
Skin	30-35*	–	TLC, colorimetry
Skin fibroblasts	6 μg/10^6 cells	77	The same
Adipose tissue	10-15*	80-90	_"_
Aorta	46*	82	_"_
Blood serum	6 -8 nmol/ml**	57-67	_"_
Blood cells			TLC, colorimetry and HPLC
erythrocytes	1.3 μg/mg protein	14	
platelets	0.6 μg/mg protein	90	The same
lymphocytes	–	72	_"_
Thyroid gland	120*	48	_"_
Adrenal medulla	0.2 mg/g wet tissue	55.8	_"_
Milk	10 mg/liter**	27	TLC, colorimetry
Brain			The same
cortex	3000-3500*	–	
white matter	1000*	4.1	
gray matter	–	3.8	

Table 1.4: GM3 ganglioside and related biochemical and physiological effects (Source: Prokazova et al., 2009)

Object	Treatment	Biochemical effect	Physiological effect
Mouse adipocytes	tTNF-α	increase in GM3 content, decrease in insulin receptor expression	insulin resistance
	PPPP + TNF-α	decrease in GM3 expression, increase in insulin receptor expression	absence of insulin resistance
Adipose tissue of diabetic Zucker fa/fa rats and ob/ob mice		increase in GM3 synthase mRNA expression, increase in TNF α content	obesity, insulin resistance
Proliferating glomerular mesangial cells of diabetic rats	high level of glucose, PDMP, TGF-β1	decrease in GM3 content, decrease in Km of GM3 synthase	proliferation
	high level of glucose or TGF-β1 + exogenous GM3		decrease in proliferation
Object	Treatment	Biochemical effect	Physiological effect
Monocyte derived human dendritic cells	exogenous GM3 and GD3	suppression of CD1a, CD54, CD80, and CD40 expression	suppression of differentiation to dendritic cells, decrease in survival, and induction of
Nerve cells precursors	intraventricular administration of GM3		decrease in proliferation, induction of apoptosis
Cell line HT22 of mouse hippocampus	exogenous glutamate	increase in GM3 content	induction of apoptosis
	exogenous GM3	the same	the same
	transfection of cells with GM3 synthase cDNA	overexpression of GM3 synthase	–"–
Zebra fish embryo	microinjection of GM3 synthase mRNA	overexpression of GM3 synthase, inhibition of production of reactive oxygen species and of entrance of extracellular	apoptosis of nerve cells
	RNA interference	calcium into cells decrease in GM3 synthase expression	prevention of glutamate induced apoptosis of nerve cells
GM3 deficient lines of tumor cells (3LL Lewis lung carcinoma cell line)	transfection of cells with GM3 synthase cDNA ("GM3 reconstruction" of cells)	synthesis of GM3, suppression of activities of caspase 3 and caspase 9, increase in content of Bcl 2	prevention of apoptotic effect of chemotherapeutic agents

GM3S deficient mice represented enhanced insulin receptor phosphorylation in response to increase insulin sensitivity (Yamashita et al., 2003). In addition, *GM3S*$^{-/-}$ mice also illustrated severe instability induced osteoarthritis by regulating the expression of MMP-13 and ADAMTS-5 and chondrocyte apoptosis (Sasazawa et al., 2014). GM3 and GT1b have role in postnatal development and maturation of normal ear (Yoshikawa et al., 2009). Thus, GM3 synthase deficient mice displayed hearing loss due to organ of corti (Yoshikawa et al., 2009). GD3S and GALGT disrupted mice represented sudden death due to sound induced seizures (Kawai et al., 2001).

1.3. Sialidases

Sialic acids exist at the terminal positions of glycoproteins, glycolipids and gangliosides (Katoh et al., 2010) Sialidases (Neuraminidases) are the member of exoglycosidases which hydrolysis α-glycosidic linkage from terminal sialic acidic residues of gangliosides and other biomolecules (Katoh et al., 2010) (Rothe et al., 1991). Neuraminidases are investigated into 4 groups; Neu1, Neu2, Neu3 and Neu4. And their concentrations change with their location.

Among these neuraminidases, Neu1 is the most highly expressed and widely distributed sialidases (Bonten & D'Azzo, 2000)(d'Azzo & Bonten, 2010). Cathepsin A have role in protection of Neu1 and β-galactosidase (β-Gal) glycosidases against proteolytic degradation by the composition of the lysosomal multienzyme complex and activates Neu1 (Bonten et al., 2014) (Calhan & Seyrantepe, 2017). Katoh reported that Neu1 have role in asthma (Katoh et al., 2010) Cathepsin A deficiency results in galactosialidosis by secondary defect in Neu1 and Beta-galactosidase (Oheda et al., 2006). And sialidosis which is an autosomal recessive lysosomal storage disease are caused due to Neu1 deficiency (d'Azzo et al., 2015). Neu1 also participate in skeletal muscle regeneration and sialidosis patient also have progressive loss of macular degeneration (cherry-red-spot) (Neves et al., 2015).

Neuraminidase 2 gene encodes functional sialidases with cytosolic localization (Monti et al., 1999). According to Chavas et al, viral sialidases inhibitors, zanamivir and peramivir but not oseltamivir, interacts with cytosolic human sialidases (Chavas et al., 2010) (Rahman et al., 2013). However, it has been reported that human sialidase

related disorders are caused due to interaction of active form of oseltamivir and Human cytosolic Neu2 (Li et al., 2007) (Rahman et al., 2013). NEU2 takes part in muscle cell and neuronal differentiation, and the rat NEU2 is highly expressed in rat skeletal muscle (Monti & Miyagi, 2015). Fanzani et al implicated that with rat Neu2 have a role in myoblast cell differentiation in C2c12 cells (Fanzani et al., 2003).

Neuraminidase 3 was first cloned Miyagi et. al. from bovine brain in 1999 (Miyagi et al., 1999) (Monti et al., 2010). Mammalian Neu3 participate in signaling of cell differentiation cell growth, apoptosis (Miyagi et al., 2008) Neu3 are also upregulated in various cancer (Miyagi et al., 2008) such as human prostate cancer by modulation apoptosis related molecules expression (Kawamura et al., 2012). Neu3 also effects in androgen signaling via PI3K and MAP kinase(Kawamura et al., 2012).

Neuraminidase 4 is located in the lysosomal and mitochondrial lumen with wide range of substrate specificity (Seyrantepe et al., 2008). *Neu4*$^{-/-}$ mice showed vacuolization and lysosomal storage in lung and spleen cell, but live like almost normal (Seyrantepe et al., 2008). In addition *Neu4*$^{-/-}$ mice also represented increase of GD1a and decrease of GM1 which is important for GM1 ganliosidosis (Seyrantepe et al., 2008). Another function of Neu4 on ganglioside are founded in by-pass mechanism in *Hexa*$^{-/-}$ mice (Seyrantepe et al., 2010). *Neu4*$^{-/-}$*Hexa*$^{-/-}$ mice are represented neuraminidases in by-mechanism can be Neu4 (Seyrantepe et al., 2010).

Table 1.5: Comparison of mammalian sialidases. a indicates two different results for Human Neu4 (Source: Monti & Miyagi, 2015).

	NEU1	NEU2	NEU3	NEU4
Major subcellular localization	Lysosomes	Cytosol	Plasma membrane	Lysosomes[a] mitochondria[a] and ER
Good substrates	Oligosaccharides Glycopeptides	Oligosaccharides Glycoproteins Gangliosides	Gangliosides	Oligosaccharides Glycoproteins
Optimal pH (in vitro)	4.4–4.6	5.6–6.5	4.6–4.8	3.2–4.5
Total amino acids				
Human	415	380	428	496,484
Mouse	409	379	418	497,413
Chromosomal location				
Human	6p21.3	2q37	11q13.5	2q37.3
Mouse	17	1	7	10

mRNA of Neu1 and Neu3 are highly expressed in mouse spleen, but Neu2 expression level was low (Wang et al., 2004)(Katoh et al., 2010). And Neu4 expression did not detected in mouse spleen (Comelli et. al., 2003) (Katoh et al., 2010). By using a homology based approach NEU1, NEU3, and NEU4 can be determined because Neu2 atomic coordinates availability (Monti & Miyagi, 2015).

1.4. Lysosomal Storage Disorders

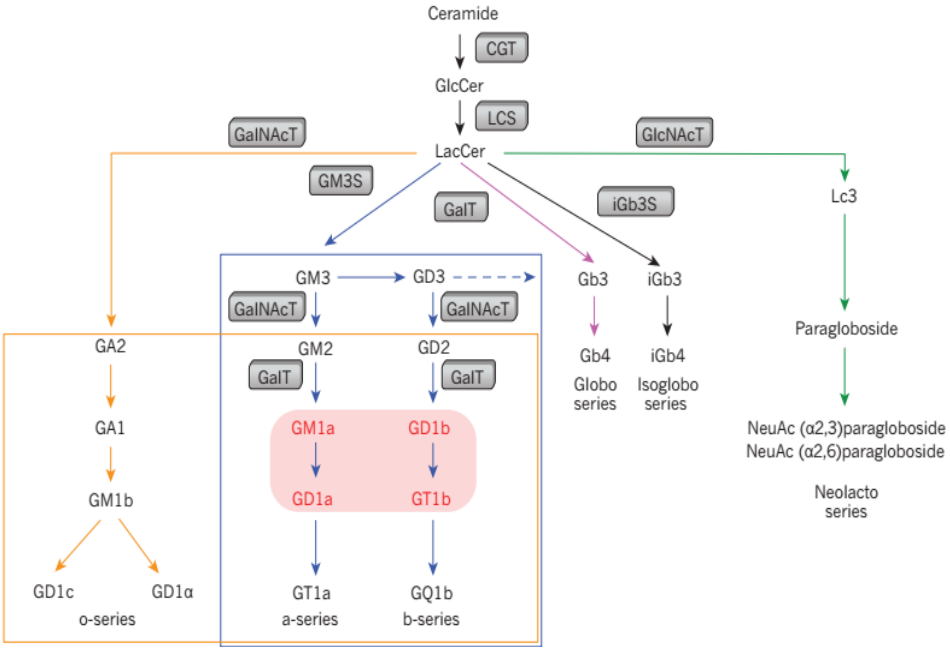

Figure 1.4: Schematic illustration of GM3 synthase (blue line)and GM2 synthase deficiency (orange line) Source: (Aronovich & Hackett, 2015).

Lysosomal storage disease (LSD) are generally defined as recessive genetic disorders which results in accumulation, or storage of macromolecules in lysosome due to mutation or other reasons and most of LSD are generally related with nervous system as well as other tissues and organs of body (Aronovich & Hackett, 2015). Genetic defectiveness, deficiency which results in lysosomal enzyme deficiency and then preventing degradation of lipids such as gangliosides and glycosphingolipids, changes cell morphology, impaired autophagy, oxidative stress and neuroinflammation, (Aronovich & Hackett, 2015) (Walkley, 2009). Some of the LSD disorders are Gaucher disease (Huang, et. al., 2015), mucopolysaccharidoses (Pastores & Maegawa, 2013),

Fabry disease (Mehta et. al., 2006) GM3 synthase and GM2 synthase deficiency (Aronovich & Hackett, 2015).

Table 1.6: Major lysosomal storage disorders with their genes and accumulating substances (Source: Aronovich & Hackett, 2015).

Metabolic defect	Disease	Biochemical defect	*Gene involved*	Protein defect	Major symptoms	CNS pathology
Biosynthetic	GM3 synthase deficiency	Loss of GM3 and downstream gangliosides	*ST3GAL5*	GM3S	Infantile onset epilepsy with developmental arrest and blindness	Yes
Biosynthetic	GM2 synthase deficiency	Loss of GM2 and downstream gangliosides	*B4GALNT 1*	GM2S	Spastic paraplegia	Yes
Catabolic (LSD)	Gaucher types 1, 2 and 3	GlcCer storage	*GBA*	Glucocerebrosidase	Hepatosplenomegaly, haematological defects, inflammation, bone disease and CNS disease in types 2 and 3	In types 2 and 3
Catabolic (LSD)	Fabry	Gb3 storage	*GLA*	α-galactosidase	Renal, cardiovascular and peripheral pain	Yes (some mild cases of cerebrovasculopathy)
Catabolic (LSD)	Tay–Sachs	GM2 ganglioside storage	*HEXA*	B-hexosaminidase α subunit	Progressive neurodegeneration	Yes
Catabolic (LSD)	Sandhoff	GM2 ganglioside storage	*HEXB*	B-hexosaminidase β subunit	Progressive neurodegeneration	Yes
Catabolic (LSD)	GM1 gangliosidosis	GM1 ganglioside storage	*GLB1*	β-galactosidase	Progressive neurodegeneration	Yes
Defect in trafficking or fusion	Niemann–Pick type C	Storage of all GSLs, cholesterol, sphingomyelin and sphingosine	*NPC1* *NPC2*	NPC1 NPC2	Progressive neurodegeneration	Yes

1.5. Tay-Sachs Disease

Tay-Sachs disease which is a neurodegenerative lysosomal sphingolipid disorder are caused by β Hexaminidase A deficiency which causes GM2 accumulation

in lysosome (Filho & Saphiro, 2004). β Hexaminidase A consists of two subunits; α and β polypeptide (Myerowitz, 1997) (Lawson & Martin, 2016)s. These subunits can hydrolyze β-N-acetylglucosamine β -Nacetylgalactosamine and the corresponding 6-sulfated β-N-acetylglucosaminides (Myerowitz, 1997). Mutation in α-chain can only disrupt catalytic activity β Hexaminidase A (Hexa) and HexS which composed of 2 α subunit because β Hexaminidase B (Hexb) has 2 β-subunit instead of α and β subunit (Myerowitz, 1997) (Lawson & Martin, 2016). Mutation in β-subunit results in deficiency in both Hexa and Hexb genes and it's called Sandhoff disease (Lawson & Martin, 2016).

Tay-Sachs disease progressive disorder are beginning at the age of 3-and 6 month range and death starts before age 4 years in infantile onset variant until adult onset variant. (Zeng et al., 2008). However, Hexa gene knockout animals do not represents such early death and severe degeneration as in Human until 1 year of age (Seyrantepe et al., 2010).

In *Hexa*$^{-/-}$*Neu4*$^{-/-}$ more severe neurological impairment are observed according to *Hexa*$^{-/-}$ mice(Seyrantepe et al., 2010). And double knockout mice also represented more GM2 accumulation in the electronmicrograph (Seyrantepe et al., 2010).

1.6. GM3 Synthase Deficiency

GM3 synthase deficiency occurs due to mutation of ST3GAL5 which converts lactosylceramide into GM3 ganglioside (Fragaki et al., 2013). In addition, GM3 synthase deficient mice are represented to live longer than 1 year (Yamashita et al., 2003). GM3S enzyme contains a transmembrane domain and two sialyl motifs; short and long (Simpson et al., 2004). Deficient GM3S enzyme probably does not contain short sialyl motifs which prevent the transportation of sialyltransferase from endoplasmic reticulum to Golgi and inhibits enzymatic activity of GM3S (Simpson et al., 2004). Lacking GM3S enzyme which causes early-onset symptomatic epilepsy in human are responsible for accumulation of Gb3 and Gb4 globosides in human syndrome and may effective on respiratory chain dysfunction (Fragaki et al., 2013). In addition, mitochondrial membrane potential loss results in apoptosis in *GM3* synthase deficiency (Fragaki et al., 2013). GM3S deficient children are born normal time and

starting age of symptoms change between 2 weeks and 3 months (Simpson et al., 2004). In first year of life, seizure activity are observed and GM3S deficient children are unable to sit unsupported, reach or walk and are nonverbal (Simpson et al., 2004).

1.7. Aim of the Study

Hexa and Neu4 gene double deficient mice represented more severe condition to the Tay-sachs disease. *Hexa*$^{-/-}$*Neu4*$^{-/-}$ mice represented GM2 accumulation with more severe contdition. And *GM3S*$^{-/-}$ mice illustrated no severe symptoms in early age and do not have GM3 related ganglioside. *Hexa*$^{-/-}$*Neu4*$^{-/-}$ mice and *GM3S*$^{-/-}$ mice are combined to decrease GM2 accumulation.

CHAPTER 2

MATERIALS AND METHODS

2.1. Animals and Genotyping

Double knockout *Neu4*$^{-/-}$*Hexa*$^{-/-}$ deficient mice were generated by Volkan Seyrantepe and *GM3S*$^{-/-}$ gene knockout mice were donated by Roger Sandhoff from Technical University of Applied Sciences in Mannheim, Germany. And double knockout *Neu4*$^{-/-}$*Hexa*$^{-/-}$ mice were crossed with *GM3S*$^{-/-}$ knockout mice. These knockout mice have neomycin cassettes compared to wild type. All mice strains have C57BL/6. Mice were produced to use in RTPCR, TLC and IHC analysis with 8 different genotypes which are shown with bold character in table 2.1.

Table 2.1: Crossing of mice

Breeding pairs	**Expected genotypes in F1 generation**
♀ *Hexa* ($^{-/-}$) *GM3S* (+/+) *Neu4* ($^{-/-}$)	
♂ *Hexa* (+/+) *GM3S* ($^{-/-}$) *Neu4* (+/+)	*Hexa* (+/-) *GM3S* (+/-) *Neu4* (+/-)
Breeding pairs	**Expected genotypes in F2 generation**
♀ *Hexa* (+/-) *GM3S* (+/-) *Neu4* (+/-)	***Hexa* (+/+) *GM3S* (+/+) *Neu4* (+/+)**
♂ *Hexa* (+/-) *GM3S* (+/-) *Neu4* (+/-)	*Hexa* (+/+) *GM3S* (+/-) *Neu4* (+/+)
	Hexa (+/-) *GM3S* (+/+) *Neu4* (+/+)
	Hexa (+/+) *GM3S* (+/+) *Neu4* (+/+)
	Hexa (+/-) *GM3S* (+/-) *Neu4* (+/+)
	Hexa (+/-) *GM3S* (+/+) *Neu4* (+/-)
	Hexa (+/+) *GM3S* (+/-) *Neu4* (+/-)
	Hexa (+/-) *GM3S* (+/-) *Neu4* (+/-)

(CONT ON NEXT PAGE)

Table 2.1: (cont).

	Hexa (+/-) *GM3S* (+/-) *Neu4* (+/-)
	Hexa (+/-) *GM3S* ($^{-/-}$) *Neu4* (+/-)
	Hexa ($^{-/-}$) *GM3S* (+/-) *Neu4* (+/-)
	Hexa (+/-) GM3S (+/-) Neu4 (+/-)
	Hexa (-/-) GM3S (-/-) Neu4 (+/-)
	Hexa (+/-) GM3S (-/-) Neu4 (-/-)
	Hexa (+/-) GM3S (+/+) Neu4 (+/-)
	Hexa (+/+) GM3S (+/-) Neu4 (+/-)
	Hexa (+/-) GM3S (+/-) Neu4 (+/+)
	Hexa (+/+) GM3S (+/+) Neu4 (+/-)
	Hexa (+/+) GM3S (+/-) Neu4 (+/+)
	Hexa (+/-) GM3S (+/+) Neu4 (+/+)
	Hexa (+/+) GM3S (-/-) Neu4 (+/+)
	Hexa (-/-) GM3S (+/+) Neu4 (+/+)
	Hexa (+/+) GM3S (+/+) Neu4 (-/-)
	Hexa (-/-) GM3S (-/-) Neu4 (+/+)
	Hexa (-/-) GM3S (+/+) Neu4 (-/-)
	Hexa (+/+) GM3S (-/-) Neu4 (-/-)
	Hexa (-/-) GM3S (-/-) Neu4 (-/-)

For Hexa gene PCR primers were 5'-GGCCAGATACAATCATACAG (*Hexa*-F) 5'-CTGTCCACATACTCTCCCCACAT (*Hexa*-R),5'-CACCAAGAAGGGAGCCGGT (PGK). For *Neu4* gene PCR primers were 5'-CTCTTCTTCATTGCCGTGCT (Neu4F), 5'- GCCGAATATCATGGTGGAAA (Neu4R), 5'-GACAAGGAGAGCCTCTGGTG (Neo). GM3S gene PCR primers were 5'-GAGCCTGTGCCACACATCT (D3), 5'-TCGCCTTCTTGACGAGTTCTGAG (D4) for knockout allele and 5'-AGCTCAGAGCTATGCTCAGGA (D1) and 5'TCACACATCGAACTGGTTGAG (D2) for wild type allele.

Mice genomic DNA was isolated from mice's tail with proteinase K isolation protocol. Tail samples were taken into eppendorf tubes and 500 µl tissue lysis buffer and 12 µl proteinase K were added into same tube. Tissue lysis buffer content was Tris with 10% 1M pH 7.6, 20 % SDS, NaCl concertation with 4% 5M, and 2.5% 0.2 EDTA. Proteinase K was used 25mg/ml solution as in previous study (Seyrantepe et al, 2010).

Tubes were put into incubator shaker at 55ºC and 70 rpm overnight. After this, tubes were centrifuged at 10 min 13000 rpm. 500 µl liquid supernatant were taken into new tube and 500 µl isopropanol were added to for each tube and gently shake to see DNA. And then DNAs of each were placed into new tubes which contain 500 µl 70% ethanol and centrifuged at 15000 rpm 1min. After then, ethanol was removed from DNA by pouring and evaporating. 200 µl pure water were added to each sample and incubated at 55ºC hour and stored at -20ºC.

In Neu4 and Hexa PCR, for 100 ng DNA, 2.5µl from 10X reaction buffer minus $MgCl_2$, 3 mM $MgCl_2$, 4% DMSO, 0.4 µM forward and PGK primer and 0.8 µM reverse primer were added into Eppendorf. After that, 300ng DNA, and 1.75-unit Taq DNA polymerase (Invitrogen) was added into tube. And final volume was adjusted to the 25 µl total volume with water. Conditions for PCR were; 1 cycle 3 minutes at 95℃; 30 cycles 45 seconds at 95℃, 45 seconds at 60℃, 45 seconds at 72℃; and 1 cycle 5 minutes at 72℃.

In GM3S knockout PCR, 1x reaction buffer without $MgCl_2$, 3 mM $MgCl_2$, 2% DMSO, 0.4 mM dNTP, 0.2 µM forward primer, 0.2 µM reverse primer, 600 ng DNA, and 4-unit Taq DNA polymerase (Invitrogen) were added into tube. And final volume was adjusted to the 50 µl total volume with water. Conditions for PCR were 5 minutes at 95ºC; 35 cycles 45 seconds at 95ºC, 35seconds at 60ºC, 1.2 minutes; 5 minutes at 72.

In GM3S wild type PCR, 1x reaction buffer minus $MgCl_2$, 4 mM $MgCl_2$, 0.8 mM dNTP, 0.4 µM forward primer, 0.4 µM reverse primer, 300 ng DNA, 2.5-unit Taq DNA polymerase (Invitrogen) were placed into tubes. And final volume was adjusted to the 25 µl total volume with water. Conditions for PCR were 5 minutes at 95ºC; 30 cycles 30 seconds at 95ºC, 45seconds at 56ºC, 1 minutes; 5 minutes at 72ºC.

2.2. Obtaining Brain Samples

3-and 6-month mice were sacrificed by cervical dislocation, brains were extracted and divided into 2 hemisphere which were right and left. And those separated brain and liver, spleen, lung, heart, kidney and testis for male were rapidly frozen in dry

ice or liquid nitrogen to decrease temperature quickly and stored -80ºC. These visceral organs except brains were washed with 0.9% saline solution before freezing.

2.3. RNA Isolation

500µl Genezol reagent (Geneaid) was added for 50 mg brain samples and homogenized with Teflon homogenized (Retsch MM100). 3-and 6-month mice with 2 replicas are used (n=2). Incubated at room temperature for 10 min and centrifuged at 16000g for 10 min. Supernatants were taken into new tubes. 100 µl chloroform were added and tubes shake vigorously for 10 sec. Tubes were then centrifuged 16000g for 15 min at 4ºC. And colorless upper phase was RNA and they were transferred into new tube. 300 µl isopropanol was added into tubes and samples were incubated at room temperature for 10 min and again tubes were then centrifuged 16000g for 10 min at 4ºC and supernatants were removed. And then, 1 ml 70% ethanol was added and vortex was made to the tubes. After this, tubes centrifuged at 16000g for 5 min at 4 ºC and supernatants were removed. Thereafter, tubes were incubated at room temperature for air-dry pellet. Later, 20-50µl RNAse free water was added to dried RNA pellet. Afterwards, to dissolve, tubes were incubated 15 min at 55ºC. Finally, RNAs were now isolated and stored at -80ºC.

2.4. cDNA Conversion

Isolated RNA concentration was measured by Nanodrop spectrophotometer (ND-1000). 4µg RNA and 4µl buffer from, 4mM dNTP mix, 4µl RT random primer from 10x primer, 50-unit MultiScribe reverse transcriptase were added to tubes. Final concentration of tubes was adjusted to the 20µl with water. For materials, high capacity cDNA reverse transcription kit from Applied Biosystems were used to cDNA conversion. Reaction conditions, first cycle is 10 min 25 ºC, 120 min at 37ºC for one cycle and 5 min at 85ºC for one cycle.

cDNAs control PCR was made with GAPDH gene. 75 ng cDNA 0.8 mM forward and reverse primer, 10 mM dNTP, 1x reaction buffer contains $MgCl_2$, 1.75-unit

Taq DNA polymerase AmpONE (GeneAll) were added to tube and water adjust to final volume 25µl. In PCR conditions, first stage was 2 minutes at 95ºC for 1 cycle. And second stage, 20 second at 95 ºC,15 second at 65ºC and 22 second at 72ºC were made for 30 cycles. Final stage was made at 1 cycle 3 min at 72ºC.

2.5. Real Time PCR

Animals RNA from 3 months and 6-months-old 8 different genotypes are examined with 13 different genes; these are Neuraminidase 1(Neu1), Neuraminidase 2 (Neu2), Neuraminidase 3 (Neu3), Neuraminidase 4(Neu4), Hexaminidase B (Hexb), GM2 activator protein (GM2AP), GM3 synthase, GD3 synthase, N-actylgalactosaminyltransferase 1 (GALGT1), Beta-galactosidase (BGAL), Galactosyl transferase (B3GALT4), Lactosylceramide synthase (B4GALT6), and Glyceraldehyde-3-Phospate Dehydrogenase (GAPDH) for internal control. Primers for these genes are given in Tables 2.2 1x Roche LightCycler 480 SYBR Green I Master Mix and 0.4 µM forward and reverse primer and 75 ng cDNA were adjusted 20 µl reaction volume with water. In Roche LightCycler 96 system, PCR conditions were 10 min 95ºC for 1 cycle and 20 secs at 95 ºC, 15 secs at 61 ºC, and 22 secs at 72 ºC were made for 45 cycles for reading. To detect primer dimer after this stage, 30 secs at 95ºC, 10 secs at 60ºC for 1 cycle are red and nonstop reading were made until temperature reaches at 99 ºC.

Table 2.2**:** Genes with primers sequences are for Real-Time PCR

GENE	PRIMER	PRIMER SEQUENCE	AMPLIFIED GENE LENGHT
Neu1	Forward	TCATCGCCATGAGGAGGTCCA	431bp
	Reverse	AAAGGGAATGCCGCTCACTCCA	
Neu2	Forward	CGCAGAGTTGATTGTCCTGA	429bp
	Reverse	TTCTGAGCAGGGTGCAGTTTCC	
Neu3	Forward	CTCAGTCAGAGATGAGGATGCT	416bp

(CONT ON NEXT PAGE)

Table 2.2: (cont).

GENE	PRIMER	PRIMER SEQUENCE	AMPLIFIED GENE LENGHT
Neu4	Forward	AGGAGAACGGTGCTCTTCCAGA	339bp
	Reverse	GTTCTTGCCAGTGGCGATTTGC	
Hexb	Forward	AGTGCGAGTCCTTCCCTAGT	412bp
	Reverse	ATCCGGACATCGTTTGGTGT	
GM2AP	Forward	GCTGGCTTCTGGGTCAAGAT	193bp
	Reverse	GCACTGTGAAGTTGCTCGTG	
GM3S	Forward	AATGATGCTGTGGACCCTG	133bp
	Reverse	GTTGATGCTGTACCTGTCCTC	
GD3S	Forward	CGATAATTCCACGTACTCCCTC	193bp
	Reverse	TTTGGAACCGACATCTCTGG	
GALGT1	Forward	TCAGGATCAAGGAGCAAGTG	124bp
	Reverse	AAGGCTTTAGTGAGGTCAACC	
BGAL	Forward	TTTCTGGGGACCGTGATGTG	432bp
	Reverse	AATCCACTGTGGCGTACAGG	
B3GALT4	Forward	GGCAGTGCCCCTTCTGTATT	407bp
	Reverse	GTGCAGTCCTCTCCCCATTC	
B4GALT6	Forward	CACCTGATTCCGATGCTCCA	410bp
	Reverse	CCTTCTGGCCGGGTTACATT	
GAPDH	Forward	CCCCTTCATTGACCTCAACTAC	347bp

2.6. Lipid Isolation

25 mg tissue samples were taken from brains, that already extracted by cervical dislocation (described above) and contains hippocampus and hypothalamus and cortex region. Tissues were diluted with 1.5 ml water and homogenized at 1 min and sonicated at 1.5 min. Sonicated tissues were lyophilized with nitrogen gas at 55 ºC to evaporate supernatant. Next, 3 ml acetone was added to tubes which contain pellet and tubes were vortex and centrifuged at 2000 rpm 5 min. This step was repeated one more time and each time supernatant are removed from tubes. After this, 1.5 ml (chloroform: 10/ methanol :10/ water: 1 ratio) extraction solution were poured onto pellet and vortex and centrifuged at 2000 rpm 5 min. This step was repeated one more time and supernatant was collected 2 ml (chloroform: 60/ methanol :30/ water: 8 ratio) solution were added

to tubes and vortex and centrifuged at 2000 rpm for 5 min. This step was repeated one more time. In 10:10:1 and 60:30:8 ratio solution step, supernatant was collected same tube.

Tubes contained total gangliosides. DEAE sephadex A25- columns were prepared to separate neutral and acidic gangliosides from total gangliosides. Columns were prepared with glass wool to prevent from falling of resin and DEAE sephadex A25 resin for separation. For DEAE sephadex A25 resin preparation (GE health care), 1.0 gr DEAE sephadex A25 resin were added 10 ml (chloroform: 30/ methanol: 60/ 0.8 mM sodium acetate: 8) solution. Resin with solution were shake and waited 5 min at room temperature. After 5 min, solution was vortex and centrifuged at 2000 rpm 1 min and supernatant colorless part were removed from. And this process was repeated 2 more times and solution with (30:60:8) solution were incubated overnight. After this, this process (5 min waiting at room temperature with resin and 30:60:8 solution) were repeated 3 times. Glass wool, which preventing resin falling, were filled at the end of Pasteur pipettes, so acidic ganglioside can bind resin and neutral gangliosides comes first. After A25 column preparation, 10:10:1 extraction solution was used to wash column. And total ganglioside was loaded to DEAE sephadex A25 column and flow through contains contain neutral gangliosides.

Neutral gangliosides were lyophilized at 55 ºC with N_2 gas and tubes had pellet and stored at +4ºC. For acidic ones, columns were washed with 4 ml 500 mM potassium acetate in methanol solution. This solution binds ganglioside and release acidic gangliosides from resin and tubes below DEAE sephadex A25 column contain now acidic gangliosides.

To separate acidic gangliosides from potassium acetate salt, Supelclean Lc-18 (Supelco) column were used. These columns were washed with 2ml methanol Chromabond Vacuum manifold with 10.132 501 Bar to vacuum. And then, they were washed with 2 ml 500 mM potassium acetate and collected acidic gangliosides from DEAE sephadex A25 column were loaded to SupelClean Lc-18 column. And then, 10 ml dH_2O were added. 4ml Methanol and 4 ml Methanol in chloroform (1:1 ratio) solution were poured to the SupelClean column for elution samples. And Those samples were lyophilized at 55 ºC with N_2 gas tubes and tubes have pellet and stored at +4ºC.

2.7. Thin Layer Chromatography and Orcinol Staining

Chambers (Camag) were incubated for 2-hour 15 min with the solution chloroform: 60 ml/ methanol :35 ml / $CaCl_{2:}$ 8 ml for two TLC chambers. 3-and 6-month mice with 2 replicas are used (n=2). Half of the solution was used for one tank. Samples were loaded to TLC plates which were incubated at 100ºC 1 hour in oven to be sure about plates were dried. Samples were loaded with chloroform: 10/ methanol:10/ water: 1 ratio solution by using Linomat V automated machine to the silica plate (Merck). sample were diluted 100 µl (10:10:1) were 30 µl. After incubation finished, plates were placed into tanks and wait approximately 1 hours to move 12 cm and 2 cm for starting space.

For visualization loaded sample movement in plates,15 ml orcinol solution were prepared in proportion to 0.06 gr orcinol, 3.75 ml sulfuric acid and 11.25 ml dH_2O within the spray. And sprayed into plates and waited 120 ºC till bands were shown.

2.8. Immunohistochemistry

6-month mice with 2 replicas are used (n=2). Brains were perfused with 4% PFA in PBS (in proportion to 0.499 mg sodium phosphate monobasic dihydrate and 2.99 sodium phosphate dibasic dihydrate within 100ml distilled water) from cardiac to whole body and embedded in optimum cutting temperature (O.C.T.) for cryosectioning and stored -80 ºC. And Brains were cut in cryostat (Leica CM1850UV) at -20 ºC and taken into slides and stored at -80 ºC.

2.9. Antibody Staining with GM2

Slides were chosen according to their hippocampal region and kept for 30 min on ice to prevent temperature shock when they were taken from -80 ºC. 10 min 1xPBS wash were made to slides. At the same time, acetone was placed to -20 to increase its effectiveness and applied 15 min to slides. After acetone, slides were washed 2 times 5

min with PBS. After this, blocking buffer which contains 160mg bovine serum albumin, 3600 µl PBS, 400 µl serum, and 0.092mg glycine were applied to each sample for 1 hour. And then, primary GM2 (KM966 Hakko-Kırın JAPAN) antibody were diluted with blocking buffer at the rate of 1:500 and distributed at the same concentration and incubated at +4 ºC overnight. After this, three times 5 min PBS wash were made, and secondary goat anti-human antibody (DyLight488 ThermoScientific) were diluted in blocking buffer at the ratio of 1:500 for 1 hour within dark place at room temperature. And then, 4 times 5min PBS wash were made. After this DAPI mounting medium which also contains DAPI (ABCAM, ab104139) were applied to show nucleus in related brain sides.

2.10. Statistical Analysis

Two-way ANOVA was used for RT PCR and TLC results. And if P value was below 0.05, it was accepted significant. For immunohistochemistry, sample t-test was used.

CHAPTER 3

RESULTS

3.1. Genotyping

To determine genotypes of mice, Hexa, Neu4 and GM3S knockout and wild type PCR are made and related gel image are shown in Figure 3.1 and 3.2.

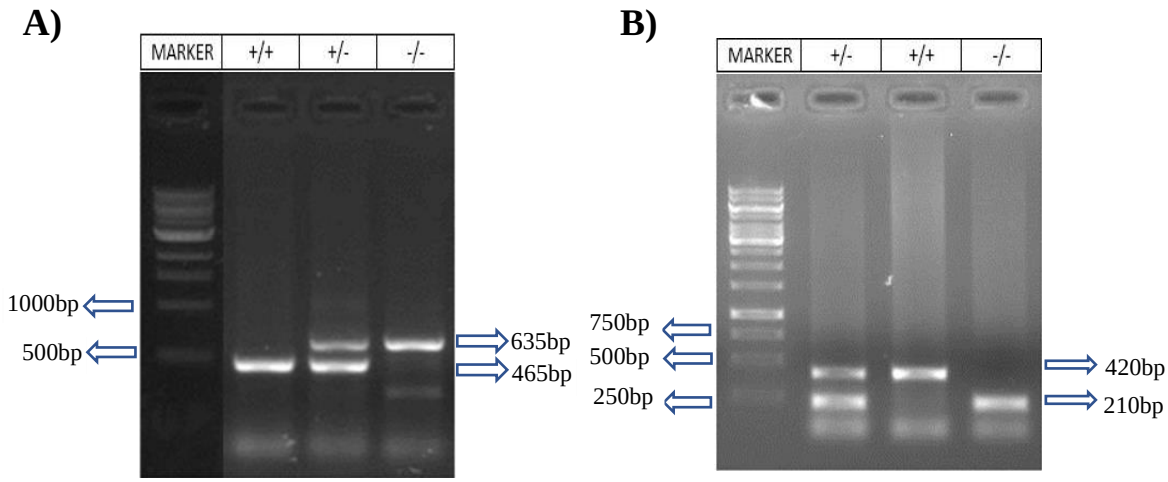

Figure 3.1:Neu4 (A) and Hexa (B) PCR results for genotyping

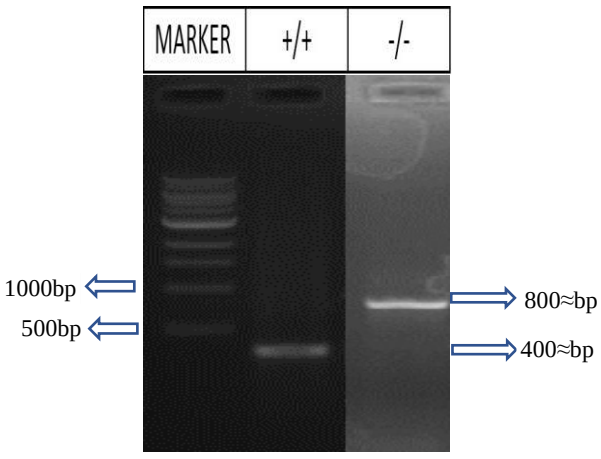

Figure 3.2: GM3S PCR results.

3.2. Realtime PCR Results

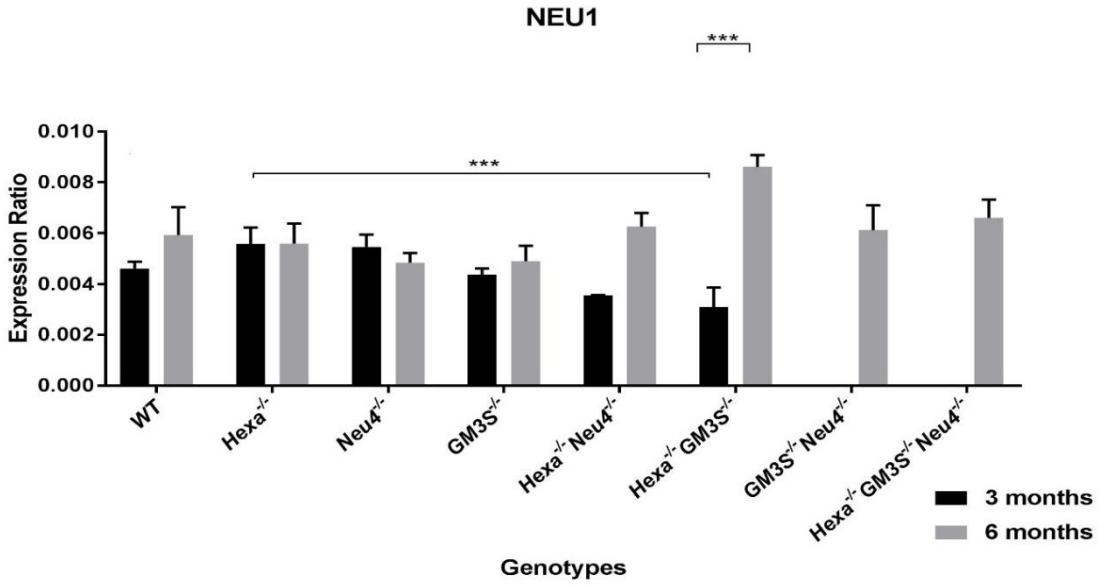

Figure 3.3: Realtime PCR results of Neu1 gene expression level in 3-and 6-month-old *WT, Hexa$^{-/-}$, Neu4$^{-/-}$, GM3S$^{-/-}$, Hexa$^{-/-}$Neu4$^{-/-}$, Hexa$^{-/-}$GM3S$^{-/-}$, GM3S$^{-/-}$Neu4$^{-/-}$, and Hexa$^{-/-}$GM3S$^{-/-}$Neu4$^{-/-}$* mice brain. WT defines wild type mice. (* describes p<0.05, ** describes p<0.01, *** describes p<005). In the experiment n=2 replicas were used. P values were calculated with ANOVA. Error bars were calculated with ±SEM.

In Figure 3.3 showed significant difference between 3 months all genotypes and 3 months *GM3S$^{-/-}$Neu4$^{-/-}$*and *Hexa$^{-/-}$GM3S$^{-/-}$Neu4$^{-/-}$* mice. In addition, 6 months *Hexa$^{-/-}$ GM3S$^{-/-}$*, *Neu4$^{-/-}$ GM3S$^{-/-}$*and *Neu4$^{-/-}$ Hexa$^{-/-}$ GM3S$^{-/-}$* mice produced Neu1 but their 3-month-old individuals did not produce Neu1. 6-months-old *Hexa$^{-/-}$ GM3S$^{-/-}$* mice exhibited significant increase to the 3-months-old *Hexa$^{-/-}$ GM3S$^{-/-}$* mice (2.47 fold). In 3-months-old *Hexa$^{-/-}$* genotyped mice represented that 1.56-fold significant increase to the 3-months-old *Hexa$^{-/-}$ GM3S$^{-/-}$* genotyped mice.

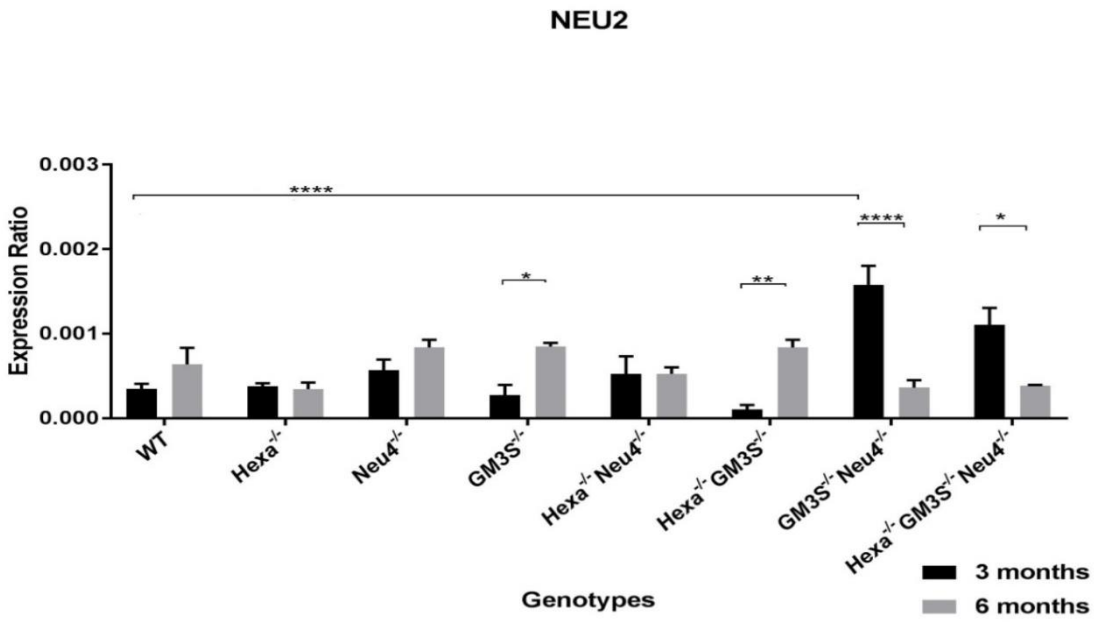

Figure 3.4: Realtime PCR results of Neu2 gene expression level in 3-and 6-month-old *WT, Hexa$^{-/-}$, Neu4$^{-/-}$, GM3S$^{-/-}$, Hexa$^{-/-}$Neu4$^{-/-}$, Hexa$^{-/-}$GM3S$^{-/-}$, GM3S$^{-/-}$Neu4$^{-/-}$, and Hexa$^{-/-}$GM3S$^{-/-}$Neu4$^{-/-}$* mice brain. WT defines wild type mice. (* describes p<0.05, ** describes p<0.01, *** describes, p<005 **** describes p<0.0001). In the experiment n=2 replicas were used. P values were calculated with ANOVA. Error bars were calculated with ±SEM.

In Figure 3.4, 3-month-old *GM3S$^{-/-}$Neu4$^{-/-}$* genotyped mice showed significant difference between other 3-months-old animal except *Hexa$^{-/-}$GM3S$^{-/-}$Neu4$^{-/-}$* mice. *GM3S$^{-/-}$Neu4$^{-/-}$* mice exhibited was 4.48-fold increase to the 3-month-old WT mice. 3-months-old *GM3S$^{-/-}$Neu4$^{-/-}$* mice exhibited 4.15-fold increase to the 3-month-old *Hexa$^{-/-}$* mice. 3-months-old *GM3S$^{-/-}$Neu4$^{-/-}$* mice. 3-months-old *GM3S$^{-/-}$Neu4$^{-/-}$* mice 2.76-fold increase to the 3-months-old *Neu4$^{-/-}$* mice. 3-months-old *GM3S$^{-/-}$Neu4$^{-/-}$* mice displayed 5.76-fold increase to the *3-month-old GM3S$^{-/-}$* mice. 3-months-old *GM3S$^{-/-}$Neu4$^{-/-}$* mice showed 3.02-fold increase to the 3-month-old and *Hexa$^{-/-}$Neu4$^{-/-}$* mice. 3-months-old *GM3S$^{-/-}$Neu4$^{-/-}$* mice exhibited 14.89-fold increase to the 3-month-old *Hexa$^{-/-}$GM3S$^{-/-}$* mice. 6-month-old *GM3S$^{-/-}$*, *Hexa$^{-/-}$GM3S$^{-/-}$*, *GM3S$^{-/-}$Neu4$^{-/-}$*, and *Hexa$^{-/-}$GM3S$^{-/-}$Neu4$^{-/-}$* mice represented significant difference to their 3-month-old same genotyped littermate. The difference between 3 months and 6-month-old *GM3S$^{-/-}$* genotyped mice was 3.09-fold. The difference between 3 months and 6-month-old *Hexa$^{-/-}$GM3S$^{-/-}$* mice was 7.90-fold. The difference between 3 months and 6-month-old *GM3S$^{-/-}$Neu4$^{-/-}$* was 3.45-fold. The difference between 3 months and 6-month-old *Hexa$^{-/-}$GM3S$^{-/-}$Neu4$^{-/-}$* mice was 2.89-fold. 6-month-old *GM3S$^{-/-}$*, and *Hexa$^{-/-}$GM3S$^{-/-}$* genotyped mice showed increase to

their 3-month-old same genotyped littermates. However, 6-month-old *GM3S*$^{-/-}$*Neu4*$^{-/-}$, and *Hexa*$^{-/-}$*GM3S*$^{-/-}$*Neu4*$^{-/-}$ mice represented decrease to the 3-month-old same genotyped littermate.

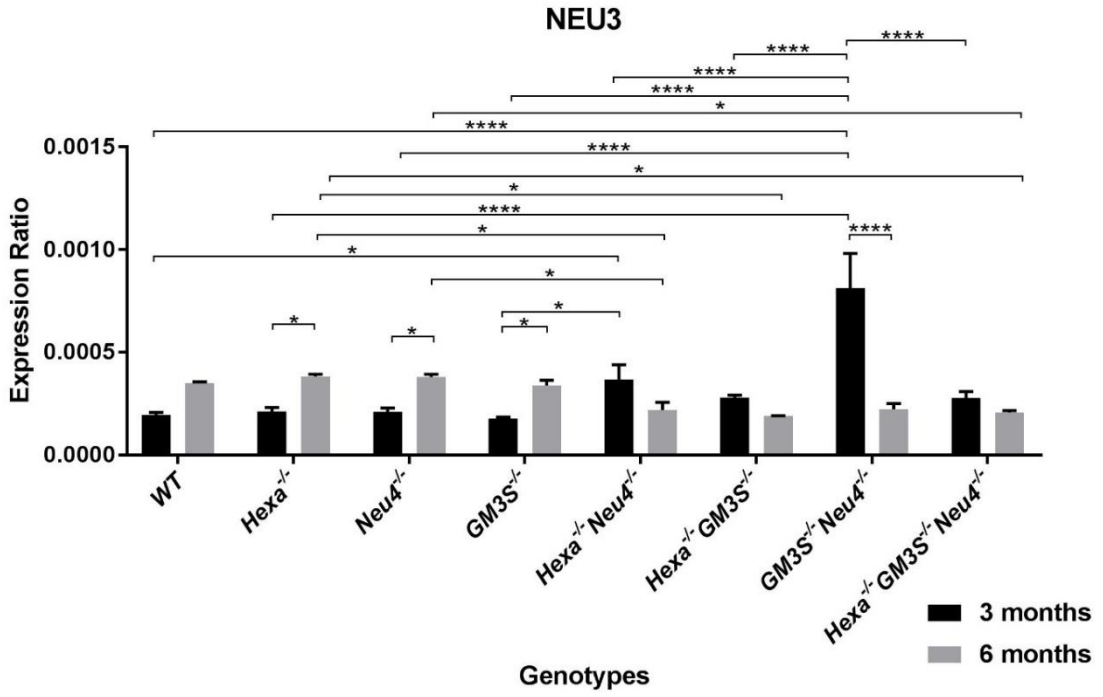

Figure 3.5: Realtime PCR results of Neu3 gene expression level in 3-and 6-month-old *WT, Hexa*$^{-/-}$*, Neu4*$^{-/-}$*, GM3S*$^{-/-}$*, Hexa*$^{-/-}$*Neu4*$^{-/-}$*, Hexa*$^{-/-}$*GM3S*$^{-/-}$*, GM3S*$^{-/-}$*Neu4*$^{-/-}$*, and Hexa*$^{-/-}$*GM3S*$^{-/-}$*Neu4*$^{-/-}$ mice brain. WT defines wild type mice. (* describes p<0.05, ** describes p<0.01, *** describes p<005, **** describes p<0.0001). In the experiment n=2 replicas were used. P values were calculated with ANOVA. Error bars were calculated with ±SEM.

In Figure 3.5, 3-month-old *GM3S*$^{-/-}$*Neu4*$^{-/-}$ genotyped mice represented noteworthy difference with other 7 genotypes; *WT*, *Neu4*$^{-/-}$, *Hexa*$^{-/-}$, *Hexa*$^{-/-}$*Neu4*$^{-/-}$, *Hexa*$^{-/-}$*GM3S*$^{-/-}$, and *Hexa*$^{-/-}$*GM3S*$^{-/-}$*Neu4*$^{-/-}$mice. 3-month-old *GM3S*$^{-/-}$*Neu4*$^{-/-}$ genotyped mice. 3-month-old *GM3S*$^{-/-}$*Neu4*$^{-/-}$ genotyped mice exhibited 4.15-fold increase to the 3-month-old WT mice. 3-month-old *GM3S*$^{-/-}$*Neu4*$^{-/-}$ mice displayed 3.80-fold increase to the 3-month-old *Hexa*$^{-/-}$ mice. 3-month-old *GM3S*$^{-/-}$*Neu4*$^{-/-}$ mice pointed out 3.85-fold increase to the 3-month-old *Neu4*$^{-/-}$ mice. 3-month-old *GM3S*$^{-/-}$*Neu4*$^{-/-}$ mice illustrated increase to the 3-month-old *Hexa*$^{-/-}$ mice. 3-month-old *GM3S*$^{-/-}$*Neu4*$^{-/-}$ mice represented showed 4.56-fold increase to the 3-month-old *GM3S*$^{-/-}$ mice. 3-month-old *GM3S*$^{-/-}$*Neu4*$^{-/-}$ mice displayed 2.20-fold increase to the 3-month-old *Hexa*$^{-/-}$*Neu4*$^{-/-}$ mice. Increase of 3-month-old *GM3S*$^{-/-}$*Neu4*$^{-/-}$ mice to the 3-month-old *Hexa*$^{-/-}$*GM3S*$^{-/-}$mice was 2.89-fold.

Increase of 3-month-old *GM3S*$^{-/-}$*Neu4*$^{-/-}$ mice to the 3-month-old *Hexa*$^{-/-}$*GM3S*$^{-/-}$*Neu4*$^{-/-}$ mice was 2.77-fold. There was 1.79-fold significant difference between 3 months and 6-month-old *Hexa*$^{-/-}$ mice. There was 1.80-fold significant difference between 3 months and 6-month-old *Neu4*$^{-/-}$ mice. 3-month-old *GM3S*$^{-/-}$ mice represented 1.89-fold increase to the 6-month-old same genotyped littermate. 3-month-old *Hexa*$^{-/-}$*Neu4*$^{-/-}$ mice exhibited 2.07-fold significant increase to the 3-month-old *GM3S*$^{-/-}$ mice. 6-month-old *Hexa*$^{-/-}$ mice have significant difference to the 6-month-old *Hexa*$^{-/-}$*Neu4*$^{-/-}$, *Hexa*$^{-/-}$ *GM3S*$^{-/-}$, and *Hexa*$^{-/-}$*GM3S*$^{-/-}$*Neu4*$^{-/-}$mice. These increases were 1.73-fold to the *Hexa*$^{-/-}$ *Neu4*$^{-/-}$ mice, 2.01-fold to the *Hexa*$^{-/-}$*GM3S*$^{-/-}$ mice, and 1.83-fold to the *Hexa*$^{-/-}$*GM3S*$^{-/-}$ *Neu4*$^{-/-}$mice. In 6-month-old *Neu4*$^{-/-}$ mice displayed 1.72-fold significant increase to the *Hexa*$^{-/-}$*Neu4*$^{-/-}$ and 1.82-fold significant increase to the *Hexa*$^{-/-}$*GM3S*$^{-/-}$*Neu4*$^{-/-}$mice. 3-month-old *Hexa*$^{-/-}$*Neu4*$^{-/-}$ mice represented 2.07-fold increase to the 3-month-old *GM3S*$^{-/-}$ mice. 6-month-old *Hexa*$^{-/-}$*GM3S*$^{-/-}$*Neu4*$^{-/-}$ mice illustrated 1.83-fold decrease to the *Hexa*$^{-/-}$ and 1.82-fold decrease to the *Neu4*$^{-/-}$ mice.

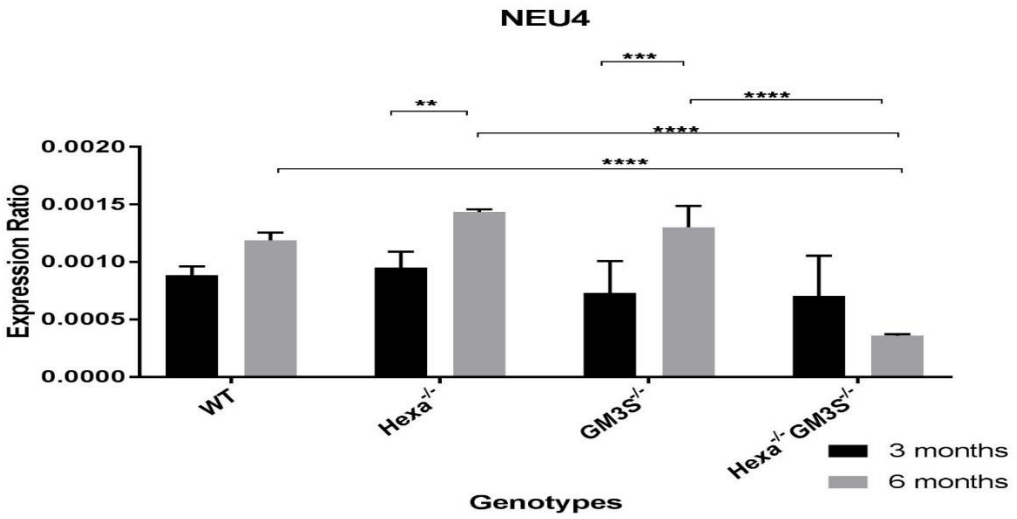

Figure 3.6 Realtime PCR results of Nue4 gene expression level in 3-and 6-month-old *WT*, *Hexa*$^{-/-}$, *GM3S*$^{-/-}$, *Hexa*$^{-/-}$*GM3S*$^{-/-}$ mice brain. WT defines wild type mice. (** describes p<0.01, *** describes p<005, **** describes p<0.0001). In the experiment n=2 replicas were used. P values were calculated with ANOVA. Error bars were calculated with ±SEM.

In Figure 3.6, as expected, *Neu4*$^{-/-}$mice, *Hexa*$^{-/-}$*Neu4*$^{-/-}$mice, *Neu4*$^{-/-}$ *GM3S*$^{-/-}$mice and *Hexa*$^{-/-}$*GM3S*$^{-/-}$*Neu4*$^{-/-}$ mice showed no Neu4 expression. 6-month-old WT displayed 3.31-fold increase to the 6-month-old *Hexa*$^{-/-}$*GM3S*$^{-/-}$ mice. 6-month-old *Hexa*$^{-/-}$ mice indicated 3.99-fold increase to the 6-month-old *Hexa*$^{-/-}$*GM3S*$^{-/-}$ mice. 6-

months-old *GM3S*$^{-/-}$ mice represented 3.62-fold increase to the 6-month-old *Hexa*$^{-/-}$ *GM3S*$^{-/-}$ mice. 6-month-old animals *Hexa*$^{-/-}$ mice showed 1.51-fold significant increase 3 months old same genotyped littermate. 6-month-old *GM3S*$^{-/-}$ mice showed 1.51-fold significant increase 3 months old same genotyped littermate.

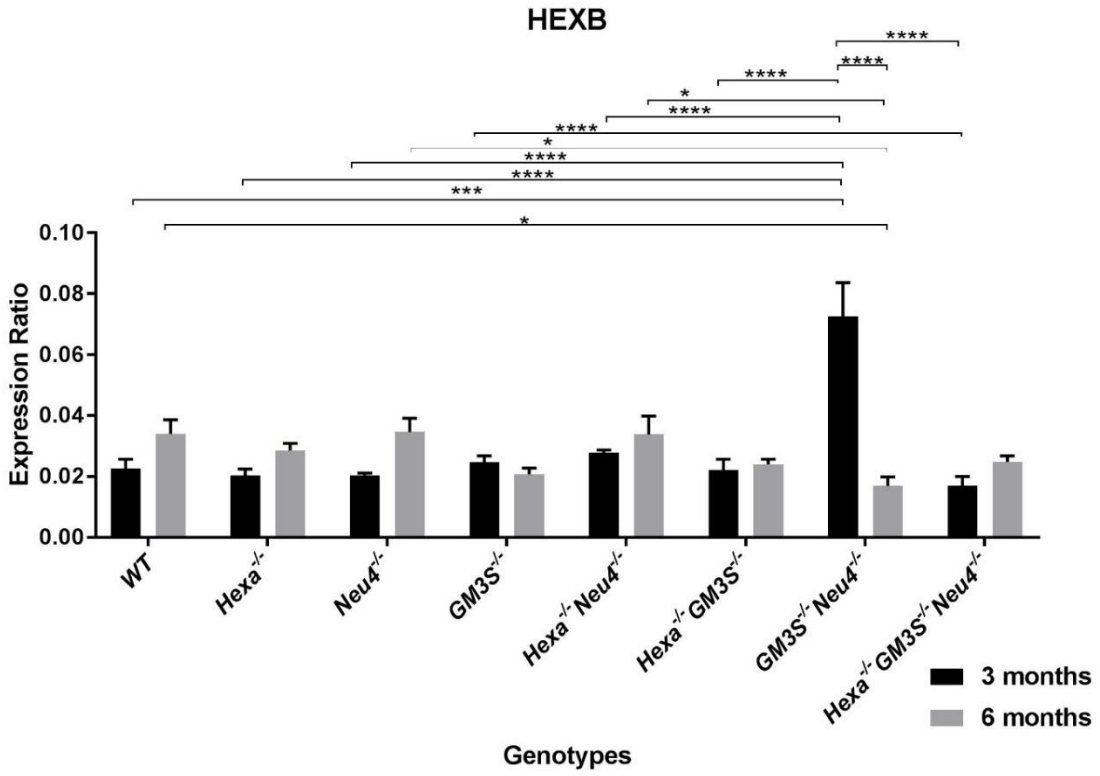

Figure 3.7**:** Realtime PCR results of HEXB gene expression level in 3-and 6-month-old *WT, Hexa*$^{-/-}$*, Neu4*$^{-/-}$*, GM3S*$^{-/-}$*, Hexa*$^{-/-}$*Neu4*$^{-/-}$*, Hexa*$^{-/-}$*GM3S*$^{-/-}$*, GM3S*$^{-/-}$*Neu4*$^{-/-}$*, and Hexa*$^{-/-}$*GM3S*$^{-/-}$*Neu4*$^{-/-}$ mice brain. WT defines wild type mice. (* describes p<0.05, ** describes p<0.01 *** describes p<005 **** describes p<0.0001). In the experiment n=2 replicas were used. P values were calculated with ANOVA. Error bars were calculated with ±SEM.

In Figure 3.7, 3-month-old *GM3S*$^{-/-}$*Neu4*$^{-/-}$ mice illustrated significant increase according to their other 3 months described genotypes. 3-month-old *GM3S*$^{-/-}$*Neu4*$^{-/-}$ mice displayed 3.20-fold increase to the 3-month-old WT mice, 3.58-fold increase to the 3-month-old *Hexa*$^{-/-}$ mice, 3.57-fold increase 3-month old *Neu4*$^{-/-}$ mice, 2.94-fold increase to the 3-month-old *GM3S*$^{-/-}$ mice, 2.61-fold increase to the 3-month-old *Hexa*$^{-/-}$ *Neu4*$^{-/-}$ mice. 3.28-fold increase to the 3-month-old *Hexa*$^{-/-}$*GM3S*$^{-/-}$ mice, 4.27-fold increase to the 3-month-old *Hexa*$^{-/-}$*GM3S*$^{-/-}$*Neu4*$^{-/-}$ mice. There was also significant 4.27-fold increase in 3-month-old *Neu4*$^{-/-}$ *GM3S*$^{-/-}$mice according to its' 6-months-old same genotyped littermate. In addition, 6-month-old wild type mice represented

significant 2.00-fold increase to the 6-month-old *GM3S*$^{-/-}$*Neu4*$^{-/-}$ mice. 6-month-old *Neu4*$^{-/-}$ mice exhibited significant 2.03-fold increase to the 6-month-old *GM3S*$^{-/-}$*Neu4*$^{-/-}$ mice. 6-month-old *Hexa*$^{-/-}$*Neu4*$^{-/-}$ mice showed significant 1.98-fold increase to the 6-month-old *GM3S*$^{-/-}$*Neu4*$^{-/-}$ mice.

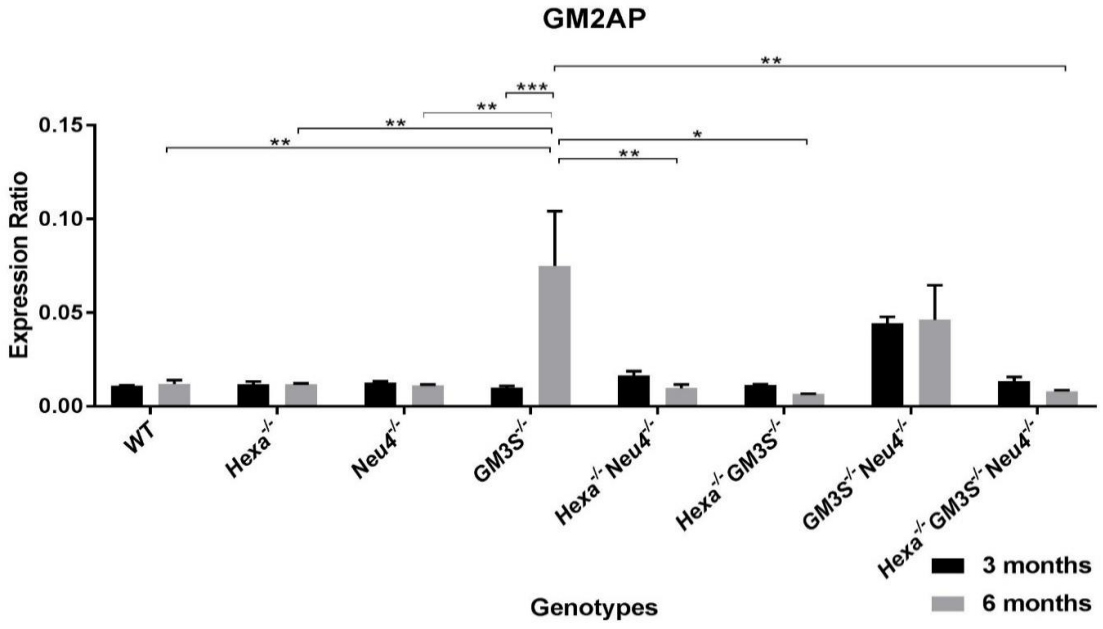

Figure 3.8: Realtime PCR results of GM2AP gene expression level in 3-and 6-month-old *WT*, *Hexa*$^{-/-}$, *Neu4*$^{-/-}$, *GM3S*$^{-/-}$, *Hexa*$^{-/-}$*Neu4*$^{-/-}$, *Hexa*$^{-/-}$*GM3S*$^{-/-}$, *GM3S*$^{-/-}$ *Neu4*$^{-/-}$, *and Hexa*$^{-/-}$*GM3S*$^{-/-}$*Neu4*$^{-/-}$ mice brains. WT defines wild type mice. (* describes $p<0.05$, ** describes $p<0.01$ *** describes $p<005$). In the experiment n=2 replicas were used. P values were calculated with ANOVA. Error bars were calculated with ±SEM.

In Figure 3.8, 6-month-old *GM3S*$^{-/-}$mice represented 7.39-fold noteworthy increase in expression to the 3-month-old same genotyped littermate. And 6-month-old *GM3S*$^{-/-}$mice also showed significant increase when compared with other 6-month-old genotypes expect *GM3S*$^{-/-}$*Neu4*$^{-/-}$ mice. 6-month-old *GM3S*$^{-/-}$mice. 6-month-old *GM3S*$^{-/-}$ mice exhibited 6.26-fold increase to the 6-month-old wildtype (WT). 6-month-old *GM3S*$^{-/-}$mice displayed 6.43-fold increase to the 6-month-old *Hexa*$^{-/-}$ mice. 6-month-old *GM3S*$^{-/-}$ mice illustrated 6.67-fold increase to the 6-month old *Neu4*$^{-/-}$ mice. 6-month-old *GM3S*$^{-/-}$ mice pointed out 7.74-fold increase to the 6-month-old *Hexa*$^{-/-}$*Neu4*$^{-/-}$ mice. And the most striking increase was 11.07-fold increase of 6-month-old *GM3S*$^{-/-}$ mice to the *Hexa*$^{-/-}$*GM3S*$^{-/-}$ mice. 6-month-old *GM3S*$^{-/-}$mice showed 9.22-fold increase to the *Hexa*$^{-/-}$*GM3S*$^{-/-}$*Neu4*$^{-/-}$mice.

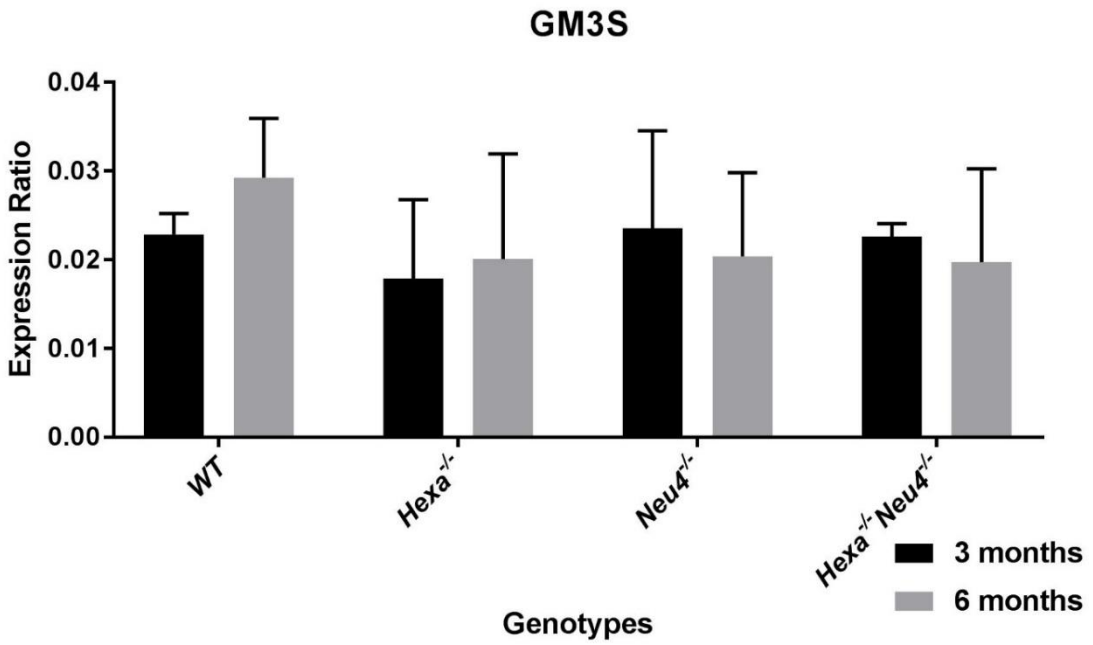

Figure 3.9**:** Realtime PCR results of GM3S gene expression level in 3-and 6-month-old *WT*, *Hexa*$^{-/-}$, *Neu4*$^{-/-}$, *Hexa*$^{-/-}$*Neu4*$^{-/-}$ mice brain. WT defines wild type mice. In the experiment n=2 replicas were used. P values were calculated with ANOVA. Error bars were calculated with ±SEM.

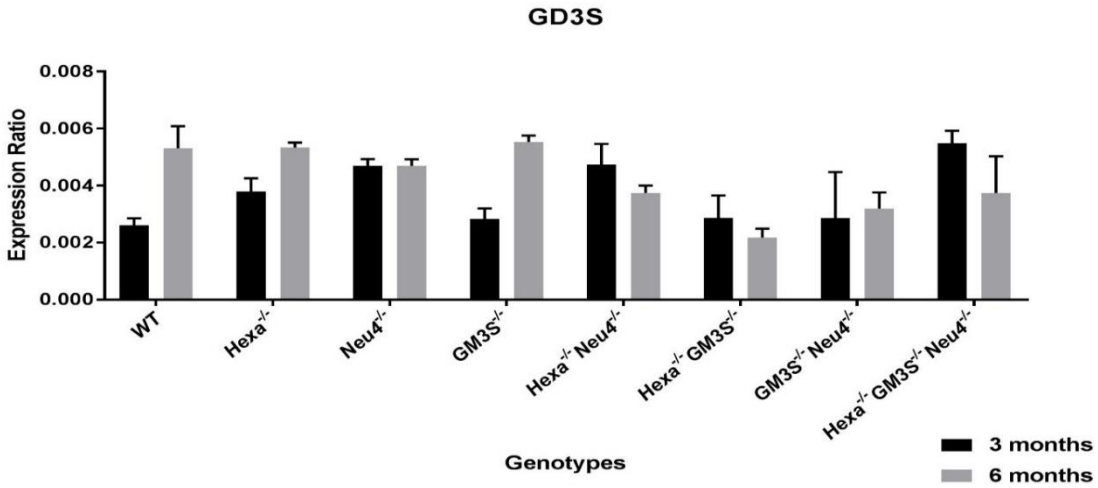

Figure 3.10: Realtime PCR results of GD3S gene expression level 3-and 6-month-old *WT*, *Neu4*$^{-/-}$, *Hexa*$^{-/-}$, *Hexa*$^{-/-}$*Neu4*$^{-/-}$, *GM3S*$^{-/-}$*Neu4*$^{-/-}$, *Hexa*$^{-/-}$*GM3S*$^{-/-}$, and *Hexa*$^{-/-}$*GM3S*$^{-/-}$*Neu4*$^{-/-}$ mice brain. WT defines wild type mice. In the experiment n=2 replicas were used. P values were calculated with ANOVA. Error bars were calculated with ±SEM.

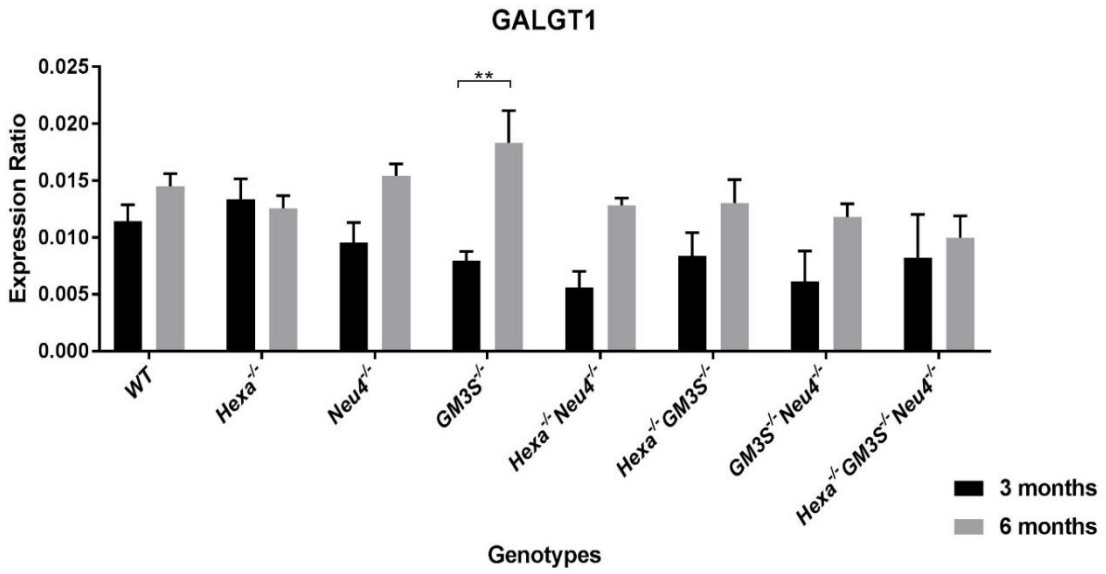

Figure 3.11**:** Realtime PCR results of GALGT1 gene expression level in 3-and 6-month-old *WT, Neu4*$^{-/-}$*, Hexa*$^{-/-}$*, Hexa*$^{-/-}$*Neu4*$^{-/-}$*, GM3S*$^{-/-}$*Neu4*$^{-/-}$*, Hexa*$^{-/-}$ *GM3S*$^{-/-}$, and *Hexa*$^{-/-}$*GM3S*$^{-/-}$*Neu4*$^{-/-}$*mice brain*. WT defines wild type mice. (* describes p<0.05, ** describes p<0.01). In the experiment n=2 replicas were used. P values were calculated with ANOVA. Error bars were calculated with ±SEM.

In Figure 3.9, as expected, *GM3S*$^{-/-}$, *Hexa*$^{-/-}$ *GM3S*$^{-/-}$, *Neu4*$^{-/-}$ *GM3S*$^{-/-}$ and *Neu4*$^{-/-}$ *Hexa*$^{-/-}$ *GM3S*$^{-/-}$ mice represented no expression. Rest of the genotypes exhibited no significant difference between each other.

In Figure 3.10, there was no significant difference between all genotypes and age groups.

In Figure 3.11, There was no significant change in GALGT1 level in these genotypes expect *GM3S*$^{-/-}$with different age groups. There was 2.29-fold increase in 6-month-old *GM3S*$^{-/-}$ mice according to its 3-months-old *GM3S*$^{-/-}$ mice and this change was accepted significant.

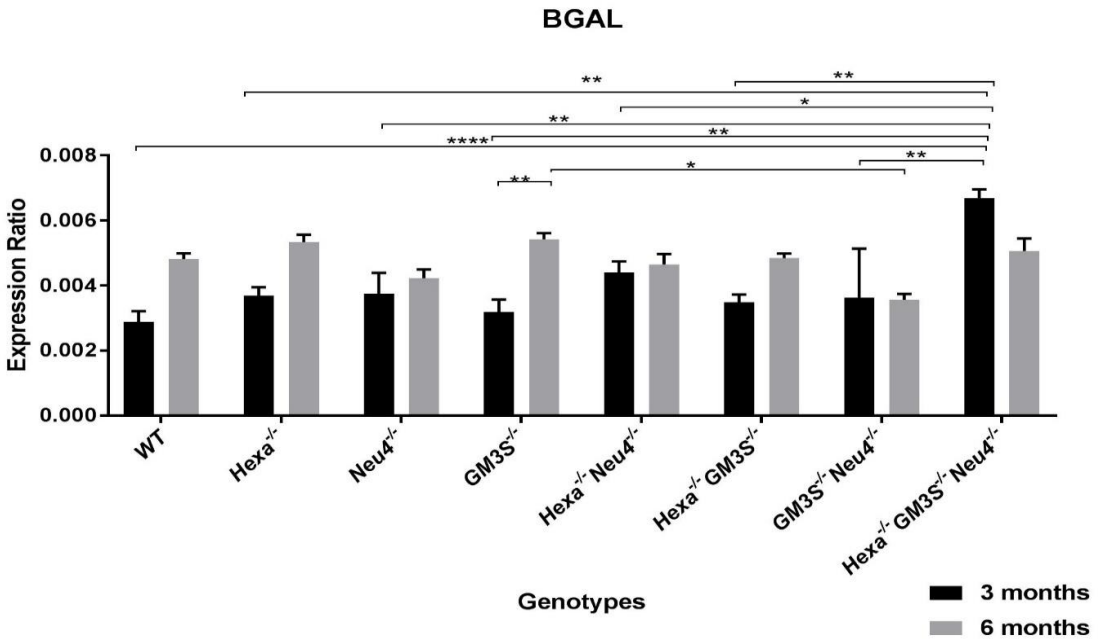

Figure 3.12**:** Realtime PCR results of BGAL gene expression level in 3-and 6-month-old *WT, Hexa*$^{-/-}$*, Neu4*$^{-/-}$*, GM3S*$^{-/-}$*, Hexa*$^{-/-}$*Neu4*$^{-/-}$*, Hexa*$^{-/-}$*GM3S*$^{-/-}$*, GM3S*$^{-/-}$ *Neu4*$^{-/-}$*, and Hexa*$^{-/-}$*GM3S*$^{-/-}$*Neu4*$^{-/-}$ mice brain. WT defines wild type mice. (* describes p<0.05, ** describes p<0.01 *** describes p<005 **** describes p<0.0001). In the experiment n=2 replicas were used. P values were calculated with ANOVA. Error bars were calculated with ±SEM.

In Figure 3.12, 3-month-old *Hexa*$^{-/-}$*GM3S*$^{-/-}$*Neu4*$^{-/-}$mice represented significant increase to other 3-month-old animals. 3-month-old *Hexa*$^{-/-}$*GM3S*$^{-/-}$*Neu4*$^{-/-}$ mice exhibited 2.32-fold increase to the 3-month-old wild type (WT) mice. 3-month-old *Hexa*$^{-/-}$*GM3S*$^{-/-}$*Neu4*$^{-/-}$ mice illustrated 1.81-fold increase to the 3-month-old *Hexa*$^{-/-}$ mice. 3-month-old *Hexa*$^{-/-}$*GM3S*$^{-/-}$*Neu4*$^{-/-}$ mice displayed 1.78-fold increase to the 3-month-old *Neu4*$^{-/-}$ mice. 3-month-old *Hexa*$^{-/-}$*GM3S*$^{-/-}$*Neu4*$^{-/-}$ mice pointed out 2.10-fold increase to the 3-month-old *GM3S*$^{-/-}$ mice. 3-month-old *Hexa*$^{-/-}$*GM3S*$^{-/-}$*Neu4*$^{-/-}$ mice showed 1.51-fold increase to the 3-month-old *Hexa*$^{-/-}$*Neu4*$^{-/-}$ mice. 3-month-old *Hexa*$^{-/-}$ *GM3S*$^{-/-}$*Neu4*$^{-/-}$ mice indicated 1.92-fold increase to the 3-month-old *Hexa*$^{-/-}$*GM3S*$^{-/-}$ mice. 3-month-old *Hexa*$^{-/-}$*GM3S*$^{-/-}$*Neu4*$^{-/-}$ mice represented 1.84-fold increase to the 3-month-old *GM3S*$^{-/-}$*Neu4*$^{-/-}$ mice. In addition, there was 1.70-fold significant increase in 6-month-old *GM3S*$^{-/-}$according to 3-month-old same genotyped littermate. There was also 1.52-fold significant increase in 6-month-old *GM3S*$^{-/-}$ mice to the 6-month-old *Neu4*$^{-/-}$ *GM3S*$^{-/-}$ mice.

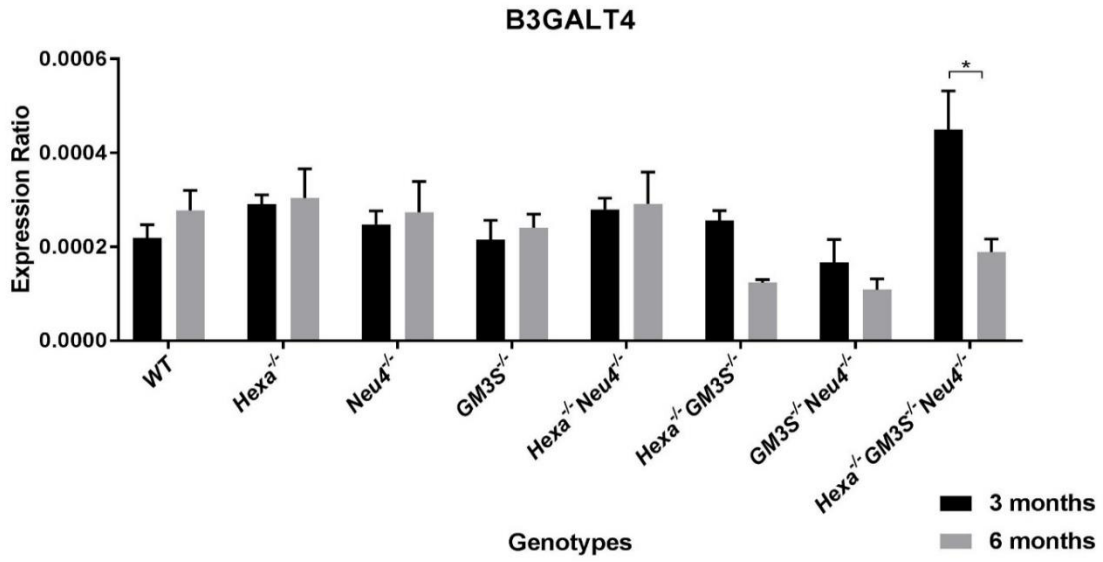

Figure 3.13**:** Realtime PCR results of B3GALT4 gene expression level in 3-and 6-month-old *WT*, *Hexa*$^{-/-}$, *Neu4*$^{-/-}$, *GM3S*$^{-/-}$, *Hexa*$^{-/-}$*Neu4*$^{-/-}$, *Hexa*$^{-/-}$*GM3S*$^{-/-}$, *GM3S*$^{-/-}$*Neu4*$^{-/-}$, *and Hexa*$^{-/-}$*GM3S*$^{-/-}$*Neu4*$^{-/-}$ mice brain. WT defines wild type mice. (* describes $p<0.05$). In the experiment n=2 replicas were used. P values were calculated with ANOVA. Error bars were calculated with ±SEM.

In Figure 3.13, there is no significant differences between all genotypes within the same months. However, 3 months *Hexa*$^{-/-}$*GM3S*$^{-/-}$*Neu4*$^{-/-}$mice exhibited 2.37-fold significant increase to the 6-month-old *Hexa*$^{-/-}$*GM3S*$^{-/-}$*Neu4*$^{-/-}$mice.

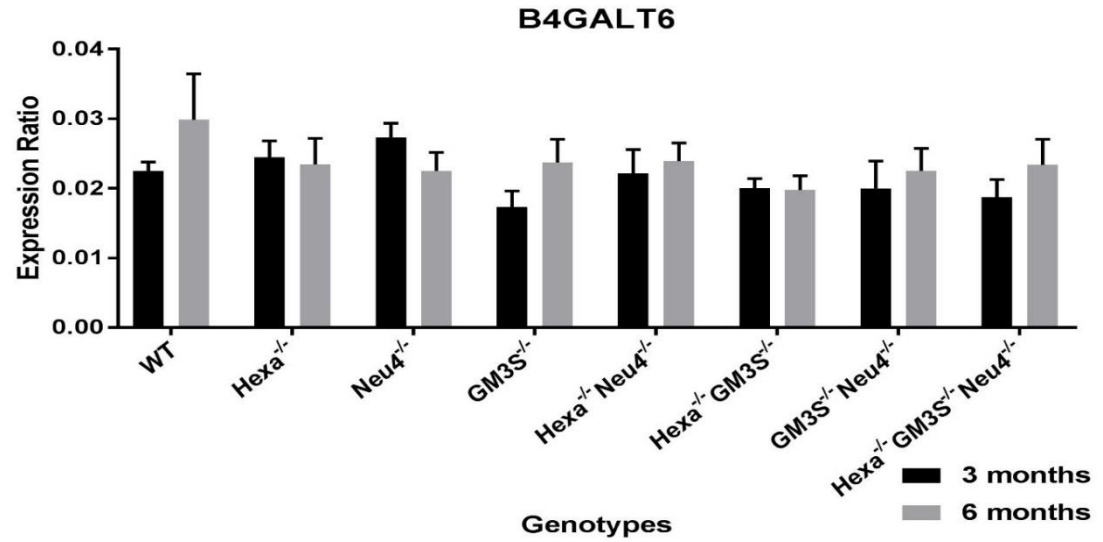

Figure 3.14**:** Realtime PCR results of B4GALT6 gene expression level in 3-and 6-month-old *WT*, *Hexa*$^{-/-}$, *Neu4*$^{-/-}$, *GM3S*$^{-/-}$, *Hexa*$^{-/-}$*Neu4*$^{-/-}$, *Hexa*$^{-/-}$*GM3S*$^{-/-}$, *GM3S*$^{-/-}$*Neu4*$^{-/-}$, *and Hexa*$^{-/-}$*GM3S*$^{-/-}$*Neu4*$^{-/-}$ mice brain. WT defines wild

type mice. In the experiment n=2 replicas were used. P values were calculated with ANOVA. Error bars were calculated with ±SEM.

In Figure 3.14, There is no significant difference between all genotypes with different age groups.

3.3. Thin Layer Chromatography

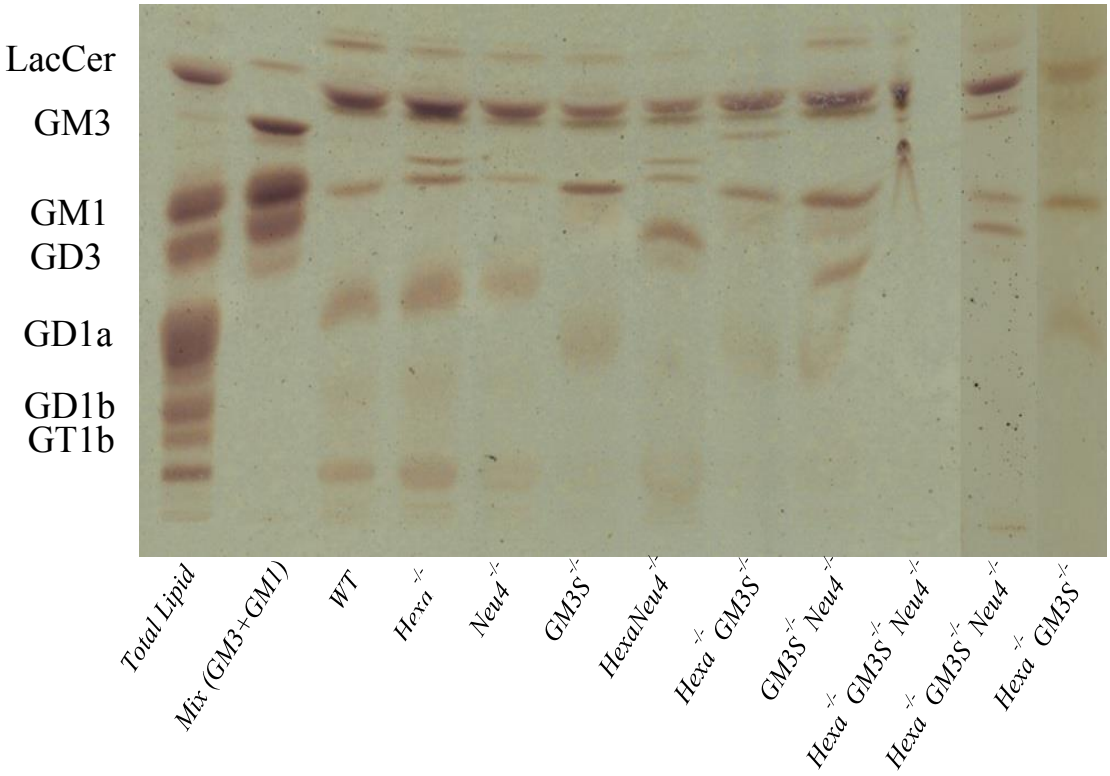

Figure 3.15: Thin layer chromatography analysis of acidic gangliosides in 3 months *WT, Hexa*$^{-/-}$, *Neu4*$^{-/-}$, *GM3S*$^{-/-}$, *Hexa*$^{-/-}$*Neu4*$^{-/-}$, *GM3S*$^{-/-}$*Neu4*$^{-/-}$, *Hexa*$^{-/-}$*GM3S*$^{-/-}$*Neu4*$^{-/-}$genotyped mice brain. Total Lipid and GM3+GM1 mixture were used as a control marker. Content of Total Lipid was Lactosylceramide (LacCer), GD3, GD1a, GD1b, and GT1b. This is for n=1 results.

In Figure 3.15, 3-months-old *Hexa*$^{-/-}$ and *Neu4*$^{-/-}$*Hexa*$^{-/-}$ genotyped mice represented GM2 band clearly, but 3-months-old *WT*, *Neu4*$^{-/-}$, *GM3S*$^{-/-}$, *GM3S*$^{-/-}$ *Neu4*$^{-/-}$, *Hexa*$^{-/-}$*GM3S*$^{-/-}$, *Hexa*$^{-/-}$*GM3S*$^{-/-}$*Neu4*$^{-/-}$ mice displayed no GM2 band. 3-months-old *WT*, *Hexa*$^{-/-}$, *Neu4*$^{-/-}$, *GM3S*$^{-/-}$, *Neu4*$^{-/-}$*Hexa*$^{-/-}$, *GM3S*$^{-/-}$ *Neu4*$^{-/-}$, *Hexa*$^{-/-}$*GM3S*$^{-/-}$, *Hexa*$^{-/-}$*GM3S*$^{-/-}$ *Neu4*$^{-/-}$ mice illustrated no GM3 band.

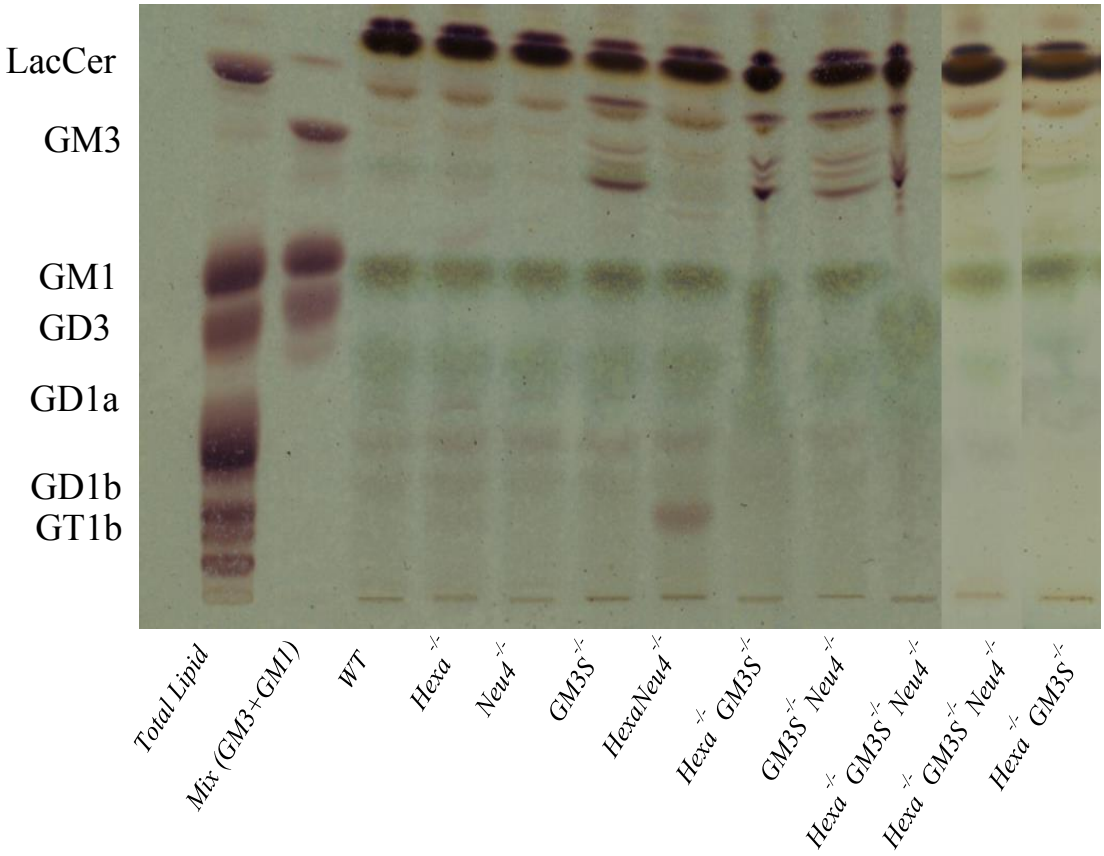

Figure 3.16: Thin layer chromatography analysis of neutral gangliosides in 3-months-old *WT*, *Hexa*$^{-/-}$, *Neu4*$^{-/-}$, *GM3S*$^{-/-}$, *Hexa*$^{-/-}$*Neu4*$^{-/-}$, *GM3S*$^{-/-}$*Neu4*$^{-/-}$, *Hexa*$^{-/-}$ *GM3S*$^{-/-}$*Neu4*$^{-/-}$genotyped mice brain. Total Lipid and GM3+GM1 mixture were used as a control marker. Content of Total Lipid was Lactosylceramide (LacCer), GD3, GD1a, GD1b, and GT1b. This is for n=1 results.

In Figure 3.16, 3-months-old *WT*, *Hexa*$^{-/-}$, *Neu4*$^{-/-}$, *GM3S*$^{-/-}$, *Neu4*$^{-/-}$*Hexa*$^{-/-}$, *GM3S*$^{-/-}$ *Neu4*$^{-/-}$, *Hexa*$^{-/-}$*GM3S*$^{-/-}$, *Hexa*$^{-/-}$*GM3S*$^{-/-}$*Neu4*$^{-/-}$ mice displayed lactosylceramide band.

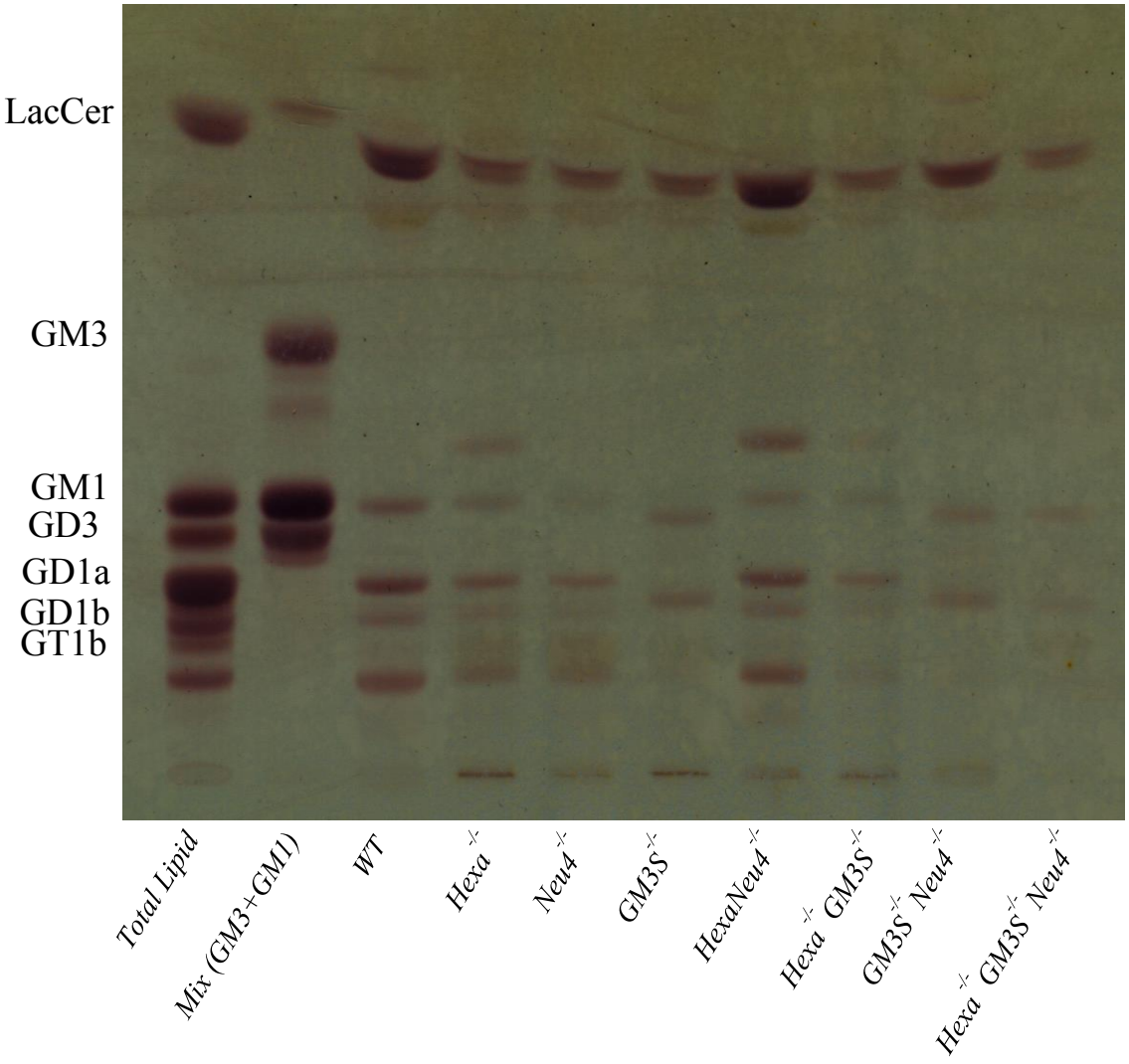

Figure 3.17: Thin layer chromatography analysis of acidic gangliosides in 6 months *WT, Hexa*$^{-/-}$, *Neu4*$^{-/-}$, *GM3S*$^{-/-}$, *Hexa*$^{-/-}$*Neu4*$^{-/-}$, *GM3S*$^{-/-}$*Neu4*$^{-/-}$, *Hexa*$^{-/-}$*GM3S*$^{-/-}$*Neu4*$^{-/-}$genotyped mice brain. Total Lipid and GM3+GM1 mixture were used as a control marker. Content of Total Lipid was Lactosylceramide (LacCer), GD3, GD1a, GD1b, and GT1b. This is for n=1 results.

In Figure 3.17, 6-months-old *Hexa*$^{-/-}$ and *Neu4*$^{-/-}$*Hexa*$^{-/-}$ genotyped mice illustrated GM2 band clearly, but 6-months-old *WT*, *Neu4*$^{-/-}$, *GM3S*$^{-/-}$, *GM3S*$^{-/-}$ *Neu4*$^{-/-}$, *Hexa*$^{-/-}$ *GM3S*$^{-/-}$, *Hexa*$^{-/-}$*GM3S*$^{-/-}$*Neu4*$^{-/-}$ mice displayed no GM2 band.

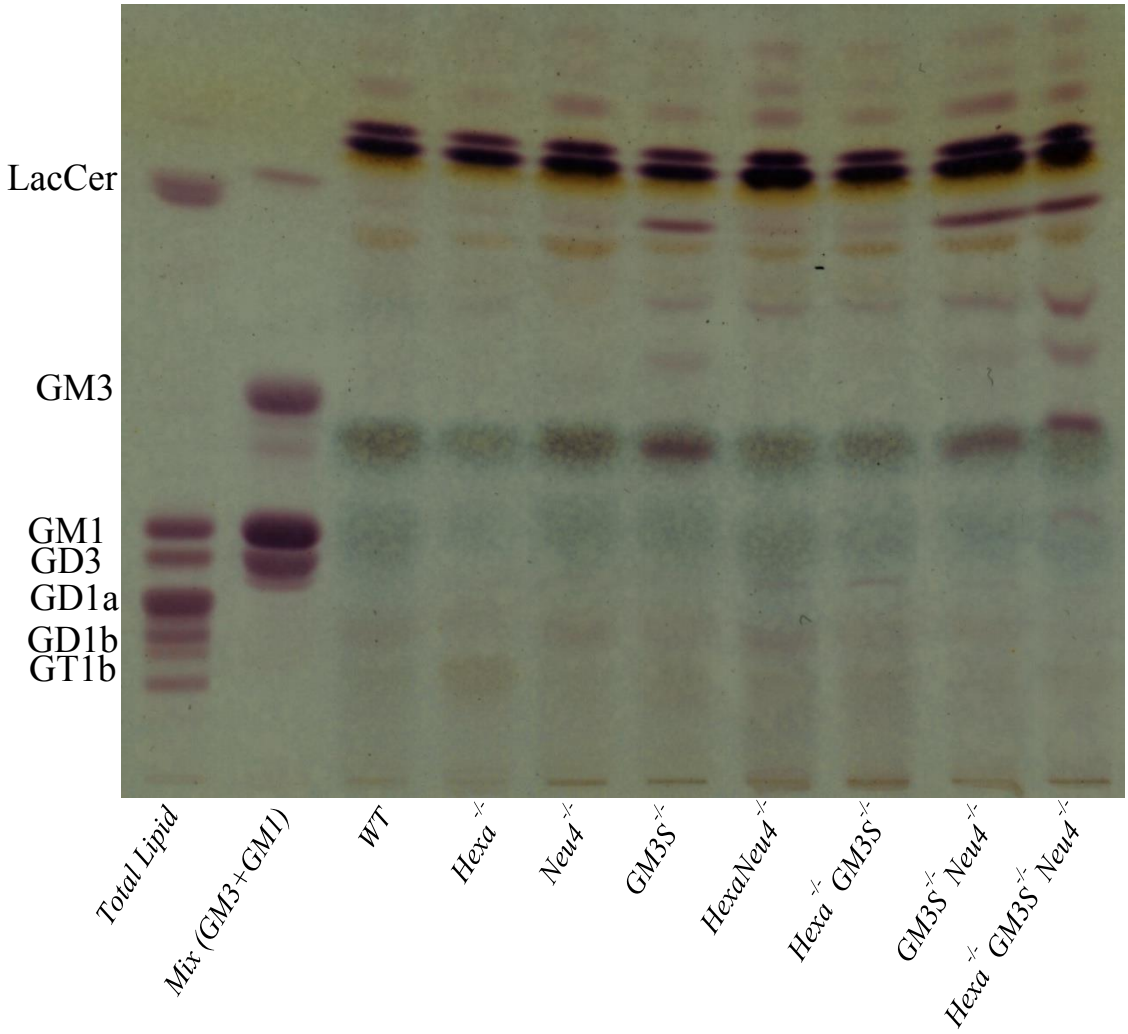

Figure 3.18: Thin layer chromatography analysis of neutral gangliosides in 6 months *WT, Hexa$^{-/-}$, Neu4$^{-/-}$, GM3S$^{-/-}$, Hexa$^{-/-}$Neu4$^{-/-}$, GM3S$^{-/-}$Neu4$^{-/-}$, Hexa$^{-/-}$GM3S$^{-/-}$Neu4$^{-/-}$*genotyped mice brain. Total Lipid and GM3+GM1 mixture were used as a control marker. Content of Total Lipid was Lactosylceramide (LacCer), GD3, GD1a, GD1b, and GT1b. This is for n=1 results.

In Figure 3.18, 6-month-old *WT, Hexa$^{-/-}$, Neu4$^{-/-}$, GM3S$^{-/-}$, Neu4$^{-/-}$Hexa$^{-/-}$, GM3S$^{-/-}$ Neu4$^{-/-}$, Hexa$^{-/-}$GM3S$^{-/-}$, Hexa$^{-/-}$GM3S$^{-/-}$Neu4$^{-/-}$* mice exhibited lactosylceramide band.

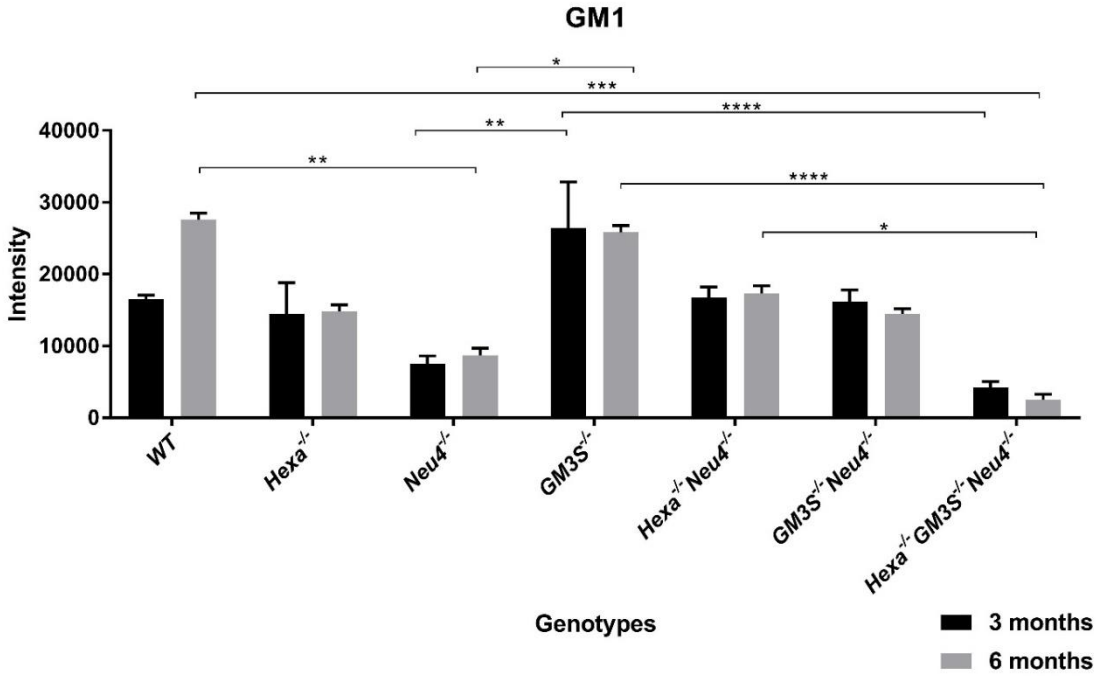

Figure 3.19: GM1 ganglioside band intensity of 3-and 6-month old *WT*, *Hexa*$^{-/-}$, *Neu4*$^{-/-}$, *GM3S*$^{-/-}$, *Hexa*$^{-/-}$*Neu4*$^{-/-}$, *GM3S*$^{-/-}$*Neu4*$^{-/-}$, *Hexa*$^{-/-}$*GM3S*$^{-/-}$*Neu4*$^{-/-}$genotyped mice thin layer chromatography results. (* describes p<0.05, ** describes p<0.01, *** describes p<005, **** describes p<0.0001) In the experiment n=2 replicas were used. P values calculated with ANOVA. Error bars were calculated with ±SEM.

In Figure 3.19, There was 3.49-fold significant increase in 3-month-old *GM3S*$^{-/-}$ mice to the 3-month-old *Neu4*$^{-/-}$ mice. There was 6.19-fold significant increase in 3-month-old *GM3S*$^{-/-}$ mice to the 3-month-old *Hexa*$^{-/-}$*GM3S*$^{-/-}$*Neu4*$^{-/-}$ mice. There was significant decrease in 6-month-old *Neu4*$^{-/-}$, and *Hexa*$^{-/-}$*GM3S*$^{-/-}$*Neu4*$^{-/-}$ mice to the wild type mice. 6-month-old wild type mice had 3.17-fold higher band intensity to the 6-month-old *Neu4*$^{-/-}$ mice. 6-month-old wild type mice had 10.92-fold higher band intensity to the 6-month-old *Hexa*$^{-/-}$*GM3S*$^{-/-}$*Neu4*$^{-/-}$ mice. 6-month-old *GM3S*$^{-/-}$ mice had 2.96-fold significant increase to the 6-month-old *Neu4*$^{-/-}$ mice. 6-month-old GM3S$^{-/-}$ mice represented 10.21-fold significant increase to the *Hexa*$^{-/-}$*GM3S*$^{-/-}$*Neu4*$^{-/-}$ mice. 6-month-old *Hexa*$^{-/-}$*Neu4*$^{-/-}$ mice exhibited 6.84-fold significant increase to the *Hexa*$^{-/-}$ *GM3S*$^{-/-}$*Neu4*$^{-/-}$ mice.

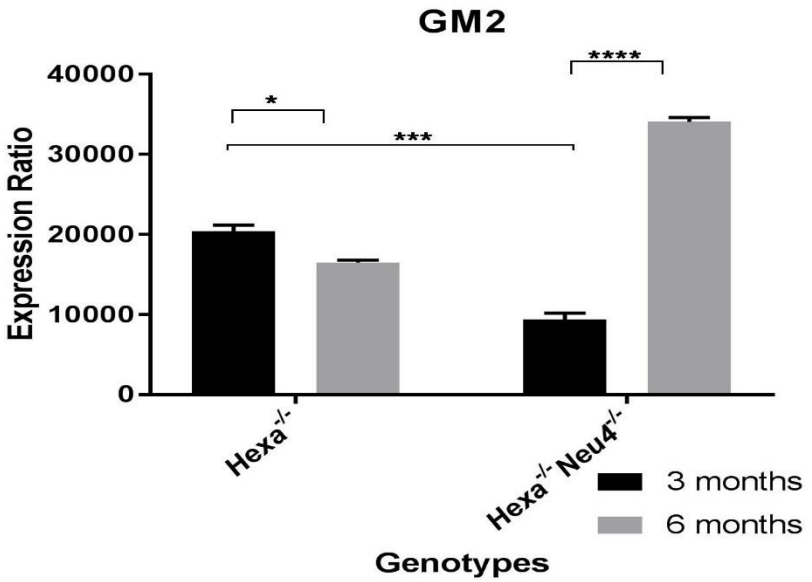

Figure 3.20: GM2 ganglioside band intensity of 3-and 6-month old Hexa$^{-/-}$, and Hexa$^{-/-}$ Neu4$^{-/-}$ genotyped mice thin layer chromatography results. (* describes p<0.05, ** describes p<0.01 *** describes p<005 **** describes p<0.0001) In the experiment n=2 replicas were used. P values calculated with ANOVA. Error bars were calculated with ±SEM.

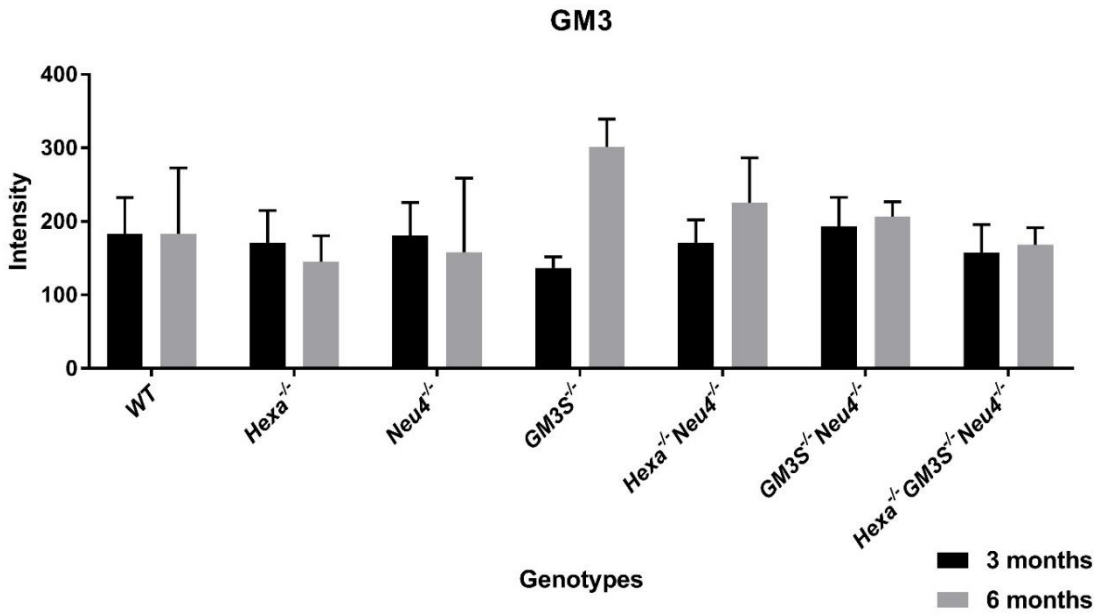

Figure 3.21: GM3 ganglioside band intensity of 3-and 6-month *WT*, *Hexa*$^{-/-}$, *Neu4*$^{-/-}$, *GM3S*$^{-/-}$, *Hexa*$^{-/-}$*Neu4*$^{-/-}$, *GM3S*$^{-/-}$*Neu4*$^{-/-}$, *Hexa*$^{-/-}$*GM3S*$^{-/-}$*Neu4*$^{-/-}$genotyped mice thin layer chromatography results. P values calculated with ANOVA. In the experiment n=2 replicas were used. Error bars were calculated with ±SEM.

In Figure 3.20, 3 months and 6-months-old *Hexa*$^{-/-}$and *Hexa*$^{-/-}$*Neu4*$^{-/-}$mice displayed significant difference with rest of the genotypes and age groups because other genotyped did not show GM2 band. There was 1.23-fold significant difference between 3 months and 6 months old *Hexa*$^{-/-}$ mice. 3.6-fold increase was also present in 6 months old *Hexa*$^{-/-}$*Neu4*$^{-/-}$ mice to the 3 months old same genotyped littermate. 3 months old *Hexa*$^{-/-}$ represented 2.16-fol significant increase to the 3-month-old *Hexa*$^{-/-}$*Neu4*$^{-/-}$mice. 6-month-old *Hexa*$^{-/-}$*Neu4*$^{-/-}$ illustrated 2.06 significant increase to the 6-month-old *Hexa*$^{-/-}$ mice.

In Figure 3.21, there is no significant difference between GM3 level between different age groups and with each other. It can also be observed by naked eye in Figure 3.15 and 3.17.

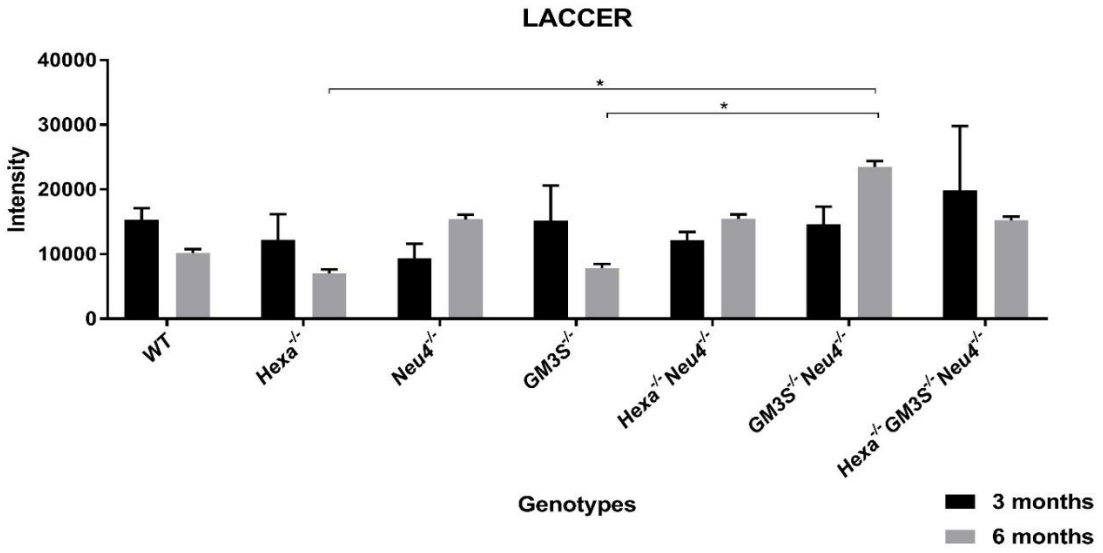

Figure 3.22: Lactosylceramide band intensity of 3 and 6-month *WT, Hexa*$^{-/-}$*, Neu4*$^{-/-}$*, GM3S*$^{-/-}$*, Hexa*$^{-/-}$*Neu4*$^{-/-}$*, GM3S*$^{-/-}$*Neu4*$^{-/-}$*, Hexa*$^{-/-}$*GM3S*$^{-/-}$*Neu4*$^{-/-}$genotyped mice thin layer chromatography results. (* describes $p<0.05$). In the experiment n=2 replicas were used. P values calculated with ANOVA. Error bars were calculated with ±SEM.

In Figure 3.22, there was 3.33-fold significant increase in 6-months-old *GM3S*$^{-/-}$ *Neu4*$^{-/-}$mice according to 6-months-old *Hexa*$^{-/-}$mice. 6-months-old *GM3S*$^{-/-}$*Neu4*$^{-/-}$mice illustrated 2.97-fold significant increase to the 6-month-old *GM3S*$^{-/-}$ mice. Rest of data shows no significant change between different and same age groups.

3.4. Immunohistochemistry

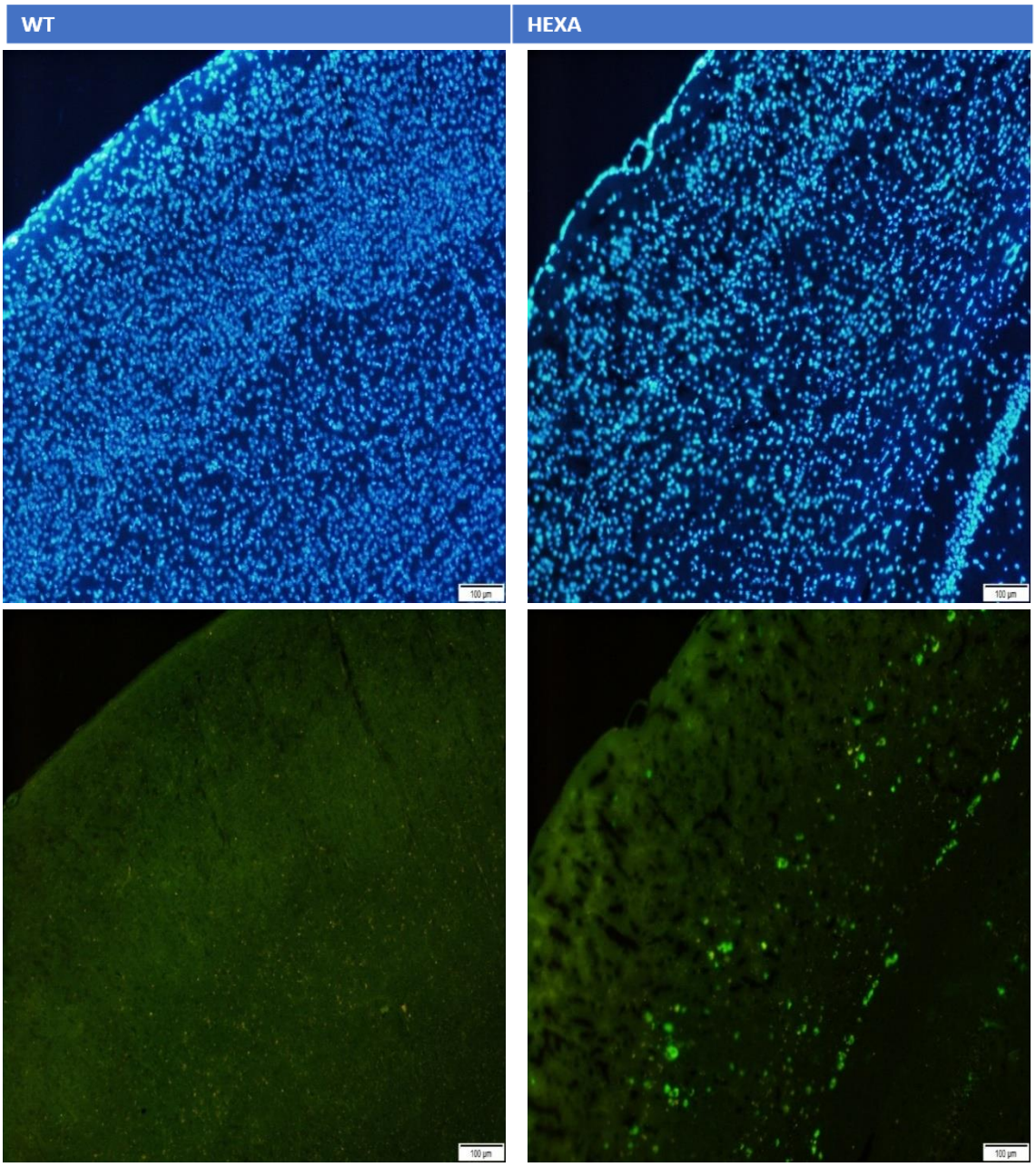

Figure 3.23: *6-months-old WT*, and *Hexa*$^{-/-}$ mice brain cortex region immunostaining with DAPI and GM2 (10x microscopic images). Blue color indicates DAPI and Green color indicates GM2 ganglioside.

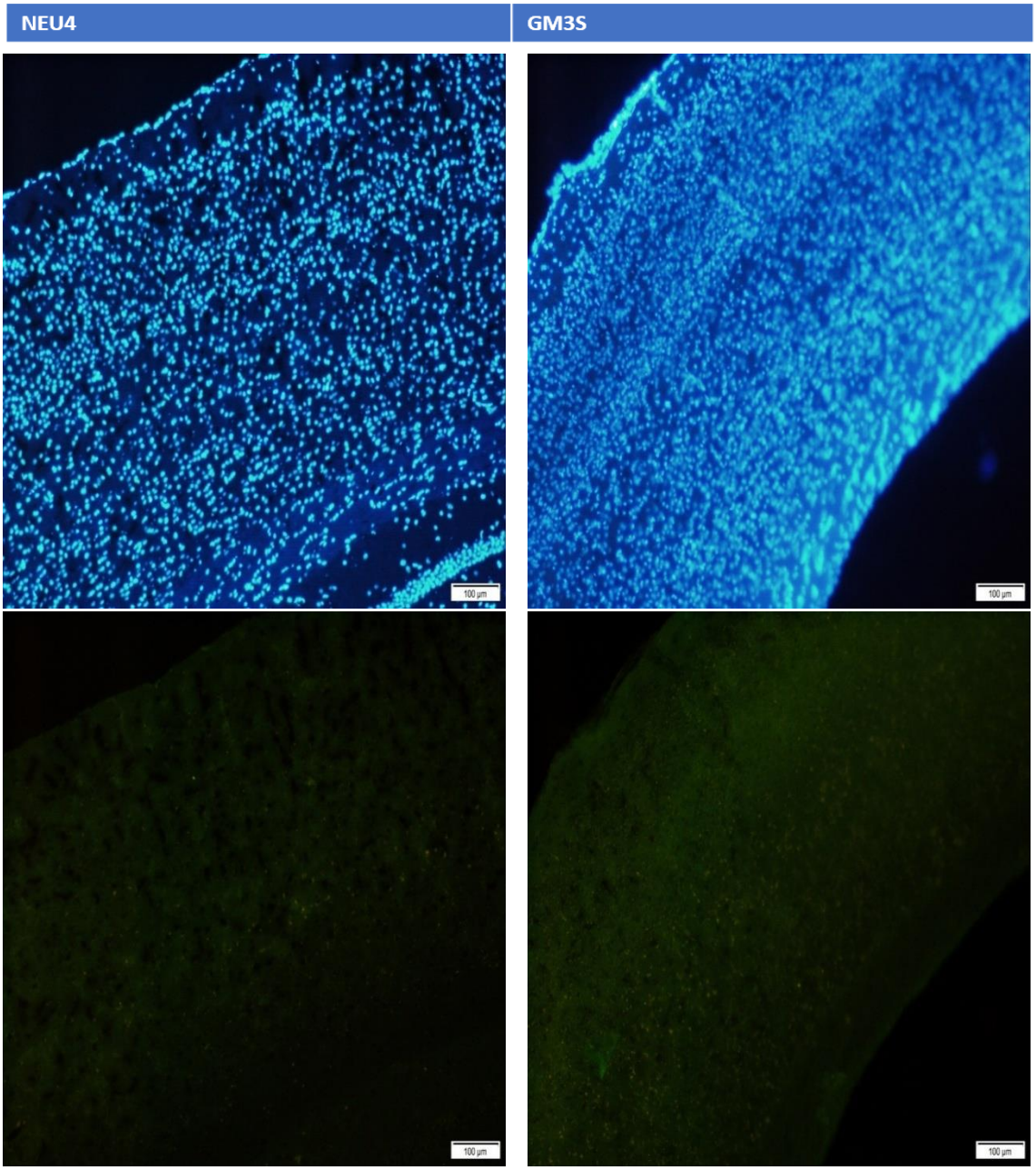

Figure 3.24: *6-months-old Neu4*$^{-/-}$, and *GM3S*$^{-/-}$ mice brain cortex region immunostaining with DAPI and GM2 (10x microscopic images). Blue color indicates DAPI and Green color indicates GM2 ganglioside.

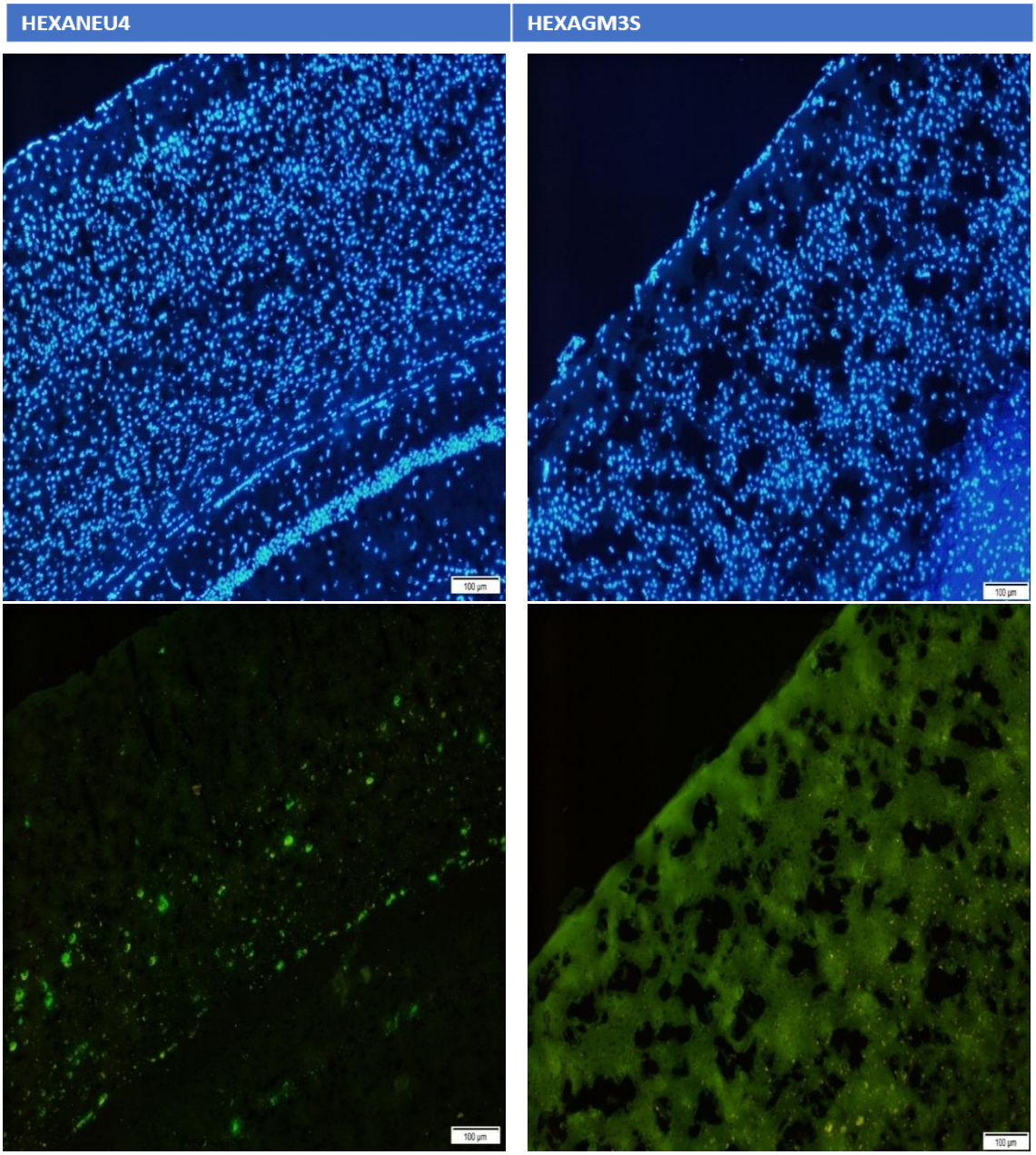

Figure 3.25: *6-months-old* Hexa$^{-/-}$GM3S$^{-/-}$, and GM3S$^{-/-}$Neu4$^{-/-}$ mice brain cortex region immunostaining with DAPI and GM2 (10x microscopic images). Blue color indicates DAPI and Green color indicates GM2 ganglioside.

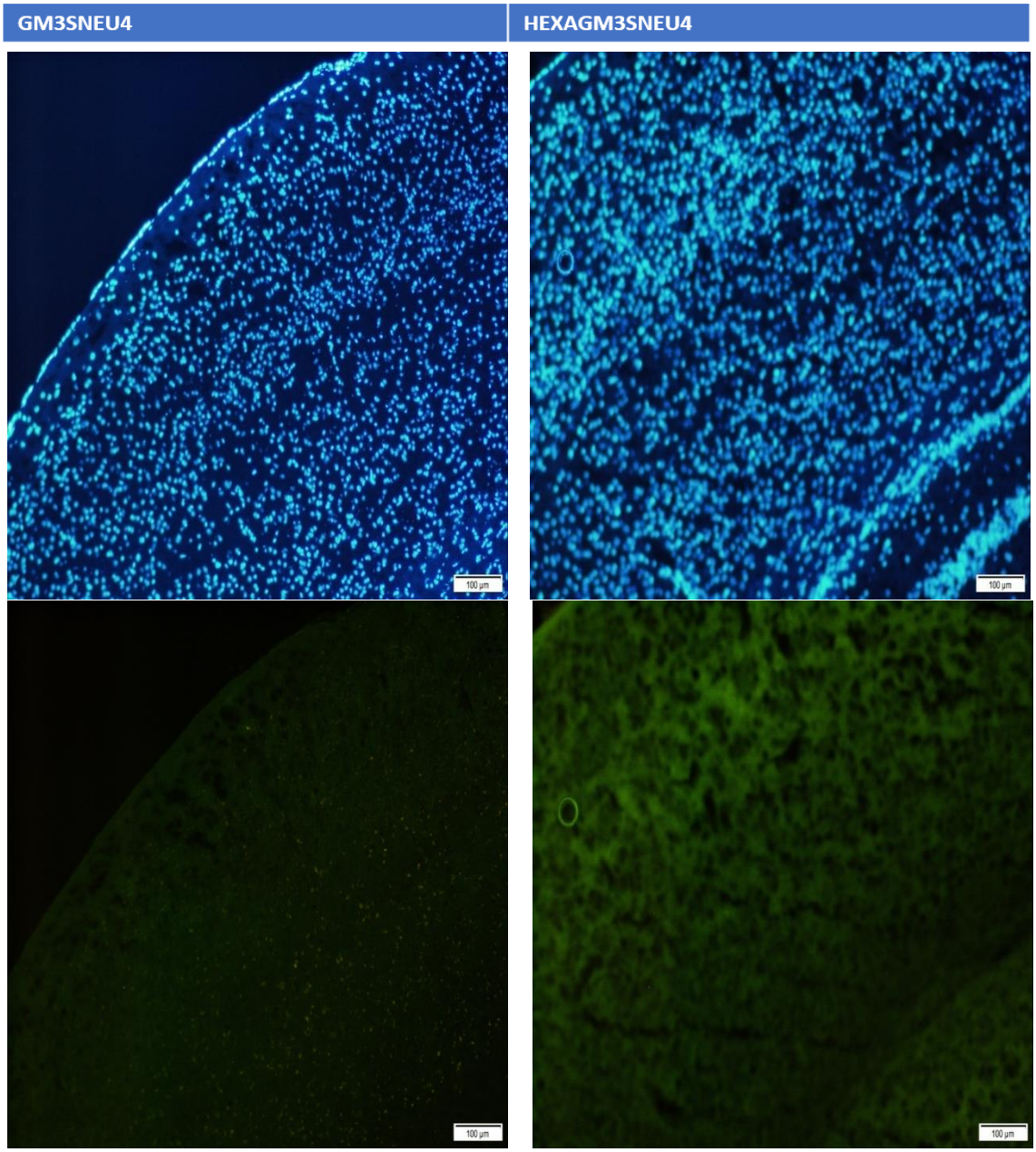

Figure 3.26: 6-months-old *GM3S*$^{-/-}$*Neu4*$^{-/-}$, and *Hexa*$^{-/-}$*GM3S*$^{-/-}$*Neu4*$^{-/-}$ mice brain cortex immunostaining with DAPI and GM2 (10x microscopic images). Blue color indicates DAPI and Green color indicates GM2 ganglioside.

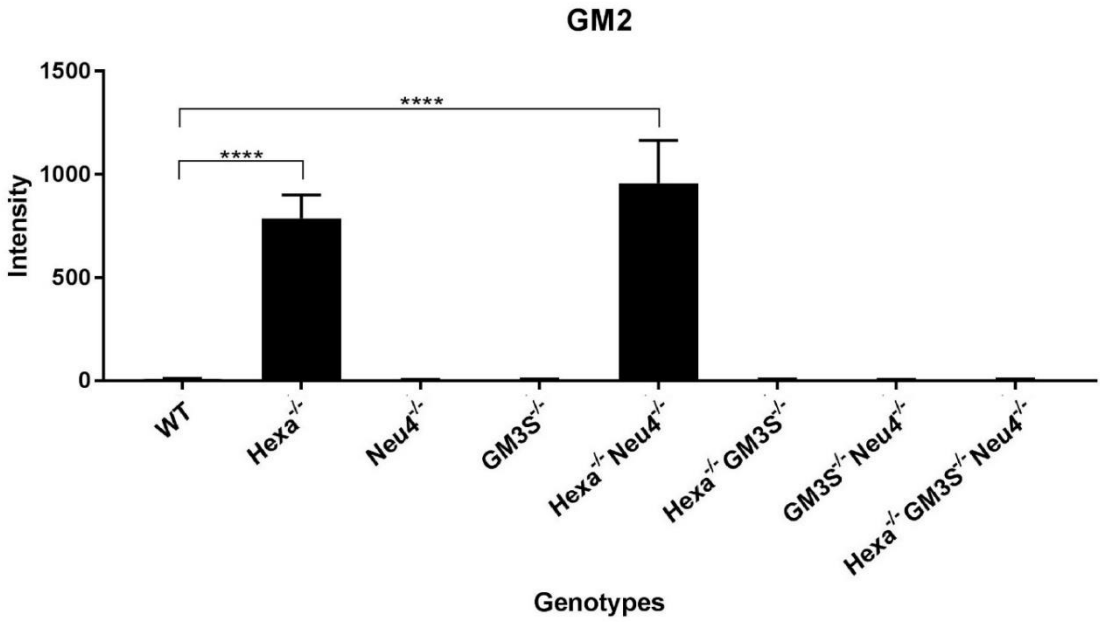

Figure 3.27: Graphs of GM2 accumulation counting on 6-months-old *WT, Hexa*$^{-/-}$, *Neu4*$^{-/-}$, *GM3S*$^{-/-}$, *Hexa*$^{-/-}$*Neu4*$^{-/-}$, *GM3S*$^{-/-}$*Neu4*$^{-/-}$, *Hexa*$^{-/-}$*GM3S*$^{-/-}$*Neu4*$^{-/-}$ mice brain cortex image (immunostained with GM2 in 10x) (* describes $p<0.05$, ** describes $p<0.01$ *** describes $p<005$ **** describes $p<0.0001$). In the experiment n=2 replicas were used from only 6-months-old animals. P values are caulculated with t-test. Error bars were calculated with ±SEM.

In Figure 3.27, green spots in GM2 staining shows in accumulation in related pictures. Blue pictures exhibit nuclei that is near to GM2 accumulation, so it means accumulation occur within the cell. There is no significant accumulation all genotypes except *Hexa*$^{-/-}$ and *Hexa*$^{-/-}$*Neu4*$^{-/-}$. This data is also observed by naked eye in Figure 3.21

.

CHAPTER 4

DISCUSSION

In this experiment, 3 months and 6-months-old *WT*, *Hexa*$^{-/-}$, *Neu4*$^{-/-}$, *GM3S*$^{-/-}$, *Hexa*$^{-/-}$*Neu4*$^{-/-}$, *Hexa*$^{-/-}$*GM3S*$^{-/-}$, *GM3S*$^{-/-}$*Neu4*$^{-/-}$, *Hexa*$^{-/-}$*GM3S*$^{-/-}$*Neu4*$^{-/-}$genotyped mice were produced for Realtime PCR analysis, and all different genotyped 3-months and 6-month-old mice were examined with 12 different gene (In Table2.2) to clarify Neu4 activity on GM3S and Hexa gene knockout mice in Figure 3.3-3.14. These 12 different genes are thought as generally as active on o-series and globo series gangliosides metabolism except GD3S. These genes were examined to see possible unknown pathway. 3-month and 6-month-old same genotyped animals and different genotyped animals with same age were compared to examine differences. Importance of these differences were indicated with * symbol. In Realtime PCR, ANOVA are used to calculate P-values. Expression level fold difference calculation between 2 dissimilar genotyped mice are determined by direct division of higher expression ratio to the lower expression ratio. In Realtime PCR genes, there was no change in B4GALT6, GD3S, and GM3S genes.

In Thin layer chromatography, *WT*, *Hexa*$^{-/-}$, *Neu4*$^{-/-}$, *GM3S*$^{-/-}$, *Hexa*$^{-/-}$*Neu4*$^{-/-}$, *GM3S*$^{-/-}$*Neu4*$^{-/-}$, *Hexa*$^{-/-}$*GM3S*$^{-/-}$*Neu4*$^{-/-}$mice brain lipids were isolated and displayed in TLC with different age groups which are 3 months and 6 months. In immunohistochemistry (IHC), 6-months-old *WT*, *Hexa*$^{-/-}$, *Neu4*$^{-/-}$, *GM3S*$^{-/-}$, *Hexa*$^{-/-}$*Neu4*$^{-/-}$, *Hexa*$^{-/-}$*GM3S*$^{-/-}$, *GM3S*$^{-/-}$*Neu4*$^{-/-}$, *Hexa*$^{-/-}$*GM3S*$^{-/-}$*Neu4*$^{-/-}$genotyped mice brain cortex regions were cut and stained with GM2 and DAPI. In TLC and IHC results, *Hexa*$^{-/-}$and *Hexa*$^{-/-}$*Neu4*$^{-/-}$deficient mice confirmed GM2 accumulation in Figure 3.15, 3.17, 3.19 and displayed by immunochemistry image with GM2 in Figure 3.23-3.27.

It is known that GM2 ganglioside accumulation present in *Hexa*$^{-/-}$and *Hexa*$^{-/-}$ *Neu4*$^{-/-}$ mice between 3 months and 6 months groups (Seyrantepe et al., 2010). TLC data of 3 and 6 months animals and Immunohistochemistry data of 6 months animals confirmed that GM2 ganglioside accumulation were shown in *Hexa*$^{-/-}$and *Hexa*$^{-/-}$*Neu4*$^{-/-}$ mice. By combination *GM3S*$^{-/-}$mice with *Hexa*$^{-/-}$and *Neu4*$^{-/-}$ *Hexa*$^{-/-}$mice, GM2

accumulation replenished and turned condition to normal because GM2 synthesis needs GM3 which are controlled by GM3 synthase enzyme. This study also confirmed that there is probably no or less active alternative pathway to synthesize GM2 from lactosylceramide in mice. In this respect, gene expression levels of these organisms indicate that *GM3S*$^{-/-}$ mice do not use GM2. Since there is no change in lifetime according to wildtype phenotype until 6 months of age, it also raises the following question about whether a, b, c series gangliosides is important or not. Since GM3 synthase deficiency are observed in human, this implies that a, b, and c series gangliosides are important. Although mice do not have GM3S synthase enzyme, mice did not display human symptoms such as unbale to sit unsupported, or walk. Therefore, mice can use alternative pathway to produce these gangliosides, or these gangliosides may not so important function in mice as in human.

In GM2 accumulation, *Hexa*$^{-/-}$ mice can escape disease by keeping GM2 accumulation below toxic level (Phaneuf et al., 1996) despite human cannot tolerate situation. *Hexa*$^{-/-}$*Neu4*$^{-/-}$ mice exhibited more serious conditions than *Hexa*$^{-/-}$ mice and GM2 accumulation (Seyrantepe et al., 2010). In this study, 6-month-old *Hexa*$^{-/-}$*Neu4*$^{-/-}$ mice showed increase to the 6-month-old *Hexa*$^{-/-}$ mice as in previous study(Seyrantepe et al., 2010). Those results are consistent with immunohistochemistry results as represented a former (Seyrantepe et al., 2010). In this study, *Hexa*$^{-/-}$*GM3S*$^{-/-}$, and *Hexa*$^{-/-}$ *GM3S*$^{-/-}$*Neu4*$^{-/-}$ mice are observed in terms of presence of alternative pathway that are mentioned above. However, there were no GM2 accumulation in immunohistochemistry (Figure 3.23-27), and no GM2 and GM3 (Figure 3.20 and 3.21) band in TLC. These results suggest that GM3 and GM2 is not produced in these organisms because if GM2 had existed in *GM3S*$^{-/-}$ genotyped mice, there would have been brief accumulation in *Hexa*$^{-/-}$*GM3S*$^{-/-}$, and *Hexa*$^{-/-}$*GM3S*$^{-/-}$*Neu4*$^{-/-}$ mice. But there was no any GM2 accumulation both *Hexa*$^{-/-}$*GM3S*$^{-/-}$, and *Hexa*$^{-/-}$*GM3S*$^{-/-}$*Neu4*$^{-/-}$ mice in Figure 3.27 and 3.20. Since *Hexa*$^{-/-}$ genotyped mice exhibited GM2 accumulation in the presence of GM2, if GM2 present, there should be accumulation in *Hexa*$^{-/-}$*GM3S*$^{-/-}$, and *Hexa*$^{-/-}$*GM3S*$^{-/-}$*Neu4*$^{-/-}$ mice. On the other hand, there is also possibility to produce small amount of GM2 and GM3 for *Hexa*$^{-/-}$*GM3S*$^{-/-}$, and *Hexa*$^{-/-}$*GM3S*$^{-/-}$*Neu4*$^{-/-}$ mice if there were alternative unknown pathway to the known ganglioside pathway. However, since there was no even small amount of accumulation in *Hexa*$^{-/-}$*GM3S*$^{-/-}$, and *Hexa*$^{-/-}$*GM3S*$^{-/-}$ *Neu4*$^{-/-}$ mice, escaping GM2 accumulation in these mice are not used due to missing of

GM2. Thus, lacking GM2 and GM3 in *Hexa*$^{-/-}$*GM3S*$^{-/-}$, and *Hexa*$^{-/-}$*GM3S*$^{-/-}$*Neu4*$^{-/-}$ mice idea is more accurate explanation for this situation. In other words, it can be predicted that there is no GM2 and GM3 in *GM3S*$^{-/-}$, *Hexa*$^{-/-}$*GM3S*$^{-/-}$, *GM3S*$^{-/-}$*Neu4*$^{-/-}$, and *Hexa*$^{-/-}$ *GM3S*$^{-/-}$*Neu4*$^{-/-}$ mice. These results are consistent with known ganglioside pathway.

Another important idea is blocking GM3 synthesis. If GM3 synthesis can be blocked in any way in Tay-Sachs mice, GM2 accumulation effects may returns normal. Blocking GM3 synthase can be also beneficial for human. Since complete blocking in GM3S enzyme caused disease, may be partial blocking of GM3S could be helpful for escaping toxic GM2 accumulation because mice can live with GM2 accumulation. On the other hand, there is no known GM3S blocking agent.

Combination Neu4 deficiency with *Hexa*$^{-/-}$*GM3S*$^{-/-}$ and *GM3S*$^{-/-}$ mice was also made to demonstrate Neu4 relation with other sialidases for o-series and globo series gangliosides and lactosylceramide. Since *GM3S*$^{-/-}$ mice which normally have o-series and globo-series ganglioside can escape from death, and *GM3S*$^{-/-}$ mice do not have a-, b- and c- series gangliosides. Sialidases may contribute ganglioside synthesis and degradation. Neu4 role is known in ganglioside metabolism by acting on GM1 but other sialidases except Neu3 are not clear. Neuraminidase 4 is also effective on bypass mechanism in Hexaminidase A deficiency. For this reason, Neuraminidase 4 preferred among other sialidases.

In 3-month-old *Hexa*$^{-/-}$*GM3S*$^{-/-}$*Neu4*$^{-/-}$mice brain cortex region, BGAL expression ratio increased in response to lack of gangliosides when compared with other genotypes. However, there was no change in B3GALT4 which is reverse enzyme of BGAL, and B3GALT4 is synthases GA1 from GA2, but BGAL degrades GA1 into GA2. And, there was no increase in Hexb activity to the wild type. There was also no significant change in lactosylceramide level according to the wild type and other genotypes. Besides, to supply the place of Neu4, 3-months-old *Hexa*$^{-/-}$*GM3S*$^{-/-}$*Neu4*$^{-/-}$ mice preferred to increase expression level of Neu2 instead of Neu3. Degradation enzyme (BGAL) were increase but synthesis enzyme (B3GALT4) concentration and lactosylceramide level and other related enzyme showed no significant change. Other gangliosides concentrations and globo series gangliosides related enzymes expression levels are required to make any interpretation about these results. On the other hand, Neu2 level increase may be absence of Neu4 and Hexa together.

In 6-months old *Hexa*$^{-/-}$*GM3S*$^{-/-}$*Neu4*$^{-/-}$mice B3GALT4 expression level were decreased according to 3-month-old *Hexa*$^{-/-}$*GM3S*$^{-/-}$*Neu4*$^{-/-}$mice. And BGAL expression level showed no difference between wild type and 3-month-old *Hexa*$^{-/-}$*GM3S*$^{-/-}$*Neu4*$^{-/-}$ mice. This may imply slight decrease of expression but this change was lesser expected.

In 3-month-old *GM3S*$^{-/-}$*Neu4*$^{-/-}$ mice, there was significant increase in Neu2, Hexb and Neu3 according to other 3-months-old other genotypes. 4.48-fold increase to the WT for Neu2, 4.15 -fold to the WT for Neu3, and 3.20-fold increase to the WT for Hexb are mentioned in results (see Figure 3.4 and 3.5). When lactosylceramide data of 3 months old *GM3S*$^{-/-}$*Neu4*$^{-/-}$mice TLC results display no significant change. In addition, B4GALT6 activity displayed no change between all genotypes. However, there was significant increase in lactosylceramide level of 6-months-old *GM3S*$^{-/-}$*Neu4*$^{-/-}$ mice to the 6-month-old *Hexa* $^{-/-}$, and *GM3S*$^{-/-}$ mice (3.33-fold and 2.97-fold respectively) in Figure 3.22. Therefore, since Hexb is degradation enzyme for lactosylceramide and GM3S enzyme is blocked. These data may relate to later slight increase lactosylceramide level in *GM3S*$^{-/-}$*Neu4*$^{-/-}$ mice due to degradation enzyme increase. In other words, degradation enzyme enhancement in *GM3S*$^{-/-}$*Neu4*$^{-/-}$ mice may not display any effect on lactosylceramide in short term because degrading and synthesizing enzyme of lactosylceramide are still active. And this change occurs the most probably due to Hexb enzyme expression increase. Although lactosylceramide level increased, mice live as normal until 6 months of age. Expression level change were generally occurring at 3-4-fold and lactosylceramide level change was approximately 3-fold. And changes in ratio may not be toxic for mice due to no abnormal situation. On the other hand, in TLC data, 3-months-old *GM3S*$^{-/-}$ mice GM1 level were increase according to *Neu4* $^{-/-}$ that may solution of depletion GM1 in Neu4. Besides, 3-months-old *GM3S*$^{-/-}$*Neu4*$^{-/-}$mice did not show significant difference among other 3-months-old mice and 6-months-old *GM3S*$^{-/-}$*Neu4*$^{-/-}$mice. Therefore, GM1 increase returns normal in *GM3S*$^{-/-}$*Neu4*$^{-/-}$mice with absence of Neu4 enzyme.

In *Hexa* $^{-/-}$ *GM3S*$^{-/-}$ mice, (2.47-fold) Neu1 and (7.9-fold) Neu2 expression increased in 6-months-old animals to the 3-months-old animals but Neu3 expression level stayed the same to the wild type. Neu4 expression level decreased to the wild type (3.31-fold). This decrease is plausible because Neu4 role on GD1a substrate conversion into GM1 in mice are known (Seyrantepe et al., 2008). In addition, GD1a is a series ganglioside that are not present in *Hexa* $^{-/-}$ *GM3S*$^{-/-}$ mice according to known

ganglioside pathway. Later increase of Neu1 and Neu2 showed that gangliosides concentration changes with age.

In 6-month-old *GM3S*$^{-/-}$ genotyped mice, there was significant change in GM2AP with other genotypes such as 6.26-fold increase to the WT. 6-month-old *GM3S*$^{-/-}$ mice have exhibited 2.29-fold increase for GALGT1, 1.70-fold increase for BGAL expression, 3.09-fold increase for Neu2 expression, 1.89-fold increase for Neu3 expression, and 1.51-fold increase for Neu4 expression according to the 3-month-old *GM3S*$^{-/-}$ mice. 3-month-old *GM3S*$^{-/-}$ mice displayed that there is no significant difference to the other genotyped. And the difference was 7.34-fold between 3-month and 6-month-old *GM3S*$^{-/-}$ mice. Thus, increase in GM2AP level in 6-month-old *GM3S*$^{-/-}$ micecan be explained by other genotypes. It can be also predicted that GM3S absence effect are observed in long term. lactosylceramide level of 6-month-old *GM3S*$^{-/-}$ mice represented no significant change to the other ganglioside. Organism may have preferred lactosylceramide conversion to other gangliosides to escape toxicity. To Prevent lactosylceramide accumulation, there may be two ways. One way is to synthesize GA2 from lactosylceramide and further o-series gangliosides. Another way is to synthesize globo series gangliosides. Since o-series related enzyme change are observed, organism in need of gangliosides may trigger to GALGT1 to synthesize GA2. And to prevent excess of these gangliosides accumulation such as GM1b and GD1c, BGAL expression level may increase to endure this harsh condition. Nevertheless, although GALGT1 expression level increase, there was no increase in the level of Hexb concentration. And B3GALT4 level illustrated also no change to 3-month-old *GM3S*$^{-/-}$ mice despite BGAL level had increase to the 3-month-old *GM3S*$^{-/-}$ mice. And since lactosylceramide level did not changed, o-series ganglioside level should as well as GA2 increase. Therefore, these results need further study for explanation. And if *GM3S*$^{-/-}$ mice are studied, higher age will be better to observe differences because 3-month-old *GM3S*$^{-/-}$ mice did not displayed notable change.

In GM1 (Figure 3.19) TLC data, 6- months-old wild type mice TLC exhibited 3.17-fold and 10.92-fold increase to the 6-month-old *Neu4*$^{-/-}$ and *Hexa*$^{-/-}$*GM3S*$^{-/-}$*Neu4*$^{-/-}$ mice. GM1 level decrease in *Neu4*$^{-/-}$ mice are known (Seyrantepe et al., 2008). Although *GM3S*$^{-/-}$*Neu4*$^{-/-}$ mice did not show any change to the other genotypes, 6-month-old *Hexa*$^{-/-}$*GM3S*$^{-/-}$*Neu4*$^{-/-}$ mice represented a significant decrease to the 6-month-old *WT*, *GM3S*$^{-/-}$ and *Hexa*$^{-/-}$*Neu4*$^{-/-}$ mice. Absence of *Hexa*$^{-/-}$ in 6-month-old

Hexa$^{-/-}$*GM3S*$^{-/-}$*Neu4*$^{-/-}$ mice may cause to decrease of GM1 level. Nonetheless, mechanism is not clear. And lack of GM3S probably have no effect on GM1.

In lactosylceramide level in Figure 3.22, there was no significant decrease in *Hexa*$^{-/-}$ mice to the wildtype although GM2 accumulation were consistent with immunohistochemistry results of *Hexa* mice. *Hexa*$^{-/-}$ mice showed significant decrease to the 6-momnth-old *GM3S*$^{-/-}$*Neu4*$^{-/-}$mice, though it is not important for *Hexa*$^{-/-}$ mice owing to no change with other genotypes. What is more, in 6-momnth-old *GM3S*$^{-/-}$ *Neu4*$^{-/-}$ mice, there was significant increase for lactosylceramide according to 6-months-old *GM3S*$^{-/-}$. Increase of lactosylceramide level in 3-month-old *GM3S*$^{-/-}$*Neu4*$^{-/-}$mice can be explained by increase of Hexb. Due to the in vitro lactosylceramide producing activity from GM3 of human Neu2 and Neu3 enzyme (T. Miyagi & Yamaguchi, 2012), *GM3S*$^{-/-}$*Neu4*$^{-/-}$ mice can be considered as having the same activity in lactosylceramide mechanism, but GM3 is not present in *GM3S*$^{-/-}$*Neu4*$^{-/-}$ mice. In addition, in vitro Neu3 activity against Gb3 degradation into lactosylceramide are also represented (Wada et al., 2007). This approach is consistent with the 1.52-fold lactosylceramide increase explanation to the wild type because lactosylceramide synthesis and degradation are controlled probably at least 6 different kind of enzyme and increase in 4.15-fold Neu3 and 3.20-fold Hexb are appear to consistent with this situation. However, 1.50 increase of lactosylceramide to the wild type is not accepted significant to the ANOVA. 3.33-fold increase to the *Hexa* $^{-/-}$ mice and 2.97-fold increase to the *GM3S*$^{-/-}$ mice were significant to the 6-month-old *GM3S*$^{-/-}$*Neu4*$^{-/-}$ mice as mentioned above. Therefore, it can be said that there is increase in lactosylceramide level in 6-month-old *GM3S*$^{-/-}$*Neu4*$^{-/-}$ mice.

Since 6-month-old *GM3S*$^{-/-}$*Neu4*$^{-/-}$mice was different from *GM3S*$^{-/-}$ in terms of Neu4 gene, absence of Neu4 in *GM3S*$^{-/-}$*Neu4*$^{-/-}$ may causes directly increase of lactosylceramide. In other words, Neu4 may have role in lactosylceramide regulation but Neu2 and Neu3 are not. When *Neu4*$^{-/-}$ and wild type mice are compared, there was Neu3 level 1.80-fold increase in 6-month-old *Neu4*$^{-/-}$ mice to the 3-month-old *Neu4*$^{-/-}$ mice. Although Neu2, Neu3, and Neu4 represented 34-40% homology to each other, amino acid identity of Neu1 are approximately 19-24% to the others (T. Miyagi & Yamaguchi, 2012). And when *GM3S*$^{-/-}$*Neu4*$^{-/-}$ and *GM3S*$^{-/-}$ mice compared together, Hexb, Neu2, and Neu3 expression levels are also increased as described above. Therefore, these changes may occur because of compensation for absence of Neu4. In

other words, since amino acid sequence is more closely to the Neu2 and Neu3 closer to the Neu4, absence of Neu4 organism can prefer increase of Neu2 and Neu3. Hexb increase may be the result of this situation. It was also known that gb3, igb3 and GM3 and GA2 can synthesize and degrade into lactosylceramide. Increase of Hexb, Neu2 and Neu3 is also exhibits that Neu4 have quite possibly role in GA2, gb3 or igb3 degradation into lactosylceramide.

In Neu1 expression level in Figure 3.3, 3-months-old *GM3S*$^{-/-}$*Neu4*$^{-/-}$ and *Hexa*$^{-/-}$*GM3S*$^{-/-}$*Neu4*$^{-/-}$ mice exhibited extremely low expression. However, it returns normal in 6-month-old animals. Due to abnormalities in crucial enzyme of *GM3S*$^{-/-}$*Neu4*$^{-/-}$ mice may cause late response to response in these organisms. In addition, 3-month-old *Hexa*$^{-/-}$*GM3S*$^{-/-}$ mice are illustrated 2.47-fold decrease to the 6-month-old *Hexa*$^{-/-}$*GM3S*$^{-/-}$ mice and 1.56-fold decrease to the 3-month-old *Hexa*$^{-/-}$ mice. These results only support that ganglioside metabolism change during development. What further elucidation can be done to these results is not uncovered.

In Neu2 (Figure 3.4), there was significant decrease in 3-month-old *GM3S*$^{-/-}$ and *Hexa*$^{-/-}$*GM3S*$^{-/-}$ ice to the 3-monnth-old *GM3S*$^{-/-}$ mice. In addition, 3-month-old *GM3S*$^{-/-}$ *Neu4*$^{-/-}$ and mice exhibited significant increase to other all genotypes within the same age. Since 3-monnth-old *GM3S*$^{-/-}$ mice showed no significant difference to the wild type and Neu4 are absent in both *GM3S*$^{-/-}$*Neu4*$^{-/-}$, and *Hexa*$^{-/-}$*GM3S*$^{-/-}$*Neu4*$^{-/-}$ mice, these results also support that *Neu4* presence have role in o series, or/and globo series ganglioside pathway and Neu2 is tried to compensate *Neu4* during early development stage (as mentioned in above). 3.5-fold mean decrease in Neu2 are also noted in 3-month-old *Hexa*$^{-/-}$*GM3S*$^{-/-}$ mice to the 3-month-old WT mice but it was not significant according to ANOVA.

In Neu3 (Figure 3.5), 3-month-old *GM3S*$^{-/-}$*Neu4*$^{-/-}$ mice exhibited increase to the wild type and other genotypes. Significant increase of Neu3 is due to compensation of Neu4 in *GM3S*$^{-/-}$*Neu4*$^{-/-}$ mice. 6-month-old. These results also strengthen the idea of Neu4 function in lactosylceramide metabolism. Increase of Neu3 in 6-month-old *Hexa*$^{-/-}$, *Neu4*$^{-/-}$, *GM3S*$^{-/-}$ mice to the 3-month-old littermate refer can explain later demand on Neu3 in these organisms. These differences were approximately 1.80-fold. These changes only describe ganglioside metabolism change by age. 6-month-old *Hexa*$^{-/-}$ *Neu4*$^{-/-}$ mice illustrated approximately 1.72-fold decrease to the *Hexa*$^{-/-}$, and *Neu4*$^{-/-}$

mice. 6-month-old *Hexa*$^{-/-}$*GM3S*$^{-/-}$*Neu4*$^{-/-}$ mice displayed roughly 1.82-fold decrease to the *Hexa*$^{-/-}$, and *Neu4*$^{-/-}$ mice. *Hexa*$^{-/-}$, and *Neu4*$^{-/-}$ mice. 6-month-old *Hexa*$^{-/-}$*GM3S*$^{-/-}$ mice illustrated 2.01-fold decrease to the *Hexa*$^{-/-}$ mice. It is hard to make a statement about these changes by alone.

In Neu4 (Figure 3.6), 6-month-old *Hexa*$^{-/-}$*GM3S*$^{-/-}$ mice have revealed roughly 3.6-fold decrease to the others including 6-month-old *GM3S*$^{-/-}$ mice. These results intimate that due to Neu4 function in a-, b-, c- series ganglioside, unnecessary Neu4 production is decreased but *GM3S*$^{-/-}$ mice also do not possess a-, b-, c- series ganglioside. Therefore, Neu4 may be indirectly effective on o-and globo series ganglioside with Hexa. Increasing Neu4 in 6-month-old *Hexa*$^{-/-}$, and *GM3S*$^{-/-}$ mice to the 3-month-old littermate also fortify that ganglioside metabolism change by age.

In Hexb (Figure 3.7), 3-month-old *GM3S*$^{-/-}$*Neu4*$^{-/-}$ mice displayed significant increase to the other genotypes. However, 6-month-old *GM3S*$^{-/-}$*Neu4*$^{-/-}$ mice illustrated decrease to the other genotypes except *Hexa*$^{-/-}$, *Hexa*$^{-/-}$*GM3S*$^{-/-}$, and *Hexa*$^{-/-}$*GM3S*$^{-/-}$*Neu4*$^{-/-}$ mice. When we compared two results with wild type, 3-month-old *GM3S*$^{-/-}$*Neu4*$^{-/-}$ mice has 3.20-fold increase to the wild type, and 6-month-old *GM3S*$^{-/-}$*Neu4*$^{-/-}$ mice has 2.00-fold decrease to the wild type. Therefore, increase of 3-month-old *GM3S*$^{-/-}$*Neu4*$^{-/-}$ mice were higher than 6-month-old *GM3S*$^{-/-}$*Neu4*$^{-/-}$ mice. In addition, 6-month-old Hexa absent mice did not show significant decrease to the 6-month-old *GM3S*$^{-/-}$*Neu4*$^{-/-}$ mice. Consequently, Hexb level increase to the all organism are not compatible with its reverse enzyme GALGT1. If there is no change in enzyme concentration for synthesis of GA2, which enzyme organism uses in reverse mechanism is unclear.

In GM2AP (Figure 3.8), 6-month-old *GM3S*$^{-/-}$ mice indicate significant difference to the other genotypes except *GM3S*$^{-/-}$*Neu4*$^{-/-}$ mice. This change was 7.39-fold to the wild type. According to these results, since wild type animals have both Hexa gene and GM2 ganglioside, there were no difference in GM2AP expression. In *Hexa*$^{-/-}$ mice, there is no Hexa gene but there is GM2 ganglioside. In *GM3S*$^{-/-}$ mice, there is no GM2 ganglioside but there is Hexa gene. In other words, in the 6-month-old *GM3S*$^{-/-}$ mice, Hexa gene may prefer to increase GM2AP for degradation of GM2, However, since there is no GM2AP, GM2AP cannot bind GM2 ganglioside. Therefore, these results represents that increase of GM2AP level ignition may be caused by Hexa gene. Other genotypes results are also support this situation except *GM3S*$^{-/-}$*Neu4*$^{-/-}$

because *GM3S*$^{-/-}$*Neu4*$^{-/-}$ mice represented no significant change although they have Hexa gene but no GM2 ganglioside. On the other hand, *GM3S*$^{-/-}$*Neu4*$^{-/-}$ mice represented 4.18-fold increase to the wild type in both 3 months and 6 months old animals. Although increase of GM2AP in *GM3S*$^{-/-}$*Neu4*$^{-/-}$ mice put forward this theory, it is not significant according to ANOVA.

In BGAL (Figure 3.9), 3-month-old *Hexa*$^{-/-}$*GM3S*$^{-/-}$*Neu4*$^{-/-}$mice indicated significant difference to the other genotypes. In addition, *GM3S*$^{-/-}$mice illustrated increase by age. There was also significant decrease 6-month-old *GM3S*$^{-/-}$*Neu4*$^{-/-}$mice to the 6-month-old *GM3S*$^{-/-}$mice. Since BGAL associated indirectly with Hexa, GM3S and Neu4 gene according to known pathway, arguing these results alone is not coherent. On the other hand, reverse enzyme of BGAL is B3GALT4, and there was no significant change in reverse enzyme of BGAL. Therefore, which enzyme takes part in this metabolism is uncertain.

In *Hexa*$^{-/-}$*GM3S*$^{-/-}$ mice comparison to the *Hexa*$^{-/-}$ mice, lacking GM3S in 3month old *Hexa*$^{-/-}$*GM3S*$^{-/-}$ mice causes Neu1 expression level decrease. This may evoke that Neu1 have a role in a-, b-, and c- series ganglioside. Lacking GM3S for the 6-month-old animals can also causes reduction in Neu4 production. This remind that Neu4 role in GM1 and GD1a which is the a-, b-, and c- series ganglioside. Neu3 level also decreased in 6-month-old *Hexa*$^{-/-}$*GM3S*$^{-/-}$ mice to the 6-month-old *Hexa*$^{-/-}$ mice. In general, substrate level decrease of Neu4, Neu1 and Neu3 may represent a cause for decrease in their concentration. Neu2 does not show any change between *Hexa*$^{-/-}$*GM3S*$^{-/-}$ mice and *Hexa*$^{-/-}$ mice. This enzyme may not have a function in a-, b-, and c- series ganglioside. On the other hand, those changes are not observed in other age. This may also be due to for temporarily defect and there may not have a relation with each other.

In *Hexa*$^{-/-}$*GM3S*$^{-/-}$ mice comparison to *GM3S*$^{-/-}$ the mice, absence of Hexa gene exhibited to decrease of Neu4 and GM2AP level. GM2AP level decrease, as mentioned, are consistent with the Hexa dependent increase of GM2AP in the absence of GM2. Neu4 level decrease refers to Hexa dependent direct/indirect function.

In *GM3S*$^{-/-}$*Neu4*$^{-/-}$ mice comparison to *GM3S*$^{-/-}$ the mice, Neu4 blocking causes increase of Hexb and Neu2 and Neu3 between 3-month-old animals. In 6-month-old animals, there was lactosylceramide increase. Since Neu4 role in synthesizing

ganglioside from lactosylceramide probability is too low, lactosylceramide increase were interpreted due to Hexb. Neu2, and Neu3 increase.

GM3S$^{-/-}$*Neu4*$^{-/-}$ mice comparison to *Neu4*$^{-/-}$ the mice and deprivation of GM3S in *GM3S*$^{-/-}$*Neu4*$^{-/-}$ mice displayed that Neu2, Neu3 and Hexb level augmented in 3 months old animals but Hexb level change went down in 6-month-old animals. In the absence of Neu4, organism preference to other sialidases are expected. However, these results refer that Neu2, Neu3 and Hexb expression increases are probably related with o-, and globo- series gangliosides. Decline in 6-month-old animal Hexb may occur due to excess augmentation of Hexb in 3-month-old animals. Another possibility is that change in Neuraminidases control Hexb expression.

In *GM3S*$^{-/-}$*Neu4*$^{-/-}$ mice comparison to *Hexa*$^{-/-}$*GM3S*$^{-/-}$*Neu4*$^{-/-}$ mice, absence of Hexa in *Hexa*$^{-/-}$*GM3S*$^{-/-}$*Neu4*$^{-/-}$ mice causes Hexb and Neu3 level decreases in 3-month-old animals. Therefore, although there is no GM2 in the medium, Hexa may have another function these organisms from degrading GM2. This function appears as not lethal because organism can live until 6-month-old age. And Hexa takes probably part in globo or o-series ganglioside metabolism owing to missing of a-, b-, and c- series gangliosides.

In *Hexa*$^{-/-}$*GM3S*$^{-/-}$ mice comparison to *Hexa*$^{-/-}$*GM3S*$^{-/-}$*Neu4*$^{-/-}$ mice, missing Neu4 leads to increase of Neu2 and BGAL. Since the only difference Neu4 in *Hexa*$^{-/-}$*GM3S*$^{-/-}$ *Neu4*$^{-/-}$ mice, Neu2 absence may related with o and globo series ganglioside function. However, it is expected absence Neu4 causes also Neu3 and Hexb level increase in the *GM3S*$^{-/-}$*Neu4*$^{-/-}$ comparison to the *GM3S*$^{-/-}$. the Since Hexb and Neu3 decreased in Hexa absence in *Hexa*$^{-/-}$*GM3S*$^{-/-}$*Neu4*$^{-/-}$ mice to the *GM3S*$^{-/-}$*Neu4*$^{-/-}$. No change in Neu3 and Hexb level are due to Hexa absence in both *Hexa*$^{-/-}$*GM3S*$^{-/-}$ and *Hexa*$^{-/-}$*GM3S*$^{-/-}$*Neu4*$^{-/-}$ mice. Therefore, deprivation of Neu4 in *GM3S*$^{-/-}$*Neu4*$^{-/-}$ mice causes Neu2 and Neu3 and Hexb level increase for the o- and globo-series gangliosides. BGAL level increase requires more experiment for clarification. When *Hexa*$^{-/-}$*Neu4*$^{-/-}$ compared with *Hexa*$^{-/-}$ *GM3S*$^{-/-}$*Neu4*$^{-/-}$ mice, *Hexa*$^{-/-}$*GM3S*$^{-/-}$*Neu4*$^{-/-}$ displayed that BGAL level increase and GM1 level decline are observed.

Consequently, Neu4 can be compensated by Neu2 and Neu3 in developmental stage, but these gangliosides return normal for later stage without a-, b- and c- series gangliosides, but it is not sufficient to reduce drawbacks of Neu4 deficiency. In this

study, *GM3S*$^{-/-}$, *Hexa*$^{-/-}$*GM3S*$^{-/-}$, *Hexa*$^{-/-}$*GM3S*$^{-/-}$*Neu4*$^{-/-}$ mice with TLC and immunohistochemistry data indicates that there is no alternative pathway to synthesize GM2 from lactosylceramide And Neu4 is essential for lactosylceramide, o-series ganglioside and globo series ganglioside metabolism due to *Hexa*$^{-/-}$*GM3S*$^{-/-}$ mice results. However, Neu4 concentration *Hexa*$^{-/-}$*GM3S*$^{-/-}$ mice may occur because of substrate in a-, b- and c- series ganglioside absence.

4.1. Future Direction

To determine what happened o-series ganglioside and globo series gangliosides with these enzyme, LC/MS/MS and DESI-MS studies are required. These experiments are going to be useful because some of their enzyme expression level determined but enzyme concentrations are not known. Some of them may not be converted into the enzyme. In addition, there is also possibility to no change in ganglioside concentration. Therefore, investigation of ganglioside concentration is also essential for determining detail function. Mass spectrometric analysis with these data will probably represent novel pathway in these mice, because in GM3S deficient symptoms in human are much advanced than mice.

For immunohistochemistry, there can be used also different marker to investigate other gangliosides changes. And lactosylceramide precursor enzyme such as glycosylceramide synthase can be also investigated.

CHAPTER 5

CONCLUSION

Absence in Neu4 leads to Neu2, Neu3 and Hexb expression level augmentation. These changes prove that Neuraminidases are try compensating Neu4 function. Hexb level increase are probably responsible for lactosylceramide increase. In addition, increase in lactosylceramide may be due to disruption of Neu4 gene. In Neu1 level represented too low expression 3-month-old *Hexa*$^{-/-}$*GM3S*$^{-/-}$ and *Hexa*$^{-/-}$*GM3S*$^{-/-}$*Neu4*$^{-/-}$ mice. However, this turn into normal concentration in 6-month-old *Hexa*$^{-/-}$*GM3S*$^{-/-}$ and *Hexa*$^{-/-}$*GM3S*$^{-/-}$*Neu4*$^{-/-}$ mice. In the GM2AP, since wild type mice have both HexA and GM2, there was no change in GM2AP concentration. Furthermore, *Hexa*$^{-/-}$ mice have GM2 but not Hexa gene. However, in *GM3S*$^{-/-}$ do not have GM2 but there is Hexa and GM2AP level increased. Therefore, GM2AP production are prompted by Hexa gene. When GM2 is absent or decreased, Hexa probably reinforce GM2AP by increase of its level to degrade GM2. *Hexa*$^{-/-}$*GM3S*$^{-/-}$, and *Hexa*$^{-/-}$*GM3S*$^{-/-}$*Neu4*$^{-/-}$ are also supported this situation. These results are plausible for 6-month-old *GM3S*$^{-/-}$, but it is not observed in 3-month-old animals. Although Hexb level increase, there was no change in GALGT1 almost all genotypes except *GM3S*$^{-/-}$ mice. Moreover, despite of BGAL level increase, its reverse enzyme B3GALt4 expression level indicate no significant change. These can cause two results. One of them may be decrease in 0-series ganglioside. It is not supported because in the absence of a-, b-, and c- series ganglioside, organism will need more o-series ganglioside. Another one may be alternative pathway presence or enzymatic function on o-series ganglioside. GM2 accumulation problem are solved with GM3S blocking. In *Hexa*$^{-/-}$*GM3S*$^{-/-}$, and *Hexa*$^{-/-}$*GM3S*$^{-/-}$*Neu4*$^{-/-}$ did not represented GM2 accumulation in immunohistochemistry and thin layer chromatography results. Those results were also compatible with Realtime PCR results. Blocking GM3S consequences no GM3 and GM3 did not converted into GM2. Partially GM3S blocking will be effective on GM2 accumulation decrease and probably increase human lifespan because mice show that GM2 accumulation can be kept below the toxic level.

REFERENCES

Allende, M. L., & Proia, R. L. (2002). Lubricating cell signaling pathways with gangliosides. *Current Opinion in Structural Biology*, *12*(5), 587–592. https://doi.org/10.1016/S0959-440X(02)00376-7

Amado, M., Almeida, R., Carneiro, F., Levery, S. B., Holmes, E. H., Nomoto, M., Clausen, H. (1998). A family of human beta3-galactosyltransferases. Characterization of four members of a UDP-galactose:beta-N-acetyl-glucosamine/beta-nacetyl-galactosamine beta-1,3-galactosyltransferase family. *The Journal of Biological Chemistry*, *273*(21), 12770–8. https://doi.org/10.1074/JBC.273.21.12770

Aronovich, E. L., & Hackett, P. B. (2015, February). Lysosomal storage disease: gene therapy on both sides of the blood-brain barrier. *Molecular Genetics and Metabolism*. https://doi.org/10.1016/j.ymgme.2014.09.011

Arthur, J. R., Lee, J. P., Snyder, E. Y., & Seyfried, T. N. (2012). Therapeutic Effects of Stem Cells and Substrate Reduction in Juvenile Sandhoff Mice. *Neurochemical Research*, *37*(6), 1335–1343. https://doi.org/10.1007/s11064-012-0718-0

Aureli, M., Samarani, M., Murdica, V., Mauri, L., Loberto, N., Bassi, R., Sonnino, S. (2014). Gangliosides and Cell Surface Ganglioside Glycohydrolases in the Nervous System. In *Advances in Neurobiology* (Vol. 9, pp. 223–244). https://doi.org/10.1007/978-1-4939-1154-7_10

Bhavanandan, V. P., & Gowda, D. C. (2014). Introduction to the Complexity of Cell Surface and Tissue Matrix Glycoconjugates. In *Glycobiology of the Nervous System* (pp. 1–31). Springer New York. https://doi.org/10.1007/978-1-4939-1154-7_1

Bobowski, M., Vincent, A., Steenackers, A., Colomb, F., Van Seuningen, I., Julien, S., & Delannoy, P. (2013). Estradiol represses the GD3 synthase gene ST8SIA1 expression in human breast cancer cells by preventing NFκB binding to ST8SIA1 promoter. *PloS One*, *8*(4), e62559. https://doi.org/10.1371/journal.pone.0062559

Bonten, E. J., Annunziata, I., & D'Azzo, A. (2014, June). Lysosomal Multienzyme Complex: Pros and Cons of Working Together. *Cellular and Molecular Lİfe Sciences : CMLS*. https://doi.org/10.1007/s00018-013-1538-3

Bonten, E. J., & D'Azzo, A. (2000). Lysosomal neuraminidase. Catalytic activation in insect cells is controlled by the protective protein/cathepsin A. *The Journal of Biological Chemistry*, *275*(48), 37657–63. https://doi.org/10.1074/jbc.M007380200

Borodzicz, S., Czarzasta, K., Kuch, M., & Cudnoch-Jedrzejewska, A. (2015). Sphingolipids in cardiovascular diseases and metabolic disorders. *Lipids in Health and Disease*, *14*(1), 55. https://doi.org/10.1186/s12944-015-0053-y

Brandenburg, K., Holst, O., Brandenburg, K., & Holst, O. (2015). Glycolipids: Distribution and Biological Function. In *eLS* (pp. 1–10). Chichester, UK: John Wiley & Sons, Ltd. https://doi.org/10.1002/9780470015902.a0001427.pub3

Bremer, E. G., Schlessinger, J., & Hakomori, S. (1986). Ganglioside-mediated modulation of cell growth. Specific effects of GM3 on tyrosine phosphorylation of the epidermal growth factor receptor. *The Journal of Biological Chemistry*, *261*(5), 2434–40. Retrieved from http://www.ncbi.nlm.nih.gov/pubmed/2418024

Calhan, O. Y., & Seyrantepe, V. (2017). Mice with Catalytically Inactive Cathepsin A Display Neurobehavioral Alterations. *Behavioural Neurology*, *2017*, 1–11. https://doi.org/10.1155/2017/4261873

Chatterjee, S., & Pandey, A. (2008). The Yin and Yang of lactosylceramide metabolism: Implications in cell function. *Biochimica et Biophysica Acta (BBA) - General Subjects*, *1780*(3), 370–382. https://doi.org/10.1016/j.bbagen.2007.08.010

Chavas, L. M. G., Kato, R., Suzuki, N., von Itzstein, M., Mann, M. C., Thomson, R. J., … Wakatsuki, S. (2010). Complexity in Influenza Virus Targeted Drug Design: Interaction with Human Sialidases. *Journal of Medicinal Chemistry*, *53*(7), 2998–3002. https://doi.org/10.1021/jm100078r

Comelli, E. M., Amado, M., Lustig, S. R., & Paulson, J. C. (2003). Identification and expression of Neu4, a novel murine sialidase. *Gene*, *321*, 155–161. https://doi.org/https://doi.org/10.1016/j.gene.2003.08.005

Cordeiro, P., Hechtman, P., & Kaplan, F. (2000). The GM2 gangliosidoses databases: allelic variation at the HEXA, HEXB, and GM2A gene loci. *Genetics in Medicine: Oficial Journal of the American College of Medical Genetics*, *2*(6), 319–27. https://doi.org/10.109700125817-200011000-00003

d'Azzo, A., & Bonten, E. (2010, December). Molecular Mechanisms of Pathogenesis in a Glycosphigolipid and a Glycoprotein Storage Disease. *Biochemical Society Transactions*. https://doi.org/10.1042/BST0381453

d'Azzo, A., Machado, E., & Annunziata, I. (2015). Pathogenesis, Emerging therapeutic targets and Treatment in Sialidosis. *Expert Opinion On Orphan Drugs*. https://doi.org/10.1517/21678707.2015.1025746

de Carvalho Neves, J., Rizzato, V. R., Fappi, A., Garcia, M. M., Chadi, G., van de Vlekkert, D., Zanoteli, E. (2015). Neuraminidase-1 mediates skeletal muscle regeneration. *Biochimica et Biophysica Acta (BBA) - Molecular Basis of Disease*, *1852*(9), 1755–1764. https://doi.org/http://dx.doi.org/10.1016/j.bbadis.2015.05.006

Fanzani, A., Giuliani, R., Colombo, F., Zizioli, D., Presta, M., Preti, A., & Marchesini, S. (2003). Overexpression of cytosolic sialidase Neu2 induces myoblast differentiation in C2C12 cells. *FEBS Letters*, *547*(1), 183–188. https://doi.org/http://dx.doi.org/10.1016/S0014-5793(03)00709-9

Fragaki, K., Ait-El-Mkadem, S., Chaussenot, A., Gire, C., Mengual, R., Bonesso, L., Paquis-Flucklinger, V. (2013). Refractory epilepsy and mitochondrial dysfunction due to GM3 synthase deficiency. *European Journal of Human Genetics*, *21*(10), 528–534. https://doi.org/10.1038/ejhg.2012.202

Funato, K., & Riezman, H. (2001). Vesicular and nonvesicular transport of ceramide from ER to the Golgi apparatus in yeast. *The Journal of Cell Biology*, *155*(6), 949–59. https://doi.org/10.1083/jcb.200105033

Furukawa, K., Ohmi, Y., Ohkawa, Y., Tajima, O., & Furukawa, K. (2014).

Glycosphingolipids in the regulation of the nervous system. *Advances in Neurobiology*, *9*, 307–20. https://doi.org/10.1007/978-1-4939-1154-7_14

Gesellschaft Deutscher Chemiker., T., & Sandhoff, K. (1962). *Angewandte Chemie. Angewandte Chemie International Edition* (Vol. 38). Verlag Chemie. Retrieved from https://www.academia.edu/15646841/Sphingolipids_Their_Metabolic_Pathways_and_the_Pathobiochemistry_of_Neurodegenerative_Diseases

Giraudo, C. G., Rosales Fritz, V. M., & Maccioni, H. J. (1999). GA2/GM2/GD2 synthase localizes to the trans-golgi network of CHO-K1 cells. *The Biochemical Journal*, 342-3, 633–40. Retrieved from http://www.ncbi.nlm.nih.gov/pubmed/10477274

Groux Degroote, S., Guérardel, Y., & Delannoy, P. (2017). Gangliosides: Structures, Biosynthesis, Analysis, and Roles in Cancer. *ChemBioChem*. https://doi.org/10.1002/cbic.201600705

Hahn, C. N., del Pilar Martin, M., Schröder, M., Vanier, M. T., Hara, Y., Suzuki, K., D'Azzo, A. (1997). Generalized CNS disease and massive GM1-ganglioside accumulation in mice defective in lysosomal acid beta-galactosidase. *Human Molecular Genetics*, *6*(2), 205–11. Retrieved from http://www.ncbi.nlm.nih.gov/pubmed/9063740

Harduin-Lepers, A., Mollicone, R., Delannoy, P., & Oriol, R. (2005). The animal sialyltransferases and sialyltransferase-related genes: a phylogenetic approach. *Glycobiology*, *15*(8), 805–817. https://doi.org/10.1093/glycob/cwi063

Hauser, E. C., Kasperzyk, J. L., D'Azzo, A., & Seyfried, T. N. (2004). Inheritance of lysosomal acid beta-galactosidase activity and gangliosides in crosses of DBA/2J and knockout mice. *Biochemical Genetics*, *42*(7–8), 241–57. Retrieved from http://www.ncbi.nlm.nih.gov/pubmed/15487588

Huang, W. J., Zhang, X., & Chen, W. W. (2015). Gaucher disease: a lysosomal neurodegenerative disorder. *European Review For Medical and Pharmacological Sciences*, *19*(7), 1219–26. Retrieved from http://www.ncbi.nlm.nih.gov/pubmed/25912581

Ichikawa, N., Iwabuchi, K., Kurihara, H., Ishii, K., Kobayashi, T., Sasaki, T., Arikawa-Hirasawa, E. (2009). Binding of laminin-1 to monosialoganglioside GM1 in lipid rafts is crucial for neurite outgrowth. *Journal of Cell Science*, *122*(2), 289–299. https://doi.org/10.1242/jcs.030338

Iqbal, J., Walsh, M. T., Hammad, S. M., & Hussain, M. M. (2017). Sphingolipids and Lipoproteins in Health and Metabolic Disorders. *Trends in Endocrinology & Metabolism*. 122, 289-99. https://doi.org/10.1016/j.tem.2017.03.005

J, F. F., & BE, S. (2004). Tay-sachs disease. *Archives of Neurology*, *61*(9), 1466–1468. https://doi.org/10.1001/archneur.61.9.1466

Katoh, S., Maeda, S., Fukuoka, H., Wada, T., Moriya, S., Mori, A., Miyagi, T. (2010, August). A crucial role of sialidase Neu1 in hyaluronan receptor function of CD44 in T helper type 2-mediated airway inflammation of murine acute asthmatic model. *Clinical and Experimental Immunology*. https://doi.org/10.1111/j.1365-2249.2010.04165.x

Kawai, H., Allende, M. L., Wada, R., Kono, M., Sango, K., Deng, C., Proia, R. L. (2001). Mice expressing only monosialoganglioside GM3 exhibit lethal audiogenic seizures. *The Journal of Biological Chemistry*, *276*(10), 6885–8. https://doi.org/10.1074/jbc.C000847200

Kawakami, Y., Kawakami, K., Steelant, W. F. A., Ono, M., Baek, R. C., Handa, K., Hakomori, S. (2002). Tetraspanin CD9 is a "proteolipid," and its interaction with alpha 3 integrin in microdomain is promoted by GM3 ganglioside, leading to inhibition of laminin-5-dependent cell motility. *The Journal of Biological Chemistry*, *277*(37), 34349–58. https://doi.org/10.1074/jbc.M200771200

Kawamura, S., Sato, I., Wada, T., Yamaguchi, K., Li, Y., Li, D., … Miyagi, T. (2012). Plasma membrane-associated sialidase (NEU3) regulates progression of prostate cancer to androgen-independent growth through modulation of androgen receptor signaling. *Cell Death and Differentiation*, *19*(1), 170–179. https://doi.org/10.1038/cdd.2011.83

Kiguchi, K., Henning-Chubb, C. B., & Huberman, E. (1990). Glycosphingolipid Patterns of Peripheral Blood Lymphocytes, Monocytes, and Granulocytes Are Cell Specific. *The Journal of Biochemistry*, *107*(1), 8–14.

Kojima, H., Suzuki, Y., Ito, M., & Kabayama, K. (2015). Structural Characterization of Neutral Glycosphingolipids from 3T3-L1 Adipocytes. *Lipids*, *50*(9), 913–7. https://doi.org/10.1007/s11745-015-4035-7

Kolter, T., Proia, R. L., & Sandhoff, K. (2002). Combinatorial ganglioside biosynthesis. *The Journal of Biological Chemistry*, *277*(29), 25859–62. https://doi.org/10.1074/jbc.R200001200

Kolter, T., & Thomas. (2012). Ganglioside Biochemistry. *ISRN Biochemistry*, 1–36. https://doi.org/10.5402/2012/506160

Krengel, U., & Bousquet, P. A. (2014). Molecular recognition of gangliosides and their potential for cancer immunotherapies. *Frontiers in Immunology*. Frontiers Media SA. https://doi.org/10.3389/fimmu.2014.00325

Kreutz, F., Petry, F. dos S., Camassola, M., Schein, V., Guma, F. C. R., Nardi, N. B., & Trindade, V. M. T. (2013). Alterations of membrane lipids and in gene expression of ganglioside metabolism in different brain structures in a mouse model of mucopolysaccharidosis type I (MPS I). *Gene*, *527*(1), 109–114. https://doi.org/10.1016/j.gene.2013.06.002

Lawson, C. A., & Martin, D. R. (2016). Animal models of GM2 gangliosidosis: utility and limitations. *The Application of Clinical Genetics*. https://doi.org/10.2147/TACG.S85354

Lecommandeur, E., Baker, D., Cox, T. M., Nicholls, A. W., & Griffin, J. L. (2017). Alterations in endo-lysosomal function induce similar hepatic lipid profiles in rodent models of drug-induced phospholipidosis and Sandhoff disease. *Journal of Lipid Research*, *58*(7), 1306–1314. https://doi.org/10.1194/jlr.M073395

Ledeen, R. W., & Wu, G. (2006). Gangliosides of the nuclear membrane: A crucial locus of cytoprotective modulation. *Journal of Cellular Biochemistry*, *97*(5), 893–903. https://doi.org/10.1002/jcb.20731

Ledeen, R. W., Yu, R. K., & Eng, L. F. (1973). Gangliosides of human myelin: sialosylgalactosylceramide (G7) as a major component. *Journal of Neurochemistry*, *21*(4), 829–839. https://doi.org/10.1111/j.1471-4159.1973.tb07527.x

Levy, M., & Futerman, A. H. (2010). Mammalian ceramide synthases. *IUBMB Life*, *62*(5), 347–56. https://doi.org/10.1002/iub.319

Li, C.-Y., Yu, Q., Ye, Z.-Q., Sun, Y., He, Q., Li, X.-M., Wei, L. (2007). A nonsynonymous SNP in human cytosolic sialidase in a small Asian population results in reduced enzyme activity: potential link with severe adverse reactions to oseltamivir. *Cell Research*, *17*(4), 357–362. https://doi.org/10.1038/cr.2007.27

Li, S. C., Chien, J. L., Wan, C. C., & Li, Y. T. (1978, August). Occurrence of glycosphingolipids in chicken egg yolk. *Biochemical Journal*.

Li, Y.-T., Sugiyama, E., Ariga, T., Nakayama, J., Hayama, M., Hama, Y., Ksama, T. (2002). Association of GM4 ganglioside with the membrane surrounding lipid droplets in shark liver. *Journal of Lipid Research*, *43*(7), 1019–25. https://doi.org/10.1194/JLR.M200010-JLR200

Malhotra, R. (2012). Membrane Glycolipids: Functional Heterogeneity: A Review. *Biochemistry & Analytical Biochemistry*, volume *1*, IP 2, https://doi.org/10.4172/2161-1009.1000108

Matsuda, J., Suzuki, O., Oshima, A., Ogura, A., Naiki, M., & Suzuki, Y. (1997). Neurological manifestations of knockout mice with/3-galactosidase deficiency. *Brain & Development*, *19*, 19–20. Retrieved from http://ac.els-cdn.com/S0387760496000770/1-s2.0-S0387760496000770-main.pdf?_tid=64f441e8-4dfa-11e7-9a0a-00000aab0f27&acdnat=1497112528_4104e290313be0d4ab1f98a5f47a06f5

Mehta, A., Beck, M., Linhart, A., Sunder-Plassmann, G., & Widmer, U. (2006). *History of lysosomal storage diseases: an overview*. *Fabry Disease: Perspectives from 5 Years of FOS*. Oxford PharmaGenesis. Retrieved from http://www.ncbi.nlm.nih.gov/pubmed/21290707

Miyagi, T., Wada, T., Iwamatsu, A., Hata, K., Yoshikawa, Y., Tokuyama, S., & Sawada, M. (1999). Molecular cloning and characterization of a plasma membrane-associated sialidase specific for gangliosides. *The Journal of Biological Chemistry*, *274*(8), 5004–11. https://doi.org/10.1074/JBC.274.8.5004

Miyagi, T., Wada, T., Yamaguchi, K., Hata, K., & Shiozaki, K. (2008). Plasma Membrane-associated Sialidase as a Crucial Regulator of Transmembrane Signalling. *The Journal of Biochemistry*, *144*(3), 279–285. https://doi.org/10.1093/jb/mvn089

Miyagi, T., & Yamaguchi, K. (2012). Mammalian sialidases: Physiological and pathological roles in cellular functions. *Glycobiology*, *22*(7), 880–896. https://doi.org/10.1093/glycob/cws057

Miyazaki, H., Fukumoto, S., Okada, M., Hasegawa, T., & Furukawa, K. (1997). Expression cloning of rat cDNA encoding UDP-galactose:GD2 beta1,3-galactosyltransferase that determines the expression of GD1b/GM1/GA1. *The Journal of Biological Chemistry*, *272*(40), 24794–9. Retrieved from

http://www.ncbi.nlm.nih.gov/pubmed/9312075

Monti, E., Bonten;, E., D'Azzo, A., Bresciani, R., Venerando, B., Borsani, G., Tettamanti, G. (2010). Sialidases in Vertebrates. *Advances in Carbohydrate Chemistry and Biochemistry*, *64*, 403–479. https://doi.org/http://dx.doi.org/10.1016/S0065-2318(10)64007-3

Monti, E., & Miyagi, T. (2015). Structure and Function of Mammalian Sialidases. In *SialoGlyco Chemistry and Biology I: Biosynthesis, structural diversity and sialoglycopathologies* (pp. 183–208). Berlin, Heidelberg: Springer Berlin Heidelberg. https://doi.org/10.1007/128_2012_328

Monti, E., Preti, A., Nesti, C., & Ballabio, A. (1999). Expression of a novel human sialidase encoded by the NEU2 gene. *Glycobiology*, *9*(12), 1313–1321. https://doi.org/10.1093/glycob/9.12.1313

Myerowitz, R. (1997). Tay-Sachs disease-causing mutations and neutral polymorphisms in the Hex A gene. *Human Mutation*, *9*(3), 195–208. https://doi.org/10.1002/(SICI)1098-1004(1997)9:3<195::AID-HUMU1>3.0.CO;2-7

Nakayama, J., Fukuda, M. N., Hirabayashi, Y., Kanamori, A., Sasaki, K., Nishi, T., & Fukuda, M. (1996). Expression cloning of a human GT3 synthase. GD3 AND GT3 are synthesized by a single enzyme. *The Journal of Biological Chemistry*, *271*(7), 3684–91. Retrieved from http://www.ncbi.nlm.nih.gov/pubmed/8631981

Oheda, Y., Kotani, M., Murata, M., Sakuraba, H., Kadota, Y., Tatano, Y., Itoh, K. (2006). Elimination of abnormal sialylglycoproteins in fibroblasts with sialidosis and galactosialidosis by normal gene transfer and enzyme replacement. *Glycobiology*, *16*(4), 271–280. https://doi.org/10.1093/glycob/cwj069

Okuda, T. (2017). PUGNAc treatment provokes globotetraosylceramide accumulation in human umbilical vein endothelial cells. *Biochemical and Biophysical Research Communications* (Vol. 487). https://doi.org/10.1016/j.bbrc.2017.04.019

Ono, M., Handa, K., Sonnino, S., Withers, D. A., Nagai, H., & Hakomori, S. (2001). GM3 ganglioside inhibits CD9-facilitated haptotactic cell motility: coexpression of GM3 and CD9 is essential in the downregulation of tumor cell motility and malignancy. *Biochemistry*, *40*(21), 6414–21. Retrieved from http://www.ncbi.nlm.nih.gov/pubmed/11371204

Pastores, G. M., & Maegawa, G. H. B. (2013, November). Neuropathic Lysosomal Storage Disorders. *Neurologic Clinics*. https://doi.org/10.1016/j.ncl.2013.04.007

Phaneuf, D., Wakamatsu, N., Huang, J.-Q., Borowski, A., Peterson, A. C., Fortunato, S. R., Gravel, R. A. (1996). Dramatically different phenotypes in mouse models of human tay-sachs and sandhoff diseases. *Human Molecular Genetics*, *5*(1), 1–14. https://doi.org/10.1093/hmg/5.1.1

Pinsky, L., Miller, J., Shanfield, B., Watters, G., & Wolfe, L. S. (1974). GM1 gangliosidosis in skin fibroblast culture: enzymatic differences between types 1 and 2 and observations on a third variant. *American Journal of Human Genetics*, *26*(5), 563–77. Retrieved from http://www.ncbi.nlm.nih.gov/pubmed/4420522

Posse de Chaves, E., & Sipione, S. (2010). Sphingolipids and gangliosides of the

nervous system in membrane function and dysfunction. *FEBS Letters*, *584*(9), 1748–1759. https://doi.org/10.1016/j.febslet.2009.12.010

Prokazova, N. V, Samovilova, N. N., Gracheva, E. V, & Golovanova, N. K. (2009). Ganglioside GM3 and its biological functions. *Biochemistry (Moscow)*, *74*(3), 235–249. https://doi.org/10.1134/S0006297909030018

Rahman, M. M., Kitao, S., Tsuji, D., Suzuki, K., Sakamoto, J.-I., Matsuoka, K., Itoh, K. (2013). Inhibitory effects and specificity of synthetic sialyldendrimers toward recombinant human cytosolic sialidase 2 (NEU2). *Glycobiology*, *23*(4), 495–504. https://doi.org/10.1093/glycob/cws221

Rothe, B., Rothe, B., Roggentin, P., & Schauer, R. (1991). The sialidase gene from Clostridium septicum: cloning, sequencing, expression in Escherichia coli and identification of conserved sequences in sialidases and other proteins. *Molecular and General Genetics MGG*, *226*(1), 190–197. https://doi.org/10.1007/BF00273603

Schnaar, R. L. (2010). Brain gangliosides in axon-myelin stability and axon regeneration. *FEBS Letters*, *584*(9), 1741–1747. https://doi.org/10.1016/j.febslet.2009.10.011

Seyfried, T. N., El-Abbadi, M., & Roy, M. L. (1992). Ganglioside distribution in murine neural tumors. *Molecular and Chemical Neuropathology*, *17*(2), 147–167. https://doi.org/10.1007/BF03159989

Seyrantepe, V., Canuel, M., Carpentier, S., Landry, K., Durand, S., Liang, F., Pshezhetsky, A. V. (2008). Mice deficient in Neu4 sialidase exhibit abnormal ganglioside catabolism and lysosomal storage. *Human Molecular Genetics*, *17*(11), 1556–1568. https://doi.org/10.1093/hmg/ddn043

Seyrantepe, V., Lema, P., Caqueret, A., Dridi, L., Bel Hadj, S., Carpentier, S., Pshezhetsky, A. V. (2010). Mice doubly-deficient in lysosomal hexosaminidase A and neuraminidase 4 show epileptic crises and rapid neuronal loss. *PLoS Genetics*, *6*(9), e1001118. https://doi.org/10.1371/journal.pgen.1001118

Shiina, T., Kikkawa, E., Iwasaki, H., Kaneko, M., Narimatsu, H., Sasaki, K., Inoko, H. (2000). The beta-1,3-galactosyltransferase-4 (B3GALT4) gene is located in the centromeric segment of the human MHC class II region. *Immunogenetics*, *51*(1), 75–8. Retrieved from http://www.ncbi.nlm.nih.gov/pubmed/10663566

Shiraishi, T., & UDA, Y. (1986). Characterization of Neutral Sphingolipids and Gangliosides from Chicken Liver. *The Journal of Biochemistry*, *100*(3), 553–561.

Shtyrya, Y. A., Mochalova, L. V, & Bovin, N. V. (2009). Influenza virus neuraminidase: structure and function. *Acta Naturae*, *1*(2), 26–32. Retrieved from http://www.ncbi.nlm.nih.gov/pubmed/22649600

Simpson, M. A., Cross, H., Proukakis, C., Priestman, D. A., Neville, D. C. A., Reinkensmeier, G., Crosby, A. H. (2004). Infantile-onset symptomatic epilepsy syndrome caused by a homozygous loss-of-function mutation of GM3 synthase. *Nature Genetics*, *36*(11), 1225–1229. https://doi.org/10.1038/ng1460

Sonnino, S., Mauri, L., Chigorno, V., & Prinetti, A. (2006). Gangliosides as components of lipid membrane domains. *Glycobiology*, *17*(1), 1R–13R.

https://doi.org/10.1093/glycob/cwl052

Svennerholm, L. (1956). Composition of Gangliosides from Human Brain. *Nature*, *177*(4507), 524–525. https://doi.org/10.1038/177524b0

Tadano, K., & Ishizuka, I. (1980). Isolation and partial characterization of a novel sulfoglycosphingolipid and ganglioside GM4 from rat kidney. *Biochemical and Biophysical Research Communications*, *97*(1), 126–132. https://doi.org/http://dx.doi.org/10.1016/S0006-291X(80)80144-6

Tokuda, N., Numata, S., Li, X., Nomura, T., Takizawa, M., Kondo, Y., Furukawa, K. (2013). ?4GalT6 is involved in the synthesis of lactosylceramide with less intensity than ?4GalT5. *Glycobiology*, *23*(10), 1175–1183. https://doi.org/10.1093/glycob/cwt054

Wada, T., Hata, K., Yamaguchi, K., Shiozaki, K., Koseki, K., Moriya, S., & Miyagi, T. (2007). A crucial role of plasma membrane-associated sialidase in the survival of human cancer cells. *Oncogene*, *26*(17), 2483–2490. https://doi.org/10.1038/sj.onc.1210341

Walkley, S. U. (2009, April). Pathogenic Cascades in Lysosomal Disease – Why so Complex? *Journal of Inherited Metabolic Dİsease*. https://doi.org/10.1007/s10545-008-1040-5

Wang, P., Zhang, J., Bian, H., Wu, P., Kuvelkar, R., Kung, T. T., Billah, M. M. (2004, June). Induction of lysosomal and plasma membrane-bound sialidases in human T-cells via T-cell receptor. *Biochemical Journal*. https://doi.org/10.1042/BJ20031896

Wu, G., Lu, Z. H., & Ledeen, R. W. (1995). GM1 ganglioside in the nuclear membrane modulates nuclear calcium homeostasis during neurite outgrowth. *Journal of Neurochemistry*, *65*(3), 1419–22. Retrieved from http://www.ncbi.nlm.nih.gov/pubmed/7643123

Yang, G.-Y., Li, C., Fischer, M., Cairo, C. W., Feng, Y., & Withers, S. G. (2015). A fret probe for cell-based imaging of ganglioside-processing enzyme activity and high-throughput screening. *Angewandte Chemie International Edition*, *54*(18), 5389–5393. https://doi.org/10.1002/anie.201411747

Yoshikawa, M., Go, S., Takasaki, K., Kakazu, Y., Ohashi, M., Nagafuku, M., Inokuchi, J. (2009, June). Mice lacking ganglioside GM3 synthase exhibit complete hearing loss due to selective degeneration of the organ of Corti. *Proceedings of the National Academy of Sciences of the United States of America*. https://doi.org/10.1073/pnas.0903279106

Yu, R. K. (1984). Gangliosides: structure and analysis (pp. 39–53). Springer US. https://doi.org/10.1007/978-1-4684-1200-0_4

Yu, R. K., Bieberich, E., Xia, T., & Zeng, G. (2004). Regulation of ganglioside biosynthesis in the nervous system. *Journal of Lipid Research*, *45*(5), 783–93. https://doi.org/10.1194/jlr.R300020-JLR200

Yu, R. K., Tsai, Y.-T., & Ariga, T. (2012). Functional Roles of Gangliosides in Neurodevelopment: An Overview of Recent Advances. *Neurochemical Research*, *37*(6), 1230–1244. https://doi.org/10.1007/s11064-012-0744-y

Yu, R. K., Tsai, Y.-T., Ariga, T., & Yanagisawa, M. (2011). Structures, biosynthesis,

and functions of gangliosides--an overview. *Journal of Oleo Science*, *60*(10), 537–44. Retrieved from http://www.ncbi.nlm.nih.gov/pubmed/21937853

Zeng, B. J., Torres, P. A., Viner, T. C., Wang, Z. H., Raghavan, S. S., Alroy, J., Kolodny, E. H. (2008). Spontaneous appearance of Tay–Sachs disease in an animal model. *Molecular Genetics and Metabolism*, *95*(1–2), 59–65. https://doi.org/https://doi.org/10.1016/j.ymgme.2008.06.010